

NONDESTRUCTIVE TESTING OF
HIGH STRENGTH STEEL WELDS
BY NEUTRON RADIOGRAPHY

J. Kenneth Edgar

LIBRARY
NAVAL POSTGRADUATE SCHOOL
MONTEREY, CALIF. 93940

NONDESTRUCTIVE TESTING OF
HIGH STRENGTH STEEL WELDS
BY NEUTRON RADIOGRAPHY

by

J. Kenneth Edgar

Lieutenant, United States Navy

B.S., United States Naval Academy

(1969)

SUBMITTED IN PARTIAL FULFILLMENT OF THE
REQUIREMENTS FOR THE
DEGREE OF MASTER OF SCIENCE IN NUCLEAR ENGINEERING AND THE
DEGREE OF MASTER OF SCIENCE IN OCEAN ENGINEERING

at the

MASSACHUSETTS INSTITUTE OF TECHNOLOGY

May 1973,

2.

NONDESTRUCTIVE TESTING OF HIGH STRENGTH

STEEL WELDS BY NEUTRON RADIOGRAPHY

by

J. Kenneth Edgar

Submitted to the Department of Nuclear Engineering and the Department of Ocean Engineering on 11 May, 1973 in partial fulfillment of the requirements for the degree of Master of Science in Nuclear Engineering and the degree of Master of Science in Ocean Engineering.

ABSTRACT

The use of neutron radiography as a method of nondestructively testing high strength steel welds is examined for technical feasibility and procedural evaluation. Four test samples constructed of HY-80 steel are used to develop accurate radiographic procedural information in order to optimize the quality and minimize error in producing neutron radiographs at MITR. Variations in the basic radiographic procedure were made in order to determine the ability of neutron radiography to find defects in the four weld samples. Attempts were also made to artificially enhance the ability of neutron radiography to pickup surface defects that conventional radiographs are unable to do. The samples were also tested by various other nondestructive test methods, namely ultrasonics, magnetic particle, and eddy current examination. The results of these test are compared against the neutron radiographs and conventional gamma radiographs of the samples.

Thesis Supervisor

D. D. Lanning

Title

Professor of Nuclear Engineering

ACKNOWLEDGEMENTS

I wish to express my appreciation to those whose assistance made this thesis possible. To Professor D.D. Lanning who supervised the work, and to Johnny Summey and his test group at Portsmouth Naval Shipyard who was a valuable source of information and help.

My wife, Sandy, deserves special credit for patience, and understanding over a long and trying period.

TABLE OF CONTENTS

Abstract	2.
Acknowledgements	3.
Table of Contents	4.
List of Figures	6.
1. Introduction	9.
1.1. Background	9.
1.2. Objectives	13.
2. Neutron Radiography	15.
2.1. Theory of Neutron Radiography	15.
2.2. Procedures and Hardware Associated with Neutron Radiography	19.
2.2.1. Neutron Sources	20.
2.2.2. Collimation	21.
2.2.3. Image Detection Techniques	31.
3. Test Facility and Procedure	36.
3.1. M.I.T. Research Reactor	36.
3.2. Radiographic Facilities	37.
3.3. Exposure Techniques	43.
3.4. Quality Control	58.
3.5. Safety Considerations	62.
4. Test Samples	65.
4.1. HY-80 Steel	65.
4.2. Test Samples	74.
4.3. Shipyard Tests	78.

5.

5.	Neutron Radiography at MIT	79.
5.1.	Characteristic Curves	80.
5.2.	Neutron Radiographs	88.
5.3.	Comparison with other Nondestructive Tests	90.
5.3.1.	Magnetic Particle Tests	90.
5.3.2.	Eddy Current Examination	91.
5.3.3.	Ultrasonic Inspection	92.
5.3.4.	Radiographic Tests	92.
6.	Recommendations and Conclusions	114.
6.1.	Recommendations	114.
6.2.	Conclusions	117.
Appendices	A. Mass Absorption Coefficients for the Elements	119.
	B. Weld Defects	123.
	C. Applications of Neutron Radiography	136.
	D. Non-Destructive Testing Methods	140.
	E. Data Sheets	155.
	F. References	165

LIST OF FIGURES

1-1	Mass Attenuation Coefficients as a Function of Atomic Number	12.
2-1	Moderating Materials	22.
2-2	Some Radioactive Sources for Neutron Radiography	25.
2-3	Collimators	28.
2-4	Geometric Unsharpness	30.
2-5	Image Detection Methods	32.
2-6	Properties of Some Thermal Neutron Radiograph Detection Converters	33.
3-1	MIT Research Reactor	38.
3-2	Medical Room and Shutter Arrangement	40.
3-3	MITR Neutron Collimator	42.
3-4	A Typical Characteristic Curve	47.
3-5	Characteristic Curves: Development Times	48.
3-6	Extrapolated Characteristic Curves for Dysprosium and Indium Foils	51.
3-7	Activation Analysis	52.
3-8	Dysprosium Decay Functions	55.
3-9	Indium Decay Functions	56.
3-10	The VISQI Neutron Radiographic Penetrameter	59.
3-11	Standard Radiographic Penetrameter	61.
4-1	Chemical and Mechanical Properties of HY-80 Steel	67.
4-2	HY-80 Welding Electrodes	71.
4-3	Mechanical Properties of HY-80 Welding Electrodes	73.

4-5	Test Samples	75.
4-6	Penetrameters	77.
5-1	Indium Foil; Characteristic Curve	82.
5-2	Comparison of Indium Characteristic Curves	84.
5-3	Normalized Characteristic Curve	85.
5-4	Effective Attenuation Coefficient	87.
5-5	Neutron Radiograph of Sample B-1	94.
5-6	Neutron Radiograph of Sample B-1	95.
5-7	Gamma Radiograph of Sample B-1	96.
5-8	Neutron Radiograph of Sample B-1	98.
5-9	Neutron Radiograph of Sample B-1	99.
5-10	Effect of Elevation Variance	100.
5-11	Neutron Radiograph of Sample F-1	102.
5-12	Neutron Radiograph of Sample F-1	103.
5-13	Gamma Radiograph of Sample F-1	104.
5-14	Neutron Radiograph of Sample B-2	106.
5-15	Gamma Radiograph of Sample B-2	107.
5-16	Gamma Radiograph of Sample B-2	108.
5-17	Gamma Radiograph of Sample F-2	109.
5-18	Neutron Radiograph of Sample F-2	110.
5-19	Neutron Radiograph of Sample B-1	113.
B-1	Porosity	130.
B-2	Slag Inclusions	130.
B-3	Incomplete Fusion	131.
B-4	Penetration	132.
B-5	Undercutting	133.

8.

B-6	Cracks	134.
B-7	Mismatch	135.
D-1	Comparison of NDT Methods	150.
E-1	Initial Characteristic Curve Data	156.
E-2	Data Sheet for Neutron Radiographs	157.
E-3	Ultrasonic Inspection Sheet	160.
E-4	Radiographic Inspection Sheet for Samples B-1	161.
E-5	Radiographic Inspection Sheet for Samples F-1	162.
E-6	Radiographic Inspection Sheet for Samples B-2	163.
E-7	Radiographic Inspection Sheet for Samples F-2	164.

CHAPTER 1

INTRODUCTION

1.1 BACKGROUND

Forty three years ago in 1935, Chadwick discovered the neutron (B-1). It was this discovery that made possible a new dimension in the young field of radiography, that is, neutron radiography. However, development in the field of neutron radiography has at best advanced slowly until recent years.

It was the German team of Kallmann and Kuhn that did the first neutron radiographic experiments in 1935. Though their work resulted in several patents in the late 30's and early 40's, it wasn't until Peter using a greatly improved and more powerful source was able to reduce radiographic exposure time from hours to minutes. Ten years later the first radiographs taken using a reactor as the neutron source were taken by Thewlis and Derbyshire at the BEPO reactor in Harwell, England (B-1).

Due to the increased availability of neutron sources and an increasing number of experiments resulting in useable purposes for neutron radiography, the field has grown from a group of scientific experiments in the 60's to a moderate size industry in the 70's. Today nearly every reactor services company offers radiographic services, accelerator manufacturers now have available radiographic attachments for their machines, and a portable neutron camera is being marketed (W-1, G-1). As a result industry now has the opportunity to exploit the full utility of neutron radiography through development of special techniques for specific inspection requirements.

This raises the question as to what advantage or disadvantages does neutron radiography have over other methods of inspection or nondestructive testing (NDT). These other methods of NDT include ultrasonic testing, dye penetrants, magnaflux testing, eddy current testing, and X-ray or gamma radiography, all of which are used and all of which have some sort of limitation. Neutron radiography also has limitations but in some cases it can be used to compliment the other methods, thus opening new areas of NDT. Dye penetrant testing is dependent on visual observations while X-ray, magnaflux, eddy current, and ultrasonic testing is highly dependent on the relative densities with-

in the test object. On the other hand, a major advantage of neutron radiography is that neutron attenuation has no strong dependence on density (B-2). Consequently, it is possible to obtain better imaging with neutron radiography through high atomic weight materials such steel, lead or uranium than with X-radiography. Similarly, the difference in neutron attenuation characteristics of materials with neighboring atomic weights often permits discrimination using neutron radiography, but their near identical densities make discrimination by other test methods extremely difficult.

The advantage of neutron radiography over other radiographic methods is best shown in Figure 1-1 in which mass absorption coefficient is plotted against atomic number for low energy or slow neutrons and 120 Kev X-rays. It can be seen from this figure that; a) the mass absorption coefficients for neutrons differ greatly and randomly from those for X-rays, b) it is often possible to distinguish neighboring elements using neutrons, c) neutrons have low attenuation in many of the heavier elements, and d) neutron coefficients are random while X-ray coefficients have a dependency on atomic number (B-1, W-2).

A more detailed development of radiographic physics

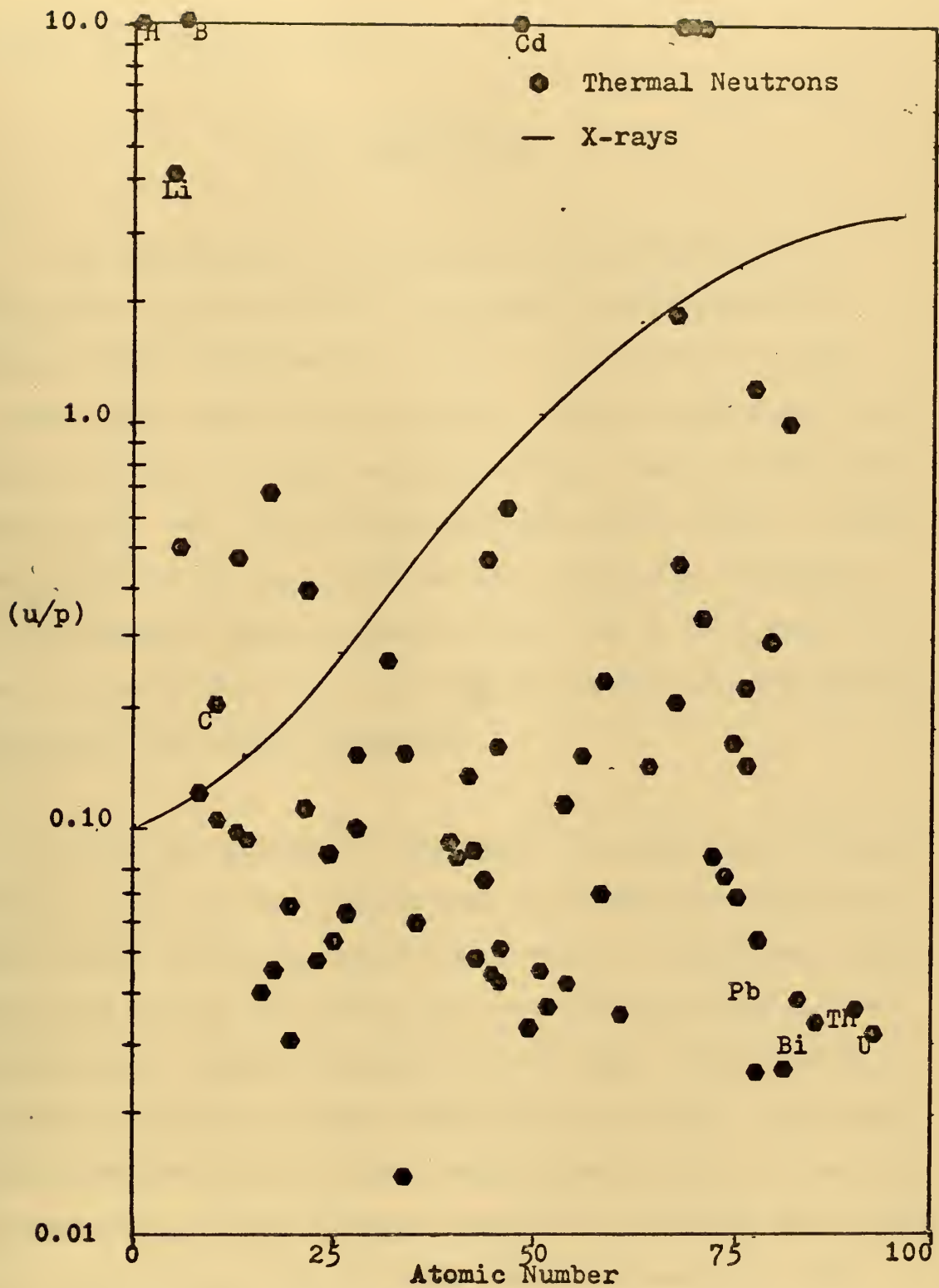


Figure 1-1. Mass-attenuation coefficients as a
Function of Atomic Number

follows in Chapter 2 and 3.

1.2 OBJECTIVES

The advancement of technology has brought with it increased requirements for materials and procedures to support man's exploration of space, his conquest of the oceans, and everything in between. These requirements have taken the form of light weight material, such as the titanium alloys, and the new high strength steel alloys. These new materials in turn require new and complex procedures to manufacture, machine and utilize, and it is because of the nature of their use and complex background that quality assurance has become paramount.

It is the purpose of this work to examine the feasibility of using neutron radiography to nondestructively test for faults in high strength steel welds. Though some work has been done in this area, the results are mixed and inconclusive. Several groups have had poor results with locating faults in welded materials (K-1, H-1). Yet other experimenters have obtained outstanding results to the point of detecting 50 ppm hydrogen content in titanium weld samples and still others have detected cracks as small as .0005 inches wide (H-2, K-2).

Other areas of interest to be investigated is the development of improved procedures and methods for taking radiographs at MITR and evaluating possible changes to the existing neutron radiographic facility. It is hopeful that the conclusion of this work may clarify previous work done in this area and provide some standard for future experiments.

CHAPTER 2NEUTRON RADIOGRAPHY2.1 THEORY OF NEUTRON RADIOGRAPHY

Neutron radiography like other forms of radiography is primarily concerned with the production of radiographs, i.e. a photographic image produced by a beam of radiation. In the case of neutron radiography the radiation is a beam of neutrons that is used either directly or indirectly to create an image on a photographic plate, and like other forms of radiation the beam of neutrons follows the general law governing the absorption of radiation as it passes through matter. This law first stated by Lambert in the 18th century, is "that fraction of the radiation absorbed in passing through a thin layer of matter is proportional to the thickness of the layer and to an absorption constant, i.e. (H-3).

$$\frac{I_0 - I}{I_0} = \mu x \quad (2.1)$$

$$I / I_0 = -\mu dx \quad (2.2)$$

and if this is applied to a homogeneous radiation and an absorber of finite thickness x , it can become.

$$I = I_0 \exp (-\mu x) \quad (2.3)$$

where: I is the transmitted radiation

I_0 is the incident radiation

x is the object thickness

μ is the linear absorption coefficient

The main difference between neutron radiography and other forms of radiography lies in the linear absorption coefficient (μ). For any type of radiation μ is a function of the radiation energy or wave length and the object material composition (H-4, L-1). For a beam of neutrons, μ is equal to the total microscopic cross section (Σ_t) which is comprised of the total microscopic cross section (Σ_t) and the number of nuclei per volume of attenuating material (N) or

$$\mu = \Sigma_t \quad (2.4)$$

$$\mu = N \Sigma_t \quad (2.5)$$

The total cross section can also be expressed as the sum of the absorption and scattering cross sections (Σ_a and Σ_s respectively) and the number of nuclei per volume can be broken down into base units which yields the attenuation coefficient for neutrons in the following form:

$$\mu = \frac{N_0 p}{A} (\sqrt{a} + \sqrt{s}) \quad (2.6)$$

where: N_0 is Avogadro's number
 p is the object density
 A is the object atomic weight
 μ, \sqrt{a} and \sqrt{s} have been previously
defined

Values of microscopic absorption and scattering cross sections for various materials and neutron energies can be found in BNL - 325, the published results of Brookhaven National Laboratory's compilation (H-4).

A similar equation for X-ray and gamma radiation linear attenuation coefficients can be developed and presented in the following form (H-3).

$$\mu_x = \frac{\rho N_0 z e \mu}{A} \quad (2.7)$$

where: μ is the linear attenuation
coefficient for gamma radiation
 ρ is the object density
 A is the object atomic weight
 z is the object atomic number
 N_0 is the Avogadro's number
 $e\mu$ is the average collision cross
section

Unlike the neutron cross section (σ_t) the average collision cross section (σ_{μ}) is a strong function of the incident energy only and not of the object material (E-1).

It should be noted that equation (2.7) contains Z , the atomic number of the object material. This is significant when one remembers X-ray and gamma radiation interacts primarily with the electrons within the object material. This accounts in part for the difference in cross sections (σ_t and σ_{μ}) between the two forms of radiation, and allows for a better understanding of the observations in Chapter 1 concerning Figure 1 (B-1, W-2):

- a) the absorption coefficients for neutrons differ greatly and randomly from those for X-rays.
- b) the possibility of distinguishing neighboring elements using neutrons.-
- c) neutrons have low attenuation in many of the heavier elements.
- d) neutron absorption coefficients are random while X-ray coefficients have a dependency on atomic number.

It is the neutron's unique attenuation characteristics that allow neutron radiography to be a potentially valuable tool in the field of NDT. A comparative table of absorption coefficients for thermal neutrons and 120

Kev X-rays is given in appendix A.

2.2 PROCEDURES AND HARDWARE

ASSOCIATED WITH NEUTRON RADIOGRAPHY

As was mentioned before, neutron radiography is primarily concerned with the production of radiographs, however producing a successful neutron radiograph encompasses many of the same problems associated with other type of radiography and several unique to this form of radiography. The reason neutron radiography has been slow in developing is the lack of suitable neutron sources. This inavailability of a suitable source of neutrons is still the major area of concern. The crux of the problem lies in finding a source of neutrons that produces a sufficient number of neutrons per unit area (neutron flux) such that after those neutrons that are unsuitable for radiographic use are removed, the usable neutron flux is sufficient for producing radiographs.

The problem of neutron selection is also important and is really a two-fold problem, that of selecting or creating neutrons of the desired energy and selecting neutrons traveling in a usable direction. These two problems are usually solved by moderation and collimation

respectively and will be discussed in detail later in this chapter.

Problems have also arisen in the areas of neutron detection, imaging, and safety. Although many of these problems have been solved as a result of experience in conventional forms of radiography, the fact that neutrons are used as the irradiating beam puts a new twist in things. For example unlike other forms of radiation, neutrons don't interact with the emulsions on conventional photographic plates, and as was mentioned before, neutrons aren't attenuated as much by heavy metals as are forms of radiation therefore shielding and activation become problems.

The following paragraphs will attempt to illuminate the above mentioned problem areas and to also serve as a guide to better understand the principles and procedures of neutron radiography.

2.2.1 NEUTRON SOURCES

No matter what the source of neutrons, they all have one thing in common, that is all neutron sources produce neutrons of energies unsuitable for use as ^aradiographic neutron beam. Most work in neutron radiography is per-

formed with thermal neutrons (average energy of .025 ev) because neutrons within that energy range exhibit the useful attenuation characteristics previously mentioned (B-2). Experiments have been conducted with neutrons in other energy ranges, but it was found that these neutrons were not nearly as useful as thermal neutrons(B-3). In order to obtain thermal neutrons, the neutrons from the source must be "moderated" or "thermalized".

This moderation is accomplished by surrounding the source or mixing the source in a material that has good moderating properties. The mechanism of moderation is scattering, that is a neutron at a high energy level strikes and imparts energy to the moderating material and thereby "slows down". It may take one or many collisions to reduce the neutrons energy to the thermal level, dependent on the initial energy and moderating material. It follows then that good moderating material is material with a high scattering cross section but low absorption cross section so as not to lower the source intensity, and the size of the moderator nuclei should be approximately the size of a neutron so that the number of collisions required to complete the thermalization is minimized thereby minimizing the amount of moderating material required.

Figure 2-1 lists the good moderating materials and their moderating characteristics (L-1, A-2).

Material	$\bar{\xi}$	$\frac{\bar{\xi}\Sigma_s}{\Sigma_a}$
Hydrogen	1.000	117.65
H2O	0.920	142.680
Deuterium	0.725	8510.0
D2O	0.509	692.197
Beryllium	0.029	159.37

Figure 2-1 Moderating Materials

$\bar{\xi}$ is the maximum fractional energy loss in a single collision.

$\frac{\bar{\xi}\Sigma_s}{\Sigma_a}$ is the moderating ratio, reflecting the influence of absorption on moderating materials.

As seen in Figure 2-1 hydrogen is a good moderating material, that is why water, wax, and other hydrocarbons have been used. Studies have also been made to evaluate TiH_2 , ZrH_2 , and BeH_2 with varied success (B-1).

As previously mentioned, neutron radiography had been limited to do the lack of adequate neutron sources. Today there are three sources of neutrons (1) reactors, (2) accelerators, and (3) radioactive sources.

Reactors have played an important part in neutron radiography ever since the BEPO reactor was used to make the first radiographs using a reactor as a source. Today firms such as "Reactor Experiments, Inc." in San Carlos, Calif, and "Western New York Nuclear Research Center, Inc." in Buffalo, New York offer neutron radiography services using their reactors. In addition studies have been undertaken to determine the feasibility of using a small non-critical reactor for neutron radiography purposes. The study showed it was possible and relatively high neutron fluxes could be obtained, but it was noncompetitive compared to other sources (B-4).

Reactors inherently produce higher fluxes and intensities than other sources; but they are bulky, nonportable and costly for industrial purposes. An example of the fluxes and intensities obtained from a reactor is the BEPO reactor in Harwell, England which has a flux (ϕ) 1.3×10^{12} N/CM²-sec and intensity (I) at the exposure area of 10^6 N/CM²-sec at 8 Mw(t) (B-2).

Though the MIT reactor was used for the experiments discussed later in this paper, a reactor should not be considered as the only practicle neutron source.

Radioactive sources show the most promise for inexpensive portable sources. The two most important reactions in radioactive neutron sources are the alpha-neutron (α, N) and the gamma-neutron (γ, N) reactions, a third and almost eclipsing reaction is the spontaneous fission reaction. Figure 2-2 shows the characteristics of several neutron sources (B-2).

The (γ, N) and (α, N) sources require two materials; a gamma or alpha source and a target. The target is struck with either gamma rays or alpha particles and neutrons are emitted from the target. Radiographic devices constructed using these radioactive sources have the advantage of being portable, rather compact, requiring no external power, and relatively inexpensive; but, they have one very serious drawback, they produce on the order of 10^6 to 10^7 n/sec per curie of activity and since a total beam of about 10^{10} n/sec is required for good results, these sources are not the best (B-5).

Also shown on Figure 2-2 is Californium - 252 (Cf^{252}) which produces neutrons from spontaneous fissions. It has a yield up to 10^{11} n/sec per curie of activity and all the advantage of other radioactive isotopes but requires more stringent shielding requirements (B-5).

SOURCE	REACTION	HALF-LIFE	AVERAGE NEUTRON ENERGY (MeV)	NEUTRON YIELD (n/sec-g)	GAMMA DOSE (rads/hr at 1 m)
$^{124}\text{Sb-Be}$	(γ, n)	60 days	0.024	2.7×10^9	4.5×10^4
$^{210}\text{Po-Be}$	(α, n)	138 days	4.3	1.28×10^{10}	2
$^{238}\text{Pu-Be}$	(α, n)	89 years	4	4.7×10^7	0.4
$^{241}\text{Am-Be}$	(α, n)	458 years	4	1×10^7	2.5
$^{241}\text{Am-}^{242}\text{-Cm-Be}$	(α, n)	163 days	4	1.2×10^9 (80% Am, 20% Cm)	Low
$^{242}\text{Cm-Be}$	(α, n)	163 days	4	1.46×10^{10}	0.3
$^{244}\text{Cm-Be}$	(α, n)	18.1 years	4	2.4×10^8	0.2
^{252}Cf	Spontaneous fission	2.65 years	2.3	3×10^{12}	2.9

Figure 2-2 Some Radioactive Sources for

Neutron Radiography (B-2)

Cf²⁵² has only recently been used as neutron source for neutron radiology. It was first used in a portable neutron camera developed by Battelle-Northwest for the AEC. The camera (NC-1) weighed 400 pounds, and was powered by a 268 millicurie source yielding 6.2×10^8 n/sec (B-1).

Since then Gamma Industries has produced a portable neutron camera for commercial use, it is 40 inches high, 33 inches in diameter, and has a total weight of less than 1000 pounds. The neutron source 322 millicuries (maximum allowable is 535 millicuries or 602 curies) yielding 1.38×10^9 n/sec (B-1). The only drawback is the large amount of shielding and moderating material required.

The third source of neutrons is the accelerator sources, accelerators produce neutrons by bombarding various targets with protons (p) or deuterons (d). The targets are light atoms with ²H, ⁹Be, or ⁷Li becoming very popular due to their favorable economics (B-5).

Accelerators are popular because they are favorable in terms of licensing, transportability and cost. Yields vary, but using sealed neutron tubes a typical yield of 10^{11} n/sec is possible. The leaders in the accelerator

field are "High Voltage Engineering" which used existing Van De Graff Accelerators to get thermal neutron yields of 1.2×10^6 n/cm²-sec, "Accelerators, Inc." which uses a Cockroft-Walton Accelerator yielding 1×10^9 thermal n/cm²-sec. "Accelerators, Inc." also has a device which attaches to X-ray machines they manufacture that produces a weak neutron beam, via a (γ ,N) reaction (W-4). However, the intensity of the beam is extremely low and not really suitable for neutron radiography.

2.2.2 COLLIMATION

Due to the moderator material surrounding the neutron source the thermal neutrons must be taken as originating from the moderator surface-a finite sized source of neutrons emitted isotropically from the surface. To handle this problem, the neutrons must be collimated either before striking the object or before reacting with the detector. Three types of collimators have been used for neutron radiography: 1) the simple straight parallel collimator 2) the Soller slit approach, and 3) the divergent beam collimator (B-2). Sketches of these various types of collimators are shown in Figures 2-3a, 2-3b, and 2-3c respectively. The important factors concerning all these collimators are the size of the entrance opening - D (diameter)

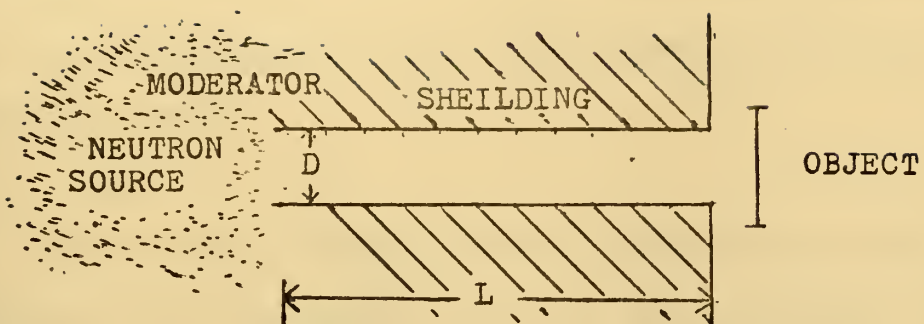


Figure 2-3a. Straight Parallel Collimator

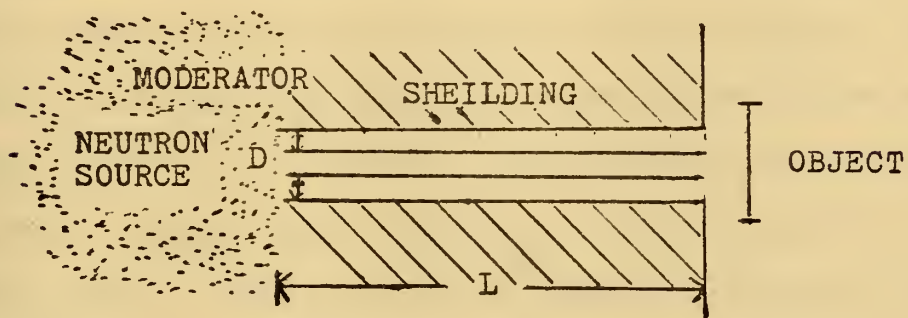


Figure 2-3b. Slit or Multichannel Collimator

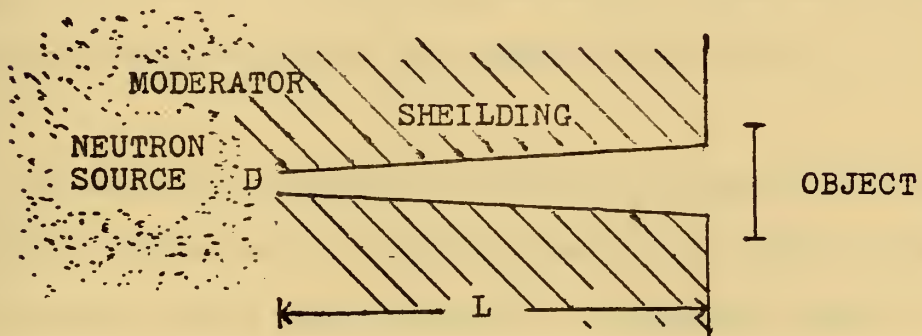


Figure 2-3c. Divergent Beam Collimator

and the length of the collimator - L , both of which define the angular divergence of the collimated beam and determine the neutron intensity at the radiographic end of the collimator (B-6).

For the usual thermal neutron situation in which the entrance of the collimator looks at an essentially isotropic neutron (thermal) flux within a moderator, D is analogous to the focal spot size of an X-ray tube and L is the same as the X-ray target to film distance. These factors determine the geometric unsharpness of the radiographs produced. In common X-radiographic situations, geometric unsharpness is about 0.1 mm for objects up to 2-3 cm thick. Values of L/D as high as 500 are in common use for X-radiography (H-3). Of course, the final radiographic unsharpness in any situation results from a combination of factors including geometry, film and intensifying screens, movement, and scattering (H-3).

In the choice between collimator systems, the simple straight collimator is usually limited in terms of useful radiographic area. The divergent collimator permits examination of a large area, but presents problems in image distortion at the edge of the field. The Soller slit or multi-channel collimator permits a large area and parallel

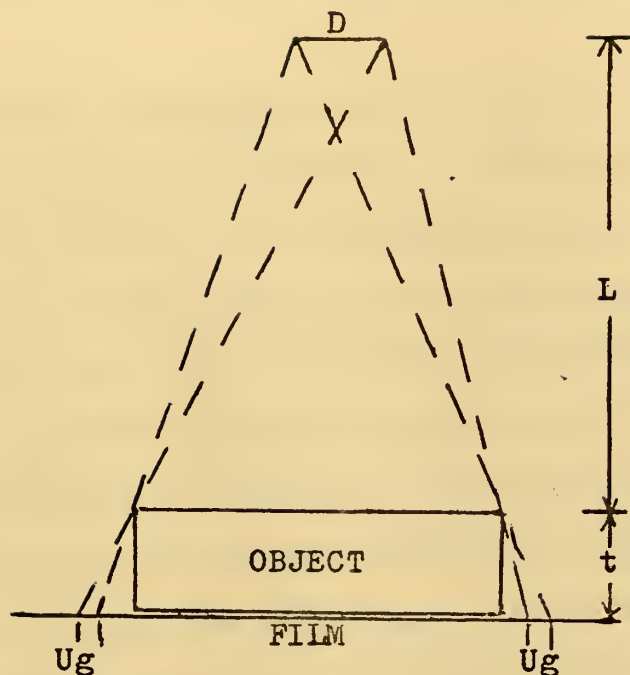


Figure 2-4. Geometric Unsharpness

where: U_g is the geometric unsharpness
 t is the object thickness
 D and L are previously defined

$$U_g = Dt / (L+t) \quad (2.8)$$

beam at the same time. However, this method can present non-uniformity problems and requires a large uniform neutron flux at the input end. All three approaches have some merit; however, the divergent collimator is most widely used (W-3).

2.2.3 IMAGE DETECTION TECHNIQUES

Photographic techniques are for the most part used for neutron radiographic detection. Typically, these methods involve X-ray films so used that they are exposed directly to the neutron beam or to a radioactive image - carrying foil in an auto-radiographic technique. These two methods are known as direct exposure and transfer methods respectively. A third and more sophisticated method involves using a neutron sensitive image tube and a TV camera to record the radiograph. This last method, real time method, along with the other two methods are shown in Figure 2-5 (G-2). In the direct exposure situation, film can be used alone but conversion or intensifying screens greatly increase the response (E-2).

For the direct exposure method, many prompt neutron - gamma (N, γ) reaction materials can be used as converter foils to enhance the neutron response of the film. Materials that yield short half-life radioactivities can also be used directly with the film because the activities decay and stimulate the film during and shortly after neutron exposure. Materials that undergo prompt neutron - alpha (N, α) reactions have also been used (S-1).

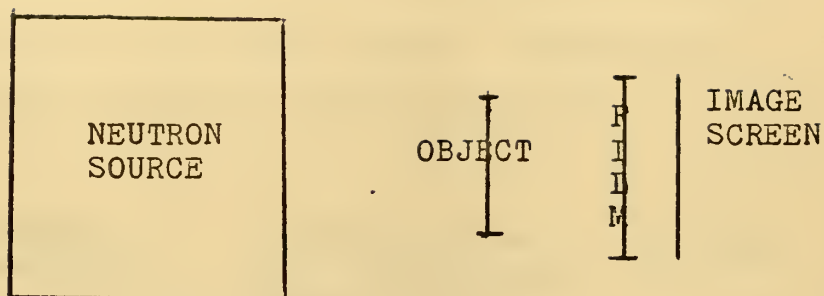


Figure 2-5a. Direct Method

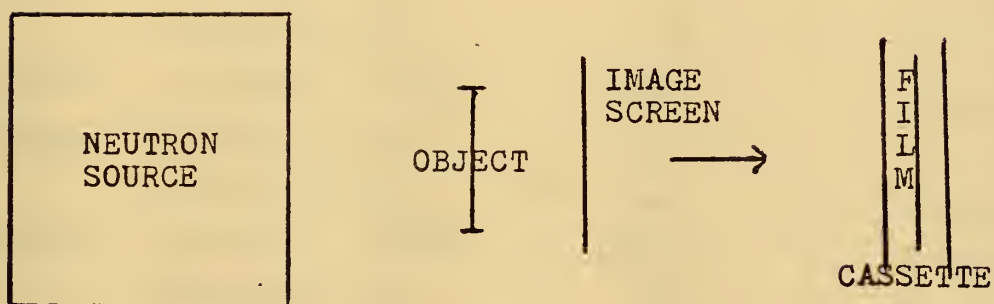


Figure 2-5b. Transfer Method

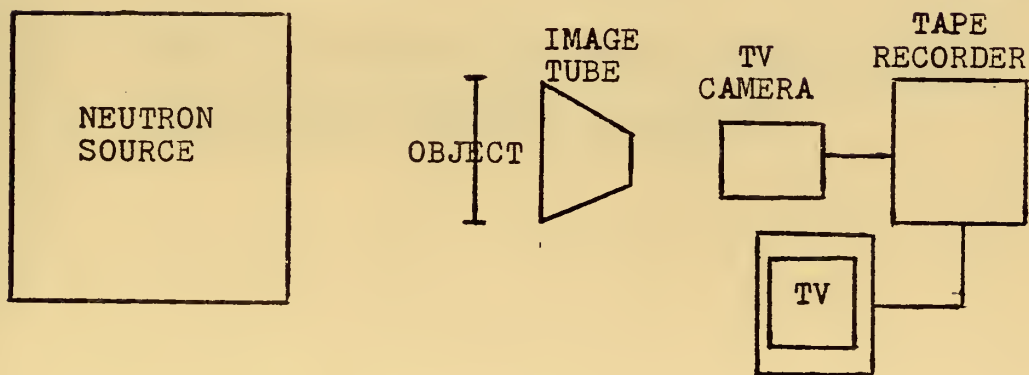


Figure 2-5c. Real Time Method

Figure 2-6 summarizes many of the properties of useful converter materials for either direct exposure or transfer method thermal neutron radiography (B-2).

Material	Useful reactions	Cross section for thermal neutrons (barns)	Half-life
Lithium	${}^6\text{Li}(n, \alpha){}^3\text{H}$	910	Prompt
Boron	${}^{10}\text{B}(n, \alpha){}^7\text{Li}$	3830	Prompt
Rhodium	${}^{103}\text{Rh}(n){}^{104\text{m}}\text{Rh}$	11	4.5 min
	${}^{103}\text{Rh}(n){}^{104}\text{Rh}$	139	42 sec
Silver	${}^{107}\text{Ag}(n){}^{108}\text{Ag}$	35	2.3 min
	${}^{109}\text{Ag}(n){}^{110}\text{Ag}$	91	24 sec
Cadmium	${}^{113}\text{Cd}(n, \gamma){}^{114}\text{Cd}$	20000	Prompt
Indium	${}^{115}\text{In}(n){}^{116\text{m}}\text{In}$	157	54 min
	${}^{115}\text{In}(n){}^{116}\text{In}$	42	14 sec
Samarium	${}^{149}\text{Sm}(n, \gamma){}^{150}\text{Sm}$	41000	Prompt
	${}^{152}\text{Sm}(n){}^{153}\text{Sm}$	210	47 hours
Gadolinium	${}^{155}\text{Gd}(n, \gamma){}^{156}\text{Gd}$	61000	Prompt
	${}^{157}\text{Gd}(n, \gamma){}^{158}\text{Gd}$	254000	Prompt
Dysprosium	${}^{164}\text{Dy}(n){}^{165\text{m}}\text{Dy}$	2200	1.25 min
	${}^{164}\text{Dy}(n){}^{165}\text{Dy}$	800	140 min
Gold	${}^{197}\text{Au}(n){}^{198}\text{Au}$	98.8	2.7 days

Fig. 2-6 Properties of Some Thermal Neutron Radiography Detection Converters

The (N, α) materials can be used directly with film or alternatively, the α emitter is intermixed with a phosphor; the resulting neutron scintillator is then used with a light-sensitive film. Because the range of the α particle is very short, the effective absorption of a loaded emulsion, is relatively low. However, if the α emitter is mixed with a phosphor powder, the light stimulated from phosphor grains adjacent to the α emitter material provides a very fast neutron detection method.

Increased sensitivity to neutrons can also be gained by utilizing two converter foils, one on each side of a double emulsion film, as is the normal case in X-radiography. Double gadolinium screens (25u or less on the source side and 50u on the backside of the film) increase the speed about 50% over that of a single gadolinium back screen. These double screen methods, with fast or medium speed films, offer a useful alternative detector for low neutron intensity situations. Although resolution properties are degraded over a single gadolinium metal screen technique, these double screen methods still display a resolution potential of 25u or better, have good informity, and present an improvement over single metal screens in relative N- γ response (B-7).

In comparing the two widely used general methods, the direct exposure method offers high speed, the best observed spatial resolution, and an immediate result because the film can be processed as soon as the exposure is completed. Transfer methods, on the other hand, offer insensitivity to γ radiation, which dictates their use in most inspections of radioactive material. A fringe benefit is improved neutron radiographic contrast, because there is no detectable background on the resultant film due to the (N, γ) interactions or γ background in the neutron beams.

Other detection methods have been used for thermal neutron radiography. One, a dynamic motion response system (real time method) has proved useful in a number of special areas. Several approaches to a dynamic, television viewing system have been studied and used. The simplest approach is to observe a neutron scintillator directly with a sensitive television camera and display useful neutron images. This method results in fair resolution, but requires a rather large neutron flux. The main advantage and principle property of the neutron television approach is its ability to detect motion. For conventional NDT problems, this system is very limited and will not be discussed beyond this point.

CHAPTER 3

TEST FACILITY AND PROCEDURE

3.1 MIT RESEARCH REACTOR

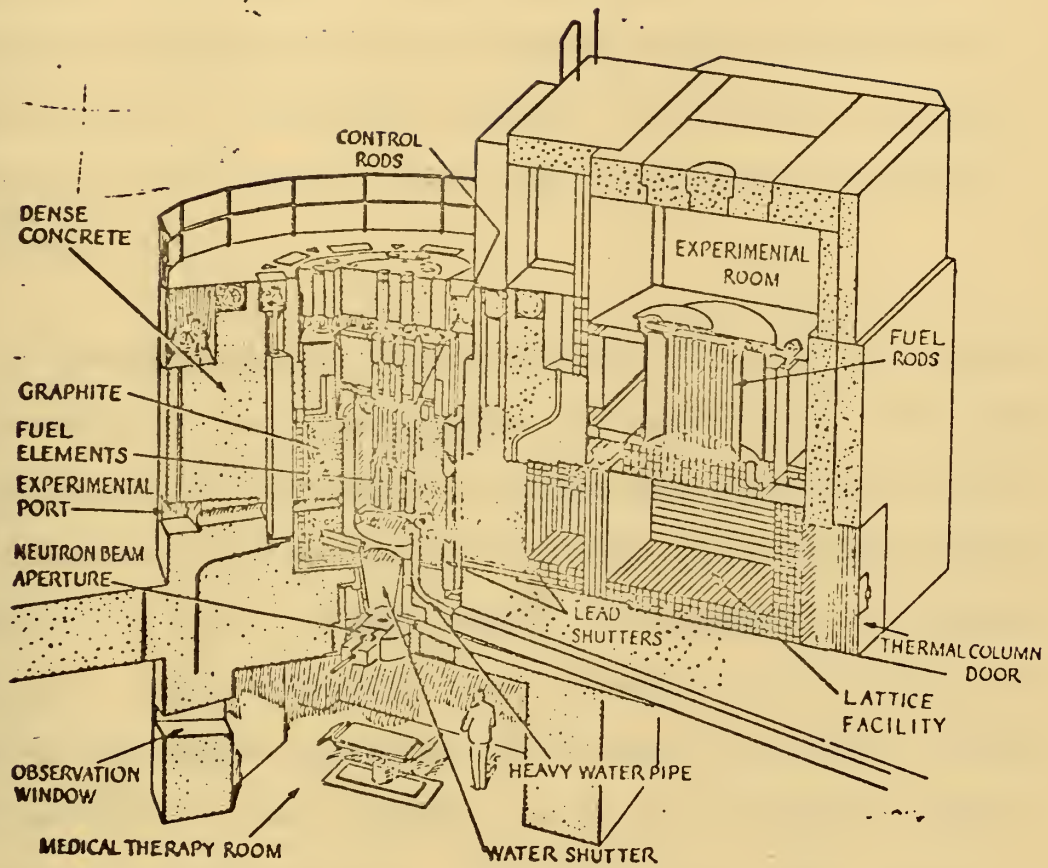
Completed in 1958 the M.I.T. Research Reactor (MITR), is one of the finest university research reactors in the world. Fueled with enriched uranium and cooled and moderated by heavy water, the 5 Mw Reactor provides first hand experience in the design; performance, and operation of nuclear reactors and serves as a source of radiations for use in laboratory instruction on radiation detection and measurement methods. A variety of research projects also make use of the intense sources of neutrons and gamma rays produced by the reactor (M-1). One such project has been the establishment of a neutron radiographic facility at the reactor. As a result of the work of several reactor and operations personnel, K. Collins, and J. Knotts, and a graduate student E. Westberg, the MITR now offers radiographic services as well as other irradiation services. A detailed description of the development and testing of the radiographic facility is given in Westberg's thesis, Neutron Radiography at the M.I.T. Research Reactor (W-2).

A complete description of the radiographic facility and procedures used at MITR is given in the following sections.

3.2 RADIOGRAPHIC FACILITIES

The Neutron Radiographic facility utilizes the beam port which leads into the Medical Therapy Room directly beneath the reactor core as shown in Figure 3-1. The room itself is constructed of thick reinforced concrete for both structural and shielding purposes, and access is accomplished through a motor driven shielding door. Controls and monitoring instruments are located on panels both inside and outside the room, however only the exterior panel is used while performing radiographic work.

The beam port itself is equipped with three shutters which when closed, allow operators and technicians to work in the Medical Therapy Room safely. The first of the three shutters is a water shutter consisting of a drainable tank containing light water with a helium cover. This tank can be completely drained or filled within two minutes time. The water level in the tank can also be varied to control the intensity of the neutron beam. The remaining shutters are 9 1/8 inch lead and 1/4 inch boron



CUT-AWAY VIEW OF THE MIT RESEARCH REACTOR

Figure 3-1 MIT Research Reactor

plates which can be opened pneumatically and closed either pneumatically or manually. The purpose of the plate shutters is to shield against gamma and neutron radiation. The controls for all three shutters are located on the previously mentioned panel outside the Medical Room. A schematic showing the shutters in relationship to the reactor core and Medical Room is shown in Figure 3-2.

A thermal neutron flux of about 10^{10} n/cm²-sec leaves the beam port when the shutters are open (M-2). The thermalization or moderation of the neutron beam occurs when the neutrons leaving the reactor core pass through approximately 1.5 feet of heavy water. The neutrons also pass through a foot of bismuth which shields out a large portion of the gamma radiation in the beam, yet still allows the neutrons to pass through due to its relatively small absorption cross section. Both the heavy water and the bismuth filter are shown in Figure 3-2.

It should be pointed out at this time that the neutron beam entering the medical room has been proven to be highly thermalized (M-2). Experimental proof is given in Chapter 3 of Westberg's thesis (W-2).

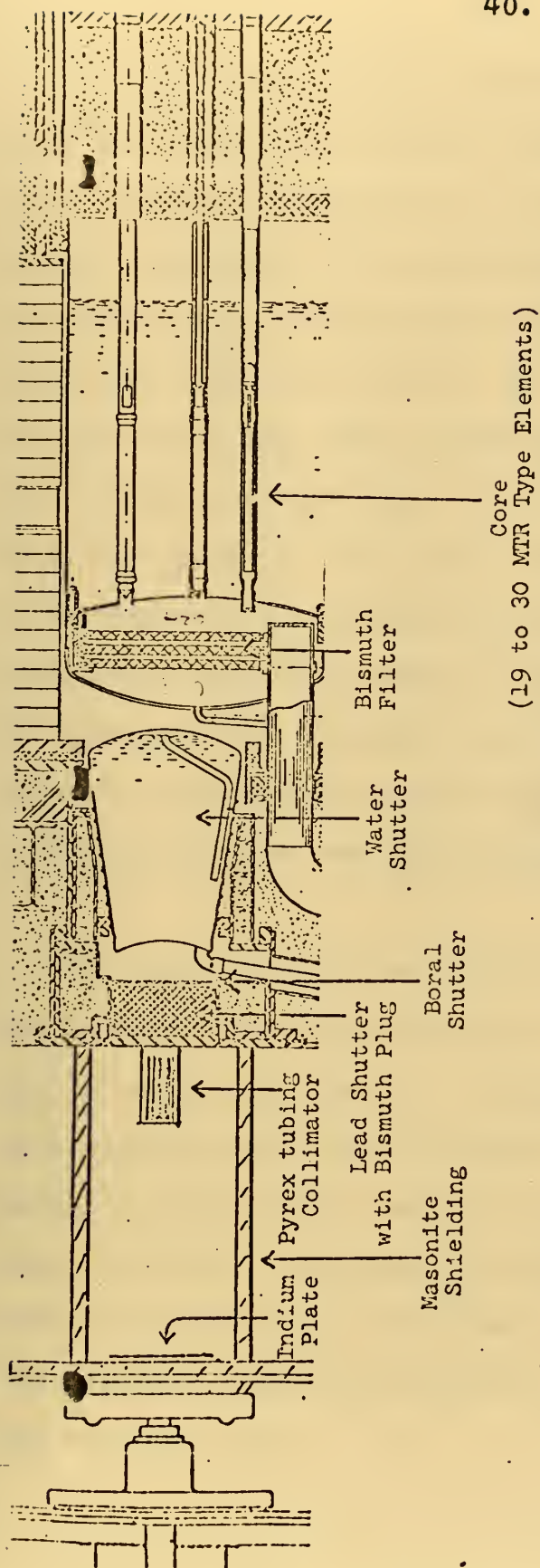


Figure 3-2 Medical Room and Shutter Arrangement

The collimator used at MITR is rather unique, both from the design and the cost point of view. The collimator consists primarily of a 6 inch ID aluminum can 11 inches long filled with pyrex tubes. A schematic of the collimator and radiographic chamber is shown in Figure 3-3. The glass tubes are 5mm ID, 7mm OD, and 9.6 inches long. The fact that the pyrex contains a sufficient amount of boron limits passage only to those neutrons traveling down the center of the tubes (M-2). As a result, only those neutrons that passed within ± 1.2 degrees of the collimator axis are used for radiography (W-2). In order to eliminate any possible "honey combed" imaging, the exposure plates are placed about three collimator lengths (28 inches) below the collimator exit.

In order to minimize irradiation of material within the medical room from both gamma rays and neutrons, shielding is used extensively. The gamma radiation and neutrons that escape around the collimator are shielded by lead and masonite split rings that fit around the outer surface of the collimator. In order to minimize irradiation by scattered neutrons, boral sheets have been placed over the masonite frame surrounding the collimator and forming the exposure area.

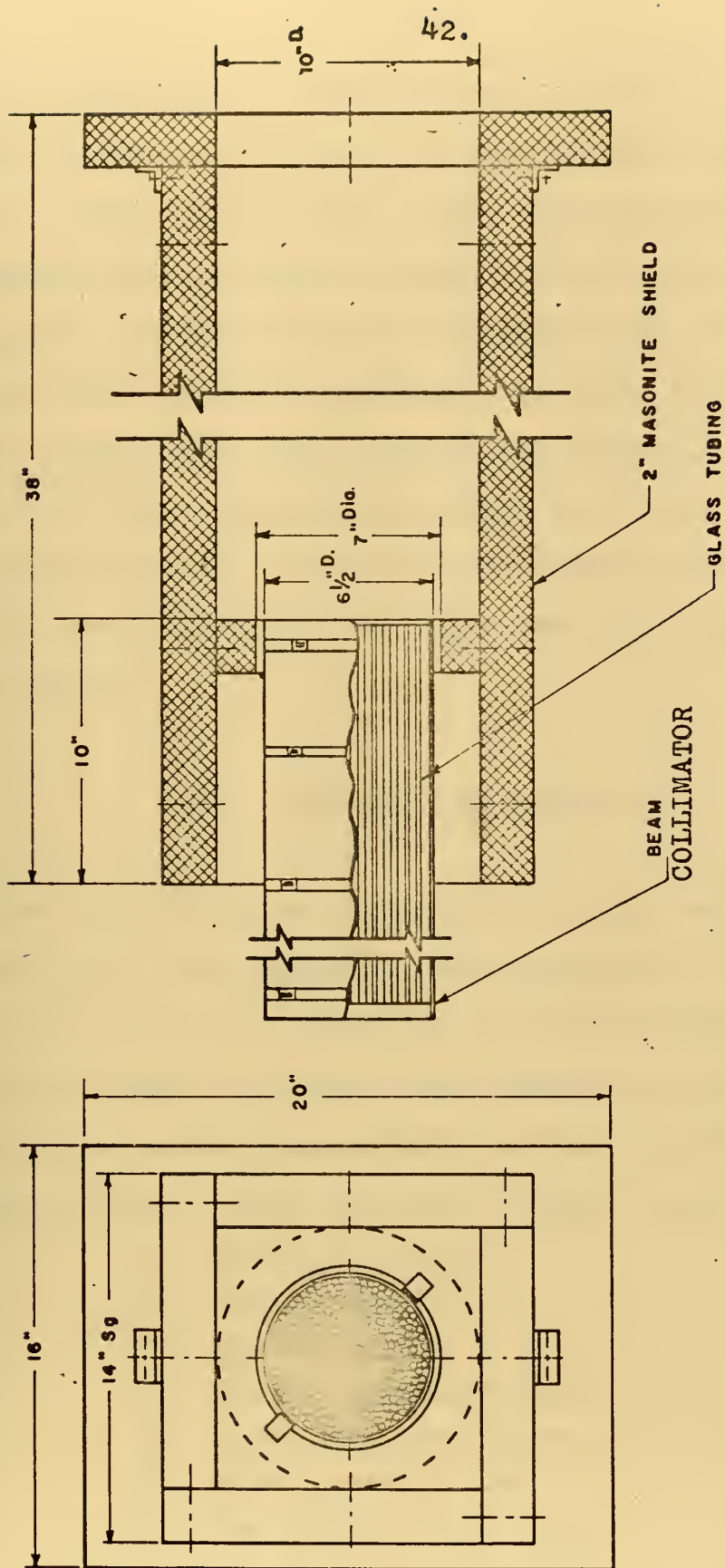


Figure 3-3 MITR Neutron Collimator

The object to be radiographed is placed in the exposure area and on top of either indium or dysprosium plate. The plate is then irradiated and an image is then irradiated and an image is then formed in the foil on the plate due to attenuation by the object and the activation of the foil. After irradiation the plate is removed from the exposure area, and film is then exposed to the activated plate and a radiographic image is formed. It must be pointed out at this time that correct radiation protection procedures must be taken when the activated plates are handled.

3.3 EXPOSURE TECHNIQUES

The critical area of producing a good neutron radiograph lies in the exposure techniques used. The reason for this is not the complexity of the procedures and techniques used, but the large number of variables associated with neutron radiography and the transfer technique in particular. These variables include the following:

- 1) Film properties
- 2) Foil properties
- 3) Neutron flux
- 4) Foil irradiation time
- 5) Transient decay time
- 6) Film exposure time
- 7) The object being tested

Ideally a neutron flux should be thermal, unidirectional, uniform and as large as possible. Since the MITR is being used for the experiments covered in this thesis, the flux level is set, although it can be reduced. As was previously mentioned the neutron beam is thermalized and well collimated when it enters the exposure area. However experiments have shown it to be not entirely uniform, and that the lack of uniformity is neglectable for all practice purposes (W-2)..

Another variable which is uncontrollable is the physical characteristics of the object being examined. Since the samples in the case of this thesis are steel weldments which may have defects due to nonfusion, voids, cracks, inclusions, and several other causes; it is then the relative attenuation between the steel and defect that is important and generally uncontrollable. The geometry of the object also affects the quality of the radiograph. As was mentioned in Chapter 2, the thickness of the object affects both the geometric unsharpness of the radiograph and the attenuation of the incident radiation. The geometry of the object can also limit the ability of the transfer foil to be placed as close to the object as possible which also affects the contrast of the radiograph (K-3).

The film properties are important since it is actually the film on which the radiographic images are reproduced. The film graininess, speed, development procedures and general quality all affect the production of a good radiograph. Graininess affects the contrast of the radiograph: the finer the grain the greater the contrast. In general all films exhibit graininess to a greater or lesser degree, and the slower films have much less graininess or finer grain than the faster films (K-3).

The resultant contrast or density of the radiograph is important in that the greater the contrast or density differences, the more definitely various details stand out, and the finer the detail that can be seen. Density is described by Van der Platts as: "When the film emulsion is exposed to radiation, the particles of silver bromide absorb energy and so become capable of photographic development. This means that when the film is placed in a reducing agent the energized grains of silver bromide are reduced to free metallic silver deposits, the density of which will be greatest at the parts which have absorbed the greatest amounts of energy. Silver is naturally opaque and when finely distributed gives the impression of being black. The transparency of the film will be least, the opacity the greatest, in those parts which contain the densest deposit of silver, that is, those which received

the greatest exposure" (K-3).

In order to assign a comparable value to density the following equation is used (L-2).

$$D = \log 1/T \quad (3.1)$$

where: D is the density

T is transmission

Transmission is defined as the ratio of the amount of light that gets through any area to the total light striking that area. In this case, the area is the film exposed to the transfer foil.

In order to demonstrate and to understand the relationship between density and exposure, "characteristic curves" are developed for different types of film. Characteristic curves are plots of density versus the log of exposure. A typical characteristic curve is shown in figure 3-4 (K-3). These curves actually describe the photographic characteristics of the film for a given development. It should be noted that curve A-B-C is for a film with the capability of exhibiting unlimited density with sufficient exposure, and curve A'-B'-C'-D' has a maximum density capability of 3.0. The important part of the curve is the so called "straight line" portion. The section B-C or B'-C' is the straight line portion of the

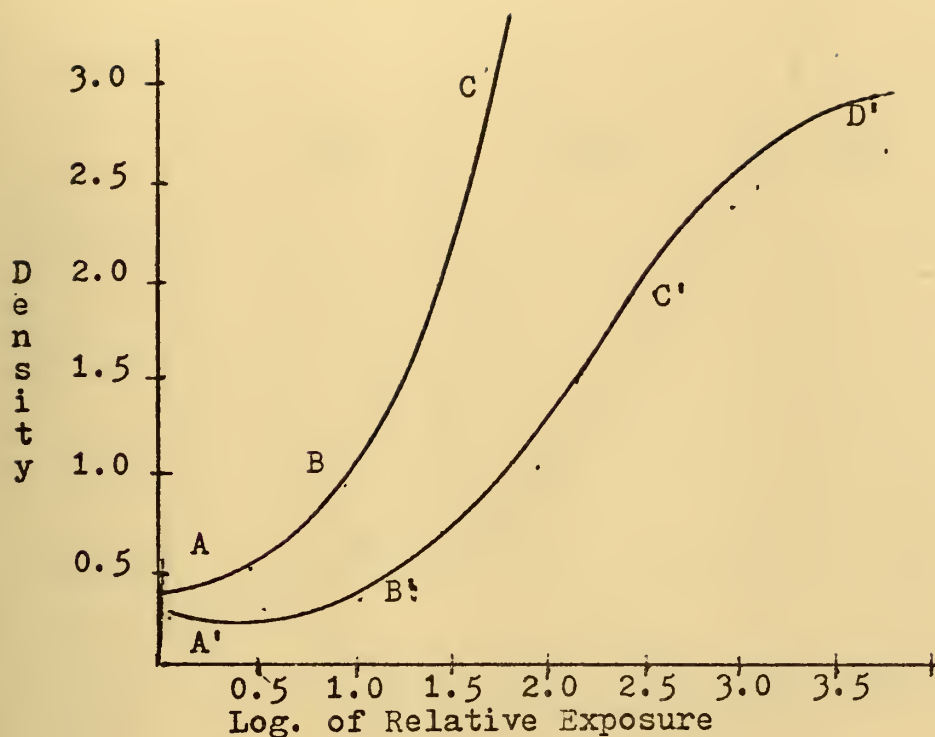


Figure 3-4. A Typical Characteristic Curve

curve; the density in the film increases proportionally with the log of the exposure. The slope of this straight - line portion of the curve is said to be film contrast; the steeper the slope, the higher the contrast.

As was mentioned in the above paragraph, the characteristic curve varies with development time, and as a result contrast varies. Figure 3-5 shows the change for various development times (L-2). As the development time increases, the contrast of the film of the slope of the curve increases. The two minute developing time yields the curve with the

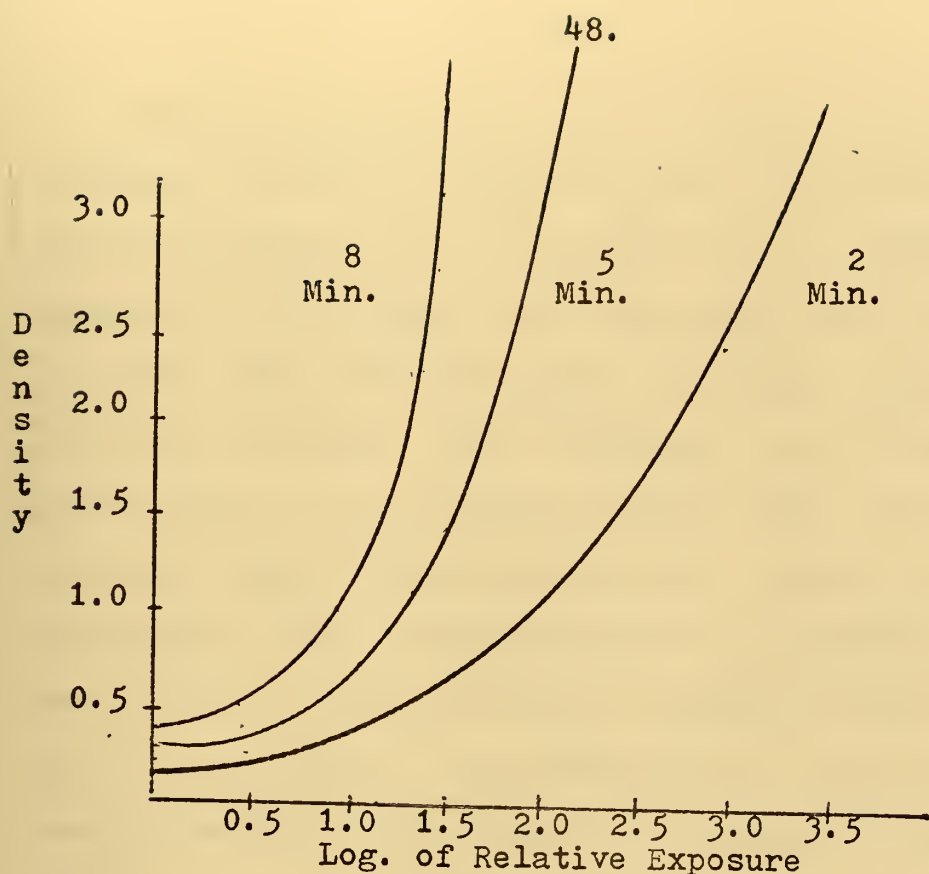


Figure 3-5. Characteristic Curves: Development Times

lowest slope and therefore has the lowest film contrast, the five minute film is intermediate and the eight minute development time is the one with the highest contrast. It should be pointed out, although increasing development time does increase the contrast, there is a point at which an increase in development time will cause an increase in base fog, or developer fog which in turn will reduce the inherent film contrast. As a result, an optimum range of development time is formed; this information is available from the film manufacturer.

Characteristic curves used in neutron radiography are somewhat different than those used in X-radiography or gamma radiography, in the latter case the exposure is defined as the exposure the film sees after the object has been irradiated with gamma or X-rays. Similarly for neutron radiography, the irradiation time is that exposure seen by the detecting medium after the neutron beam has passed through the object. However, for neutron radiography the detecting medium is an activation foil not the film. Then the film is exposed to the radioactive foil. As a result, the characteristic curves for film used in neutron radiography are a function of the detection foil used. The effect of the foils on a characteristic curve for a particular film is to move it left or right along the abscissa and to limit the density of the film.

A table of the properties of thermal neutron detection converters is given in Figure 2-6 of Chapter 2. As can be seen there are several suitable materials which can be used as transfer foils. However, for the purpose of this thesis only indium and dysprosium foils were used with effective half-lives of 54 minutes and 139.2 minutes respectively. In addition to the type of converter foil used, the thickness of the foil also affects the film

density. A study of foil thickness versus film density was done at Argonne National Laboratory and a concise summary is given in Berger's text (B-1). Characteristic curves for dysprosium foil and Kodak type AA X-ray film were developed by Bruce Momsen for the Nuclear Reactor Operations course (22.39) in the spring of 1972. The curve he developed is shown in Figure 3-6 (M-3). *

However a characteristic curve for indium foil and type AA X-ray film was not developed. In order to get a feel for the contrast capabilities of the indium foil, a characteristic curve for indium foil was developed from the back files of neutron radiographs presently stored in the reactor operations office. This curve is also shown in Figure 3-6. In order to verify these curves and attempt to improve their accuracy, additional points were plotted as the experiments for this thesis progressed. The final curves are given in the experimental results in Chapter 6

In order to understand the characteristic curves one should understand the theory of the transfer technique.

* Note: The relative exposure used for these curves is explained in detail on page 57 of this chapter.

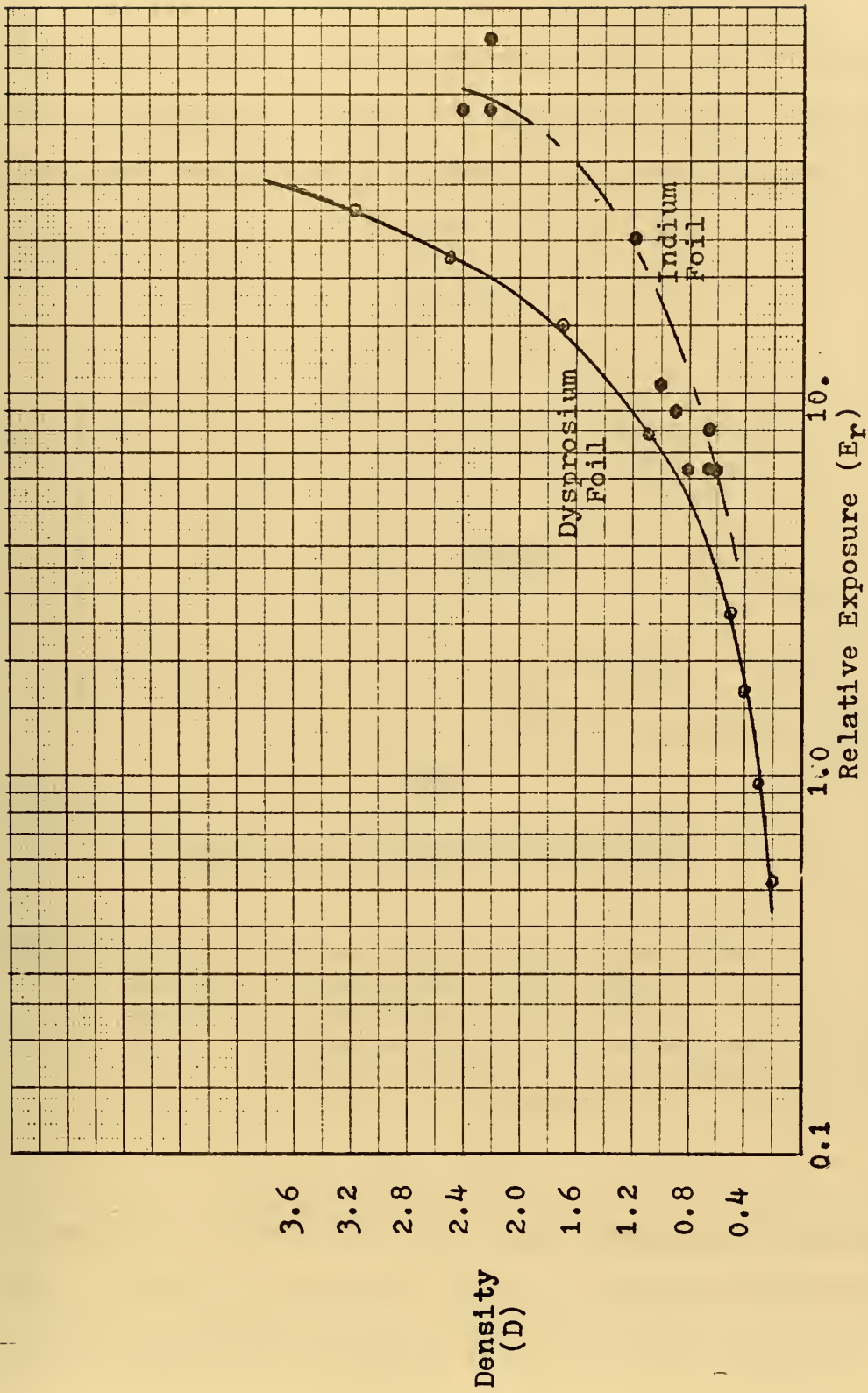


Figure 3-6. Characteristic Curves for Indium and Dysprosium Transfer Foils
Extrapolated

The transfer technique used in neutron radiography is identical to activation analysis except that the activity in radiography is detected by exposing film. The transfer technique can be shown diagrammatically as in Figure 3-7.

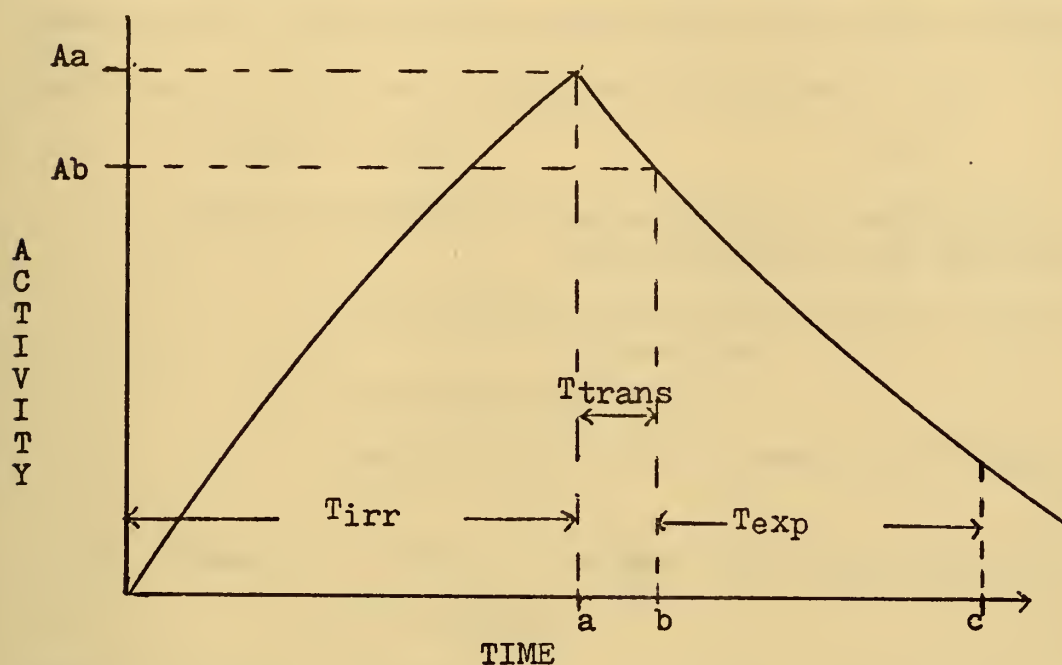


Figure 3-7. Activation Analysis

where: T_{irr} is the foil irradiation time
 T_{trans} is transient decay time
 T_{exp} is the film exposure time
 A_a is the activity at the end of irradiation
 A_b is the activity at the beginning of film exposure

It should be noted that the three remaining variables T_{irr} , T_{trans} , and T_{exp} are most readily controlled variables of the seven originally mentioned earlier in this chapter.

The dose during exposure is the area under the curve between b. and c. However the film does not receive all the irradiation as the foil decays, and not all of that irradiation causes film darkening. Therefore for constant transfer foil properties ie half-life and cross section, the film exposure can be written as follows: (M-3)

$$E \text{ film} = CD, \quad (3.2)$$

where: E film is the exposure of radiation
darkening the film emulsion,

C= constant containing activity and foil
properties,

D= normalized dose,

$$D = (1 - e^{-\lambda T_{irr}}) (e^{-\lambda T_{trans}}) (1 - e^{-\lambda T_{exp}}), \quad (3.3)$$

where: λ = decay constant for a particular foil,

$$\lambda = .693/T_{1/2} \quad \text{or} \quad (3.4)$$

A more detailed development of equation 3.2 is given in Chapter 2 of Westberg's thesis (W-2).

In order to eliminate the constant and to simplify the results, a reference exposure (E_o) is defined:

$$E_o = C D_o \quad (3.5)$$

$$\text{where: } D_o = \frac{1}{1000} = .001,$$

$$\text{therefore } E_o = .001C \quad (3.6)$$

From equations 3.2 and 3.6 a relative exposure (ER) can be defined as follows:

$$ER = E_{\text{film}}/E_0,$$

$$ER = CD/C(.001)$$

$$ER = 1000D \quad (3.7)$$

$$ER = (1000) (1 - e^{-\lambda T_{\text{irr}}}) (e^{-\lambda T_{\text{trans}}}) (1 - e^{-\lambda T_{\text{exp}}}) \quad (3.8)$$

$$(M-3)$$

Equation 3.8 was used to calculate the relative exposure in Figure 3.6. The equation can also be used to get a good radiograph. For a good radiograph it is desirable to have the highest contrast possible or be in the area of the characteristic curve where the slope is the greatest. So to get a good radiograph one would enter the characteristic curve for the film and transfer foil being used and pick off the relative exposure (ER) in the area of highest contrast. With ER now known and at the MITR, T_{trans} is set at about 10 minutes for safety reasons, it is possible to use equation 3.8 and Figure 3-8 or 3-9 to determine T_{irr} and T_{exp} that will give the desired contrast.

One is usually not irradiating a bare foil through an object. It is then desirable to correct the relative exposure for attenuation through the object. From the radiation principles shown in Chapter 2 the following relationship can be developed:

Dysprosium

 $(\lambda = .004978 \text{ min}^{-1})$

$t(\text{min})$	$e^{-\lambda t}$	$1-e^{-\lambda t}$	$t(\text{min})$	$e^{-\lambda t}$	$1-e^{-\lambda t}$
.5	.9975	.0025	360	.166	.834
1.0	.995	.005	420	.123	.877
1.5	.993	.007	480	.0917	.9083
2.0	.990	.0098	540	.068	.932
2.5	.988	.012	600	.050	.950
3.0	.985	.0146	660	.0374	.9626
3.5	.983	.017	720	.0278	.9722
4.0	.980	.020	780	.0206	.9794
4.5	.978	.022	840	.015	.985
5.0	.975	.025	900	.0113	.9887
10	.951	.049			
15	.928	.072			
20	.905	.095			
25	.883	.117			
30	.861	.139			
35	.840	.160			
40	.819	.181			
45	.799	.201			
50	.780	.220			
55	.760	.240			
60	.742	.258			
90	.639	.361			
120	.550	.450			
150	.475	.525			
180	.408	.592			
210	.351	.649			
240	.302	.698			
270	.261	.739			
300	.225	.775			
330	.193	.807			

Figure 3-8
Dysprosium Decay Functions

Indium		$(\lambda = .01280 \text{ min}^{-1})$	
$t(\text{min})$	$e^{-\lambda t}$	$1 - e^{-\lambda t}$	
1	.987	.013	
5	.938	.062	
10	.879	.121	
15	.825	.175	
20	.774	.226	
25	.726	.274	
30	.681	.319	
35	.639	.361	
40	.599	.401	
45	.562	.438	
50	.527	.473	
55	.495	.505	
60	.464	.536	
90	.316	.684	
120	.215	.785	
150	.147	.853	
180	.0999	.900	
210	.068	.932	
240	.0463	.954	
270	.0316	.968	
300	.0214	.979	
360	.0099	.991	

Figure 3-9
Indium Decay Functions

$$ER' = ER e^{-\mu x}, \quad (3.9)$$

where: ER' is the exposure through the object
 ER is the exposure of the unperturbated beam,
 μ is the linear attenuation coefficient of the object,
 x is the object thickness,

As was done previously, one now picks ER' off the characteristic curves and knowing the properties of the test sample one can calculate ER from equation 3.9. Again using equation 3.8 and Figure 3-8 and 3-9 T_{irr} and T_{exp} can be determined.

In summation: of the seven original variables mentioned, the important or controllable variables are the film, transfer foil irradiation time, and film exposure time. The film and transfer foil must be selected for speed, contrast ability and price; the selection of the film and foil set of the characteristic curve and the exposure and irradiation times must be used to obtain the desired contrast. Though the remaining three variables ^f influence the control of the radiographic process, for most cases they are either constant or uncontrollable as in the case of the object of interest.

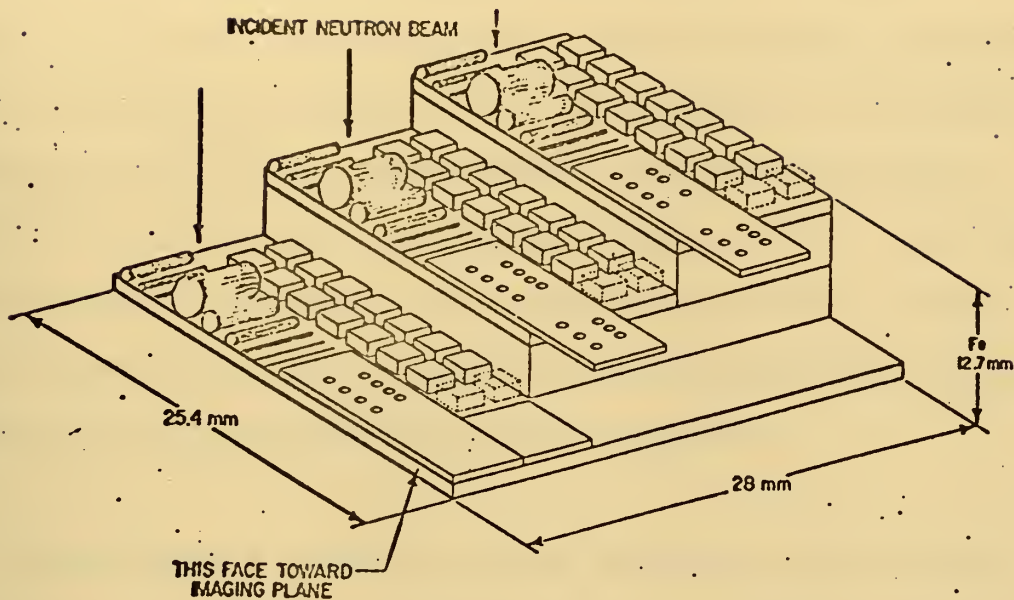
A more detailed and exact procedural description of how the radiographs were taken for this thesis is given in the experimental procedure in Chapter 5.

3.4 QUALITY CONTROL

Neutron radiography or any form of radiography is used to check on the quality of a process of material i.e. "Quality Assurance" or "Quality Control". It is also necessary to ensure the quality of the radiograph, that is, to obtain evidence on a radiograph that the technique used was satisfactory. To do this a standard test device is radiographed at the same time the test sample is radiographed. Current industrial practice is to use a penetrometer. This device used by Gamma and X-radiographers shows the sensitivity of the radiograph. A penetrometer was also used in the neutron radiographs in this thesis for comparison against X and Gamma radiographs. Another device is the "Visual Reading Image Quality Indicator" or VISQI which is specifically designed for neutron radiography.

The Visual Reading Image Quality Indicator or VISQI is shown in figure 3-10 is a composition of different materials, holes and various thicknesses on three different levels.

59.
VISQI Construction



		6 PLASTIC WIRES						3 Cd WIRES		
		01	02	035	075	150	250	02	050	075
HOLES IN OVERHANG	HOLES (0.50 mm DIA.) IN Cd (0.50 mm THICK)									
2nd & 3rd STEPS ONLY	SEPARATION → 0.5 → 0.25									
Pb 0.50 mm 1st STEP ONLY	1 Fe 0.63	2 Cd 0.25	3 In 2.0	4 Cd 0.10	5 Gd 0.012	6 Cd 0.05	7 In 1.0	8 CH ₂ 1.50		
	16 Fe 1.27	15 Pb 0.25	14 Pb 0.50	13 Pb 1.50	12 CH ₂ 0.25	11 CH ₂ 0.75	10 Dy 0.12	9 In 0.50		
ALL DIMENSIONS IN mm										

Figure 3-10 The VISQI Neutron Radiographic
Penetrameter

As seen in several radiographs in subsequent chapters, the VISQI gives a good indication of radiographic quality. A more detailed description and the procedures for proper uses are found in the manufacturers instruction manual on file in the Reactor Operations Office (P-2). The VISQI was not used extensively or exclusively for this thesis due to the desire to use current and convential industrial radiographic procedures as much as possible.

The standard quality control procedures were those established by the "American Society for Testing Materials" (ASTM). As a result a standard penetrameter was used to obtain evidence insuring satisfactory radiographic quality. It should be pointed out that penetrameters are not intended for judging discontinuity sizes or establishing acceptance limits, but to indicate the sensitivity of the radiograph. As a result of maintaining this standard, a good comparison of sensitivity between gamma, X-ray, and neutron radiographs can be made.

The standard penetrameter as specified by ASTM is of the same or similar material as the object and placed on top of the object as it is being radiographed. The thickness of the penetrameter is also specified to be a given percentage of the thickness of the test object. This

thickness is generally one or two percent and the two percent thick penetrameter being preferred (A-3). As an example suppose an object four inches thick were being radiographed. Then a two percent penetrameter, 80 mills thick would be used.

Holes bored through the penetrameter serve as the means for evaluating the radiograph. ASTM requires at least three holes, of 1T, 2T, and 4T diameters where T is the penetrameter thickness (A-3). A sketch of a standard penetrameter is shown below:

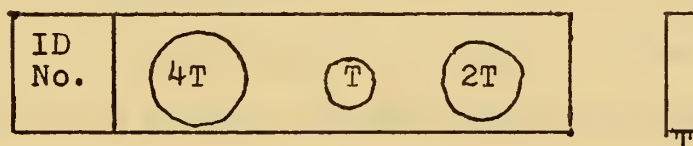


Figure 3-11

where: T is the penetrameter thickness

The length and width of the penetrameter are also specified by ASTM, but these dimensions vary somewhat with intended application.

Sensitivity is determined from the following equation (Y-1):

$$S = \frac{(\sqrt{2t} \quad (x)^{\frac{1}{2}}) \quad 50T}{t} \quad (3.10)$$

where:

S is the radiographic sensitivity in percent,
 T is the penetrameter thickness,
 X is the diameter of the smallest visible
 hole as a function of T (1,2, or 4),
 t is the object thickness.

For most applications radiographic specifications demand that a 2-2T hole be visible and for some extremely high quality work a 2- T hole must be visible (A-3). The first number in the previous notation indicates the percent thickness of the penetrameter and the second indicates the diameter of the hole that must be visible. Other specifications demand that a given sensitivity be maintained. In the earlier example where the object was 4 inches thick, seeing a 2-2T hole on a radiograph indicates a sensitivity of 3.97%. The U.S. Navy requires that for non-nuclear related objects a radiographic sensitivity of 2% be maintained (Y-1). This means that for the 4 inch thick example a 1-2T hole must be visible for non-nuclear acceptance and a 1-1T hole visible for nuclear acceptance.

3.5 SAFETY CONSIDERATIONS

Radiation is essentially undetectable to human senses. It can't be seen, heard, or felt until it's too

late. For this reason safety procedures must always be followed and safety apparatus always used and insured to be operating correctly.

Radiographers are trained to work with radiation and they must know the correct procedures in order to safely operate their X-radiation or gamma sources. They must also remember to post the correct warnings and barriers to insure that some unknowing, individual does not become exposed to radiation. Neutron radiography like gamma and X-radiation requires the same care and caution. However, using a neutron source, one must be familiar with the shielding and penetrating power of the neutrons, as well as the background gamma. To even further compound the problem some types of neutron radiography use transfer foils which decay by alpha and/or beta decay.

It is therefore essential that a radiographer working with a neutron source be aware of all types of radiation and their characteristics, and if the transfer foils have to be handled, he must be particularly careful not to receive a high radiation dose and to ensure that activated foils are carefully secured from accidentally exposing anyone or anything. A neutron radiographer must also be familiar with activation analysis theory and must use

caution when he irradiates an object that becomes highly activated.

Though it appears that neutron radiography requires such stringent safety and radiation requirements that it is industrially unfeasible, the majority of these safety considerations are already in use with conventional radiographic methods. It is felt that the potential of radiation hazards must be pointed out and that they are easily handled. Detailed information on safety requirements, doses and safety procedures can be found in "MIT Required Procedures For Radiation Protection" (M-4) or from the Radiation Protection Office in building NW-12.

CHAPTER 4

TEST SAMPLES

With the increased design requirements being placed on structures, new high strength materials have had to be developed to meet these requirements. One of the most widely used high strength materials is HY-80 steel. HY-80 is the government terminology for "High Yield Stress - 80,000 psi minimum". It is used extensively for ships, submarines, and pressure vessels, the commercial equivalent to HY-80 is ASTM A517-67 (contains less nickel) which is also used for pressure vessels, storage tanks, merchant ships, and other high strength structures (M-6). Due to its high applicability and availability HY-80 was chosen for the construction of the test samples for this research work.

4.1 HY-80 Steel

HY-80 steel was developed in the late 1940's but did not come into extensive use until the early 60's. HY-80 was created as a low carbon hardenable steel which obtains

its properties from heat treatments, that is it derives its strength and toughness from quenching and tempering. A summary of the chemical and mechanical properties is shown in Tables I and II of Figure 4-1 (H-6).

The chemical composition of the steel is important, the different elements all contribute in some manner or another to its mechanical properties or to its workability. The limit on the carbon and phosphorous is to assure both notch toughness and weldability, while sulfur is undesirable because it forms iron sulfide which melts at normal rolling and forging temperatures. Manganese is added to defer the effect of the sulfur but not enough to cause embrittlement during heat treatments. Slight quantities of nickel and molybdenum reduce temper embrittlement and the nickel improves toughness (M-6).

HY-80 steel is produced through an open hearth or electric furnace method. The result is that the steel is fully killed and finely grained. The final heat treatment or quenching and tempering is needed for strength and toughness. The heat requirements during the steel-making process specify not less than 1100°F and a microstructure at mid-thickness of the plate containing no less than 80% martensite (H-6).

TABLE I - Specification Limits of HY-80 Chemical Composition

LADLE ANALYSIS - PER CENT

C	Mn	P*	S*	Si	Ni	Cr	Mo	Ti	Va	Cu
.18	.10	.025	.025	.15	2.00	1.00	.20	.02	.03	.25
Max.	to	Max.	Max.	to	to	to	to	Max.	Max.	Max.
40				35	3.25	1.80	.60			
CHECK ANALYSIS-PER CENT-OVER UPPER LIMIT										
.02	.05	.003	.000	.03	.07	.06	.03			
CHECK ANALYSIS-PER CENT-UPPER LOWER LIMIT										
--	.00	--	--	.03	.07	.06	.03			

Figure 4-1. Summation Of Chemical and Mechanical Properties of HY - 80

TABLE II - Chemical Composition for HY-80 Thin, Thick,
and Insert Plates

Thickness	C	Mn	P	S	Si	Ni	Cr	Mo
Thin plate								
(Up to 1½ in. Incl)	.14	.30	.015	.020	.20	2.35	1.15	.30
Thick plate								
(Over 1½ in. to 3 in. Incl)	.16	.30	.015	.020	.20	2.85	1.55	.45
Insert plate								
(over 3 in. to 6 inc. Incl)	.17	.30	.015	.020	.20	3.10	1.65	.55

68.

Figure 4-1. Summation of Chemical and
Mechanical Properties of HY-80

TABLE III - Specification Limits of HY-80
Mechanical Properties

Property	Plate Thickness	
	Less than 5/8 in.	5/8 in. and over
Ultimate strength (psi)	For information	For information
Yield strength at 0.2% Offset (psi)	80,000 to 100,000	80,000 to 100,000
Min. Elongation in 2 in. (percent)	19	20
Reduction in area (percent)		
Longitudinal	--	55
Transverse	--	50

69.

Figure 4-1. Summation of Chemical and
Mechanical Properties of HY-80

The goal when welding any material is to produce weld metals with the same properties of the base metal. This is not easy, even with common low strength materials, but with a notch-tough high strength steel such as HY-80 it is almost impossible. So far it has not been possible to develop electrodes which produce weld metals as notch tough as HY-80 base metal (M-6). The various types of electrodes and their chemical properties are shown in Figure 4-2. Similarly, the mechanical properties are shown in figure 4-3 (H-6).

In addition to the electrode type designation, the welding process, welding position, and applicable specifications are usually given for a particular structure. However, standard and codes are published by the American Society of Mechanical Engineers (ASME), American Society for Testing Materials (ASTM), and American Welding Society (AWS) and the government has a series of specifications one of which is a group of military specifications (Mil Specs) published by the Department of Defense. The welding process used in the construction of the test samples is Mil Spec. 0900-006-0910 and electrodes used was MIL-10018 the properties of which are found in Figures 4-2 and 4-3.

An outstanding reference for understanding basic

HY-80 Welding Electrodes and Application

Elec. Type	Spec.	Process	Position	Application
MIL-11018	MIL-E-22200/1	Shielded metal arc	All	All
MIL-10018	MIL-E-22200/1	Shielded metal arc	All	Fillet, Fillet Groove or Groove joints
MIL-9018	MIL-E-22200/1	Shielded metal arc	All	Limited use
MIL-B88	MIL-E-19822	Semi-Automatic or Automatic Metal Inert-Gas Arc	Flat or Horizontal	All
MIL-EB82*	MIL-E-22749	Submerged arc	Flat	All
MIL-MI88**	MIL-E-22749	Submerged arc	Flat	All
MIL-8218Y QT	MIL-E-22200/5	Shielded metal arc	All	Limited to Pro- cedure Approval

* Granular Flux Particle Size 10 x 50.

** Granular Flux Particle Size 12 x 150.

Figure 4-2 HY-80 Welding Electrodes

Specification Limits of Deposited Weld Metal

Chemical Compositions

	MIL-9018	MIL-10018	MIL-11018	MIL-B88	MIL-MI88	MIL-8218 QT
Carbon	.10	.10	.10	.08	.06	.10-.15
Manganese	.60-1.25	.75-1.70	1.30-1.80	1.15-1.55	1.00-1.50	.80-1.15
Phosphorous	.030	.030	.30	.025	.010	.030
Sulfur	.030	.030	.030	.025	.010	.030
Silicon	.80	.80	.60	.35-.65	.50	.30-.60
Nickel	1.40-1.80	1.40-1.80	1.25-2.50	1.15-1.55	1.40-1.90	1.50-2.00
Chromium	.15	.35	.40	--	.10-.30	.90-1.20
Molybdenum	.35	.25-.50	.30-.55	.30-.60	.20-.40	.45-.75
Vanadium	.05	.05	.05	.10-.20	.05	.02
Copper					.10-.30	
Titanium					.10	
Zirconium					.10	
Aluminum					.10	

Figure 4-2 HY-80 Welding Electrodes

Specification Limits of Deposited Weld Metal

Mechanical Properties

	MIL-9018	MIL-9018	MIL-11018	MIL-B88	MIL-MI88	MIL-8218YQT
Ultimate						
Strength 90,000 (psi)	100,000	110,000	---	110,000	---	---
Yield Strength 78,000	90,000	95,000	88,000	88,000	82,000	
at 0.2% Offset 90,000 (psi)	102,000	107,000				
Elongation in 24	20	20	14	20	18	
2 inc. (percent)						
At - 600F	20	20	20	30	20	

73.

Figure 4-3 Mechanical Properties of HY-80 Electrodes

welding principals and techniques is Current Welding Processes published by the American Welding Society (P-1).

4.2 TEST SAMPLES

The sample design chosen are simple butt and fillet welds constructed of one and two inch plate. The reason for choosing the butt and fillet welds for the samples is that they are the most common welds encountered in structural welding. Other types of welds, such as cylindrical or plug welds, are no more than special cases of the butt and fillet welds. The choice of one and two inch thickness in the sample construction was again like the welds. The one and two inch plates are within a common range of use and they also provided the needed variation for test purposes.

Though the samples were welded to the afore mentioned Mil Spec, defects were placed in the sample intentionally. These defects were not necessarily large enough to fail the weld during the tests, but were large enough to be detected by one of the conventional test methods. These defects are used to give an indication as the effectiveness of the various test methods.

Figure 4-5 (a-d) shows the samples designated B-1, B-2,

75.

75.

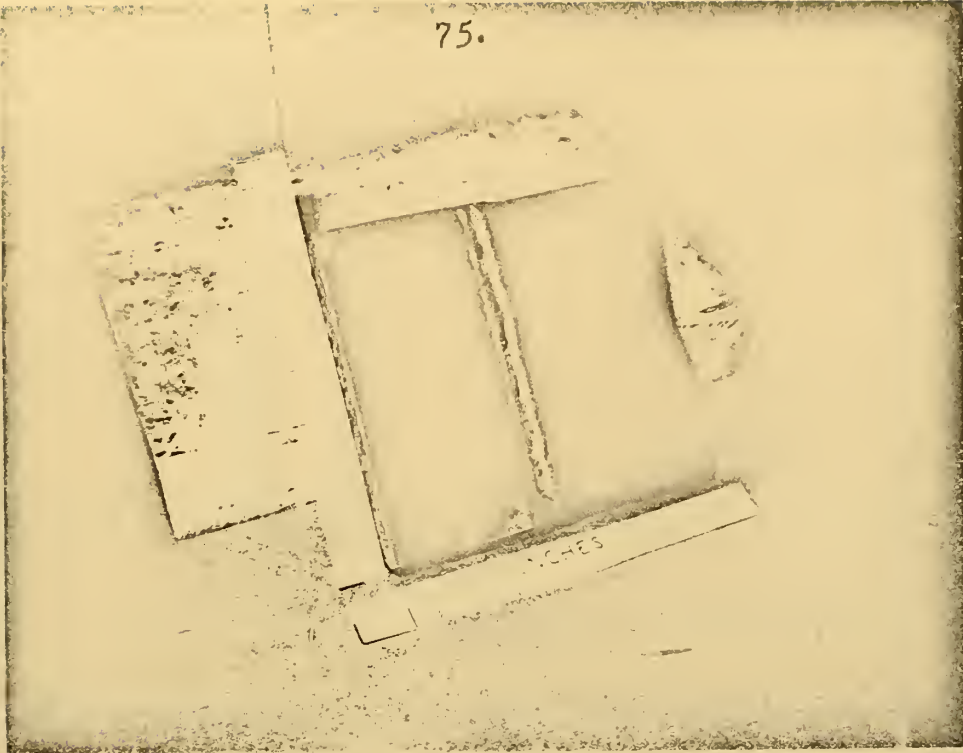


Figure 4-5a. Sample B-1



Figure 4-5b. Sample B-2

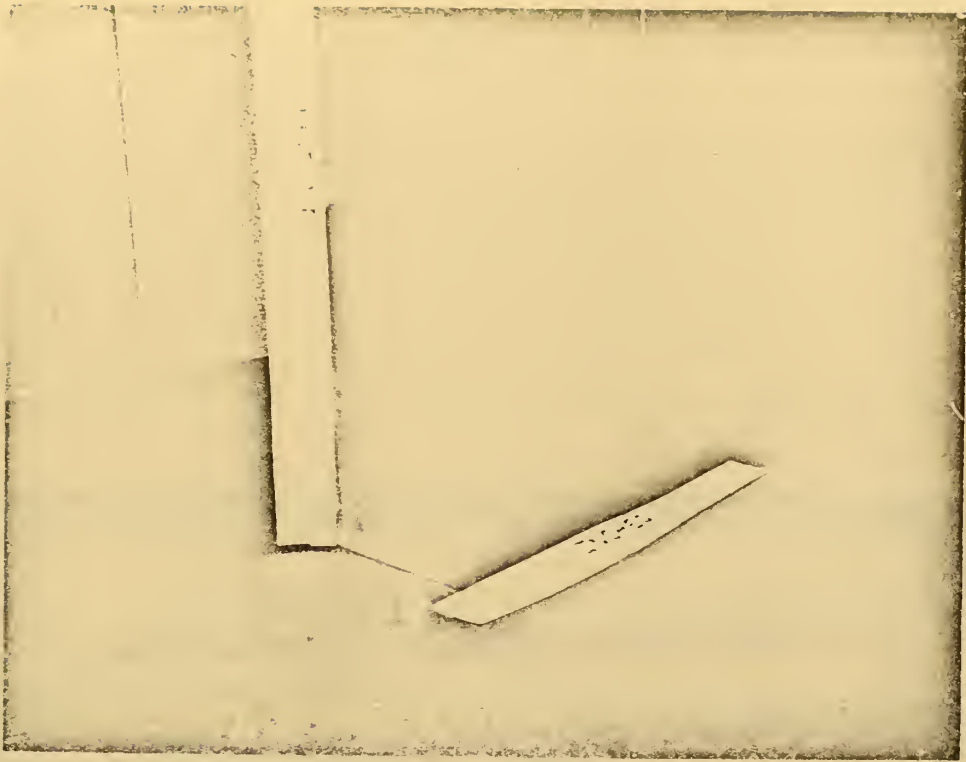


Figure 4-5c. Sample F-2



Figure 4-5d. Sample F-2

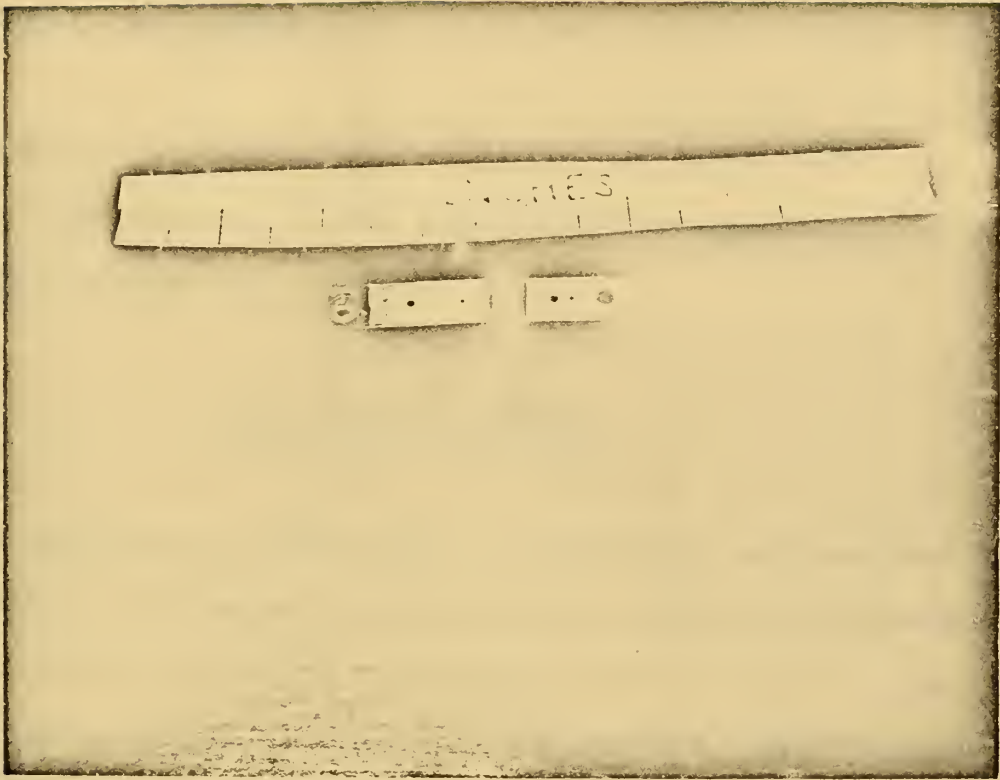


Figure 4 -6. Penetrameters

F-1, and F-2 where the B stands for butt and F for fillet and the number is the plate thickness. All the samples are approximately six inches square and six inches high.

The penetrameters used during the radiographing are standard 20 mill and 40 mill iron penetrameters designated 1.0 and 2.0 respectfully.

The two penetrameters are shown in figure 4-6. A detailed description of the penetrameters and their use is given in Chapter 3.

4.3 SHIPYARD TESTS

In addition to procuring the materials and constructing the samples, Portsmouth Naval Shipyard offered the services of their Non Destructive Test Branch (Code 133.1) to run an extensive series of tests on the samples. The tests included conventional radiographs; ultrasonic tests, eddy current tests, and magnetic particle tests. The record sheets for many of these tests appear in Appendix E and the results of these tests are compared to the neutron radiographic results in Chapter 7. Also given in Chapter 7 are the limitations and where and when to use the various test methods. These again are compared to the neutron radiography characteristics.

CHAPTER 5NEUTRON RADIOGRAPHY AT M.I.T.

The first radiographs taken at MITR were taken to become more familiar with the radiographic procedures and to develop an accurate set of characteristic curves for both indium and dysprosium foils. The next step was to radiograph the four weldments using the characteristic curves to obtain the highest contrast possible, these radiographs could then be compared against the X-rays and test results from PNSY. Finally, improvements to the established procedures and technique were proposed in order to improve the radiographic quality and to optimize the procedure.

The established radiographic procedure used at MITR was developed by Eric Westberg and Jim Knotts in 1971-72, as was mentioned in Chapter 3. The procedure utilizing the transfer technique to produce radiographs, consists of placing the object to be radiographed on a transfer foil in the neutron camera located in the Medical Room. The object and foil are then irradiated when the shutters leading to the Medical Room aperture are opened. After the desired irradi-

iation, the shutters are closed, the residual radiation in the Medical Room is allowed to decay and the transfer foil is removed. The transfer foil is then placed on a sheet of photographic film which is allowed to expose as the transfer foil decays. A detailed description of the procedure is given in Chapter 3.

Control of the radiograph is maintained by varying the irradiation time, film exposure time, and to some extent the time foil decays before it is placed on the film. As was also discussed in Chapter 3, the above mentioned times are determined from the characteristic curves for the particular transfer foil. It is then essential that the characteristic curves for two types of transfer foils (indium and dysprosium) be accurate.

5.1 CHARACTERISTIC CURVES

The first radiographs taken using the indium transfer foil did not agree with the indium characteristic curve extracted from operation records and shown in Figure 3-6. This disagreement with the indium curve had to be investigated and the reason for the disagreement determined before serious radiographing could continue. However, in order to obtain maximum utilization out of the radiographs, complete

records were kept of the data accumulated from each radiograph and the resultant data sheets are shown in Appendix E.

The first step to developing the characteristic curve for indium was to check the accuracy of the characteristic curve for dysprosium foil. Several radiographs were taken using the dysprosium foil and the density measurements agreed extremely well with the characteristic curve developed by Momsen (M-3). Next the operations files were rechecked and an allowance for the darkening of the negatives due to age was made and still the characteristic curve for indium did not agree with experimental data. Further investigation led to the possibility that the assumption of a 10 minute decay time (T_{trans}) was erroneous. A deviation of 5 minutes in T_{trans} results in a deviation of 12 percent in the relative exposure (E_r) and a deviation of 10 minutes results in a E_r deviation of 23.5 percent. (See Figure 3-9 for variation in T_{trans}). In any case, the fact that there is insufficient information contained within the neutron radiography file at Reactor Operations, plus the fact the information there is not experimentally accurate for the purpose of deriving an accurate characteristic curve for indium meant additional radiographs using the indium transfer foils had to be taken to get the needed curve. The resultant characteristic curve for the indium foil is shown in Figure 5-1.

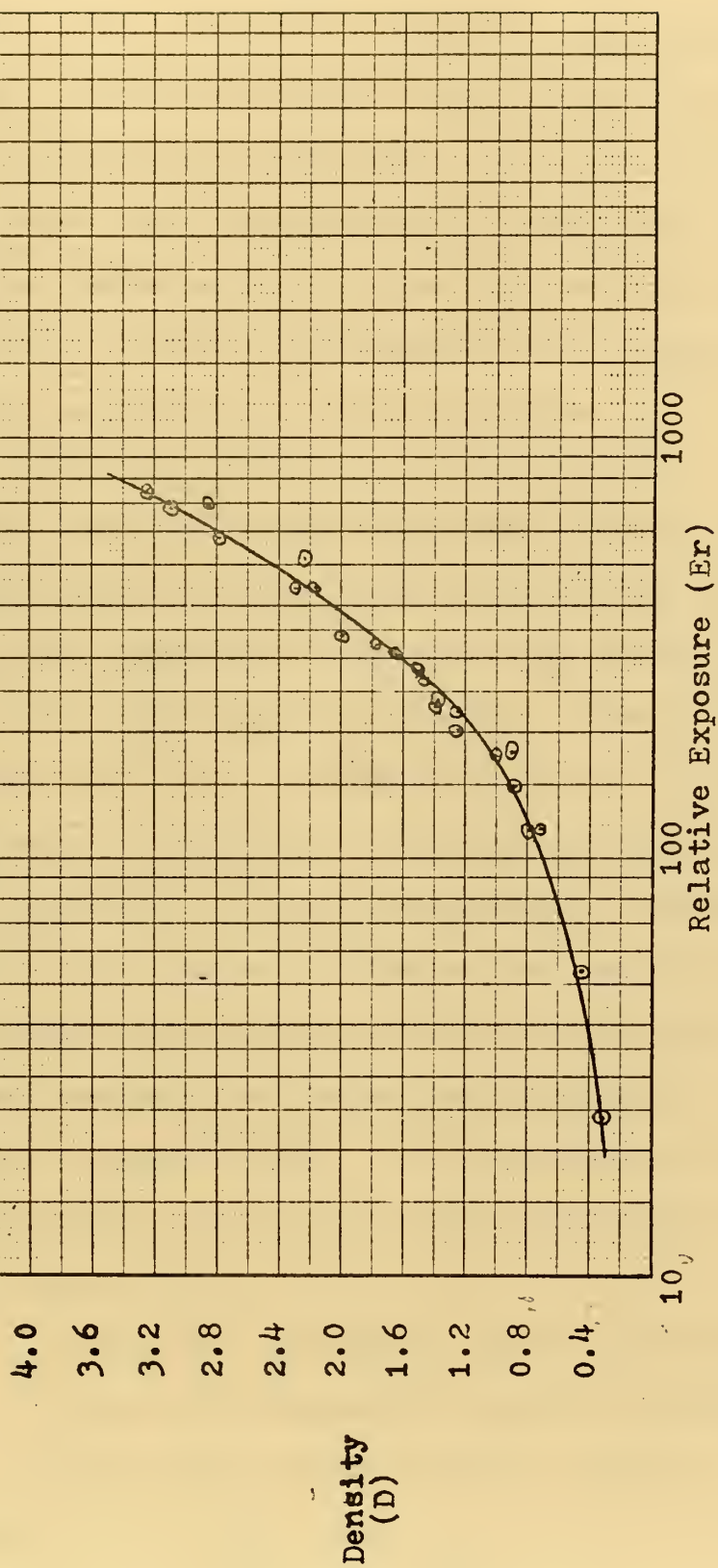


Figure 5-1. Density vs Relative Exposure for Indium Foil
Experimental

Figure 5-2 shows the points taken from the operations files with a 10 percent deviation in E_r plotted over the experimentally derived characteristic curve for indium foil. It should be noted that these points now correlate rather roughly with the characteristic curve, and an even better correlation could be made if an allowance for density were made due to the various ages of the negatives.

Upon close examination and comparison of both the indium and dysprosium characteristic curve it was found that the two curves are identical except that the indium curve is shifted to the right along the abscissa. The fact the curves are identical can be expected due to the fact that the same film was used (Kodak AA X-ray film) and as was pointed out in Section 3.3 the film determines the shape of the characteristic curve. Similarly, the shift to the right of the indium curve can be accounted for by the difference in decay constants of indium and dysprosium (.01280 and .004978 min^{-1} respectively). It is possible to normalize the indium curve and lay it on the dysprosium curve, the result is Figure 5-3.

where: E_{rn} is the normalized relative exposure
 E_{rd} is the dysprosium relative exposure
 E_{ri} is the indium relative exposure

Note $E_{rd} = E_{rn}$
 $E_{ri} = 22.2 E_{rn}$

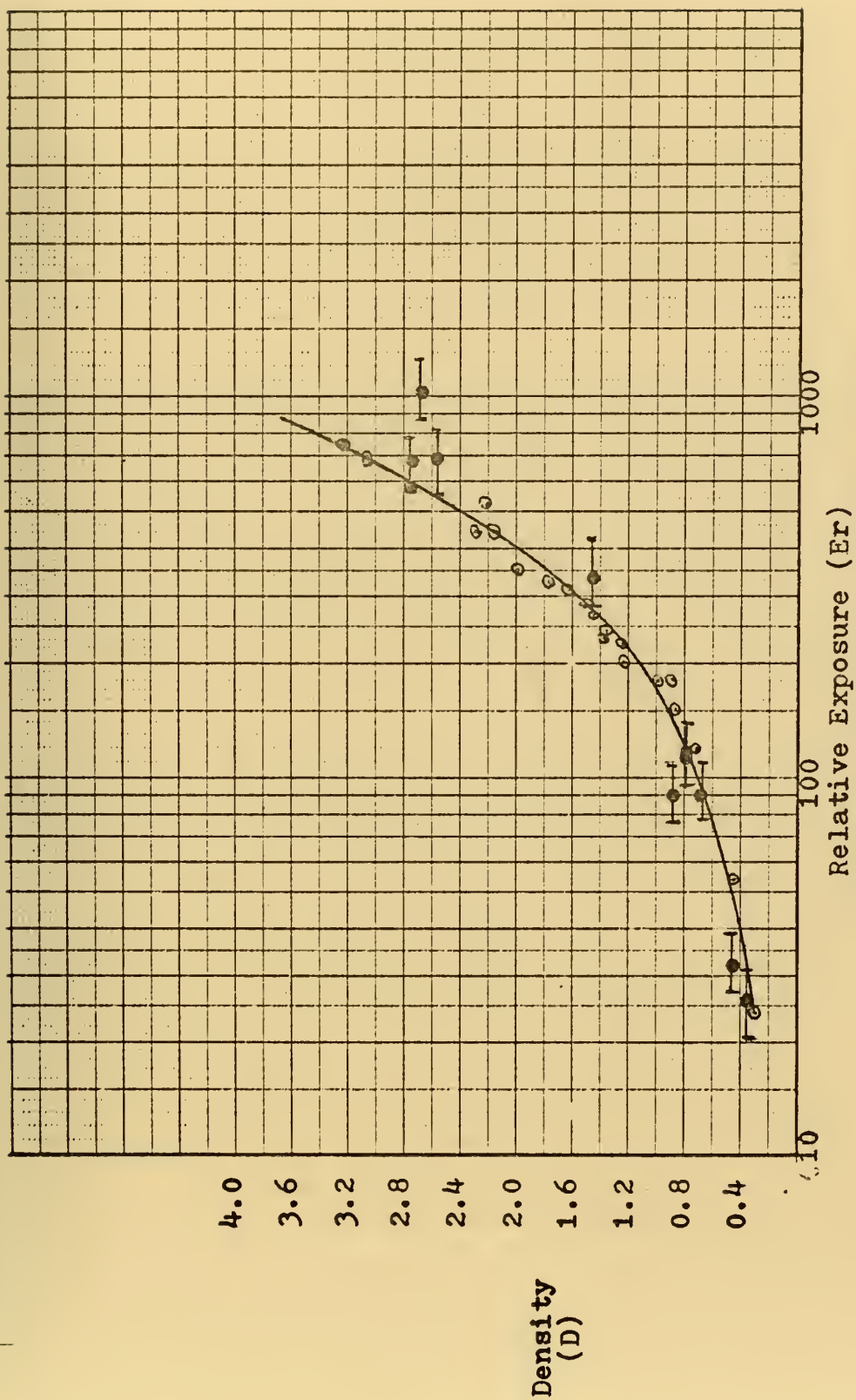


Figure 5-2. Comparison of Indium Characteristic Curves

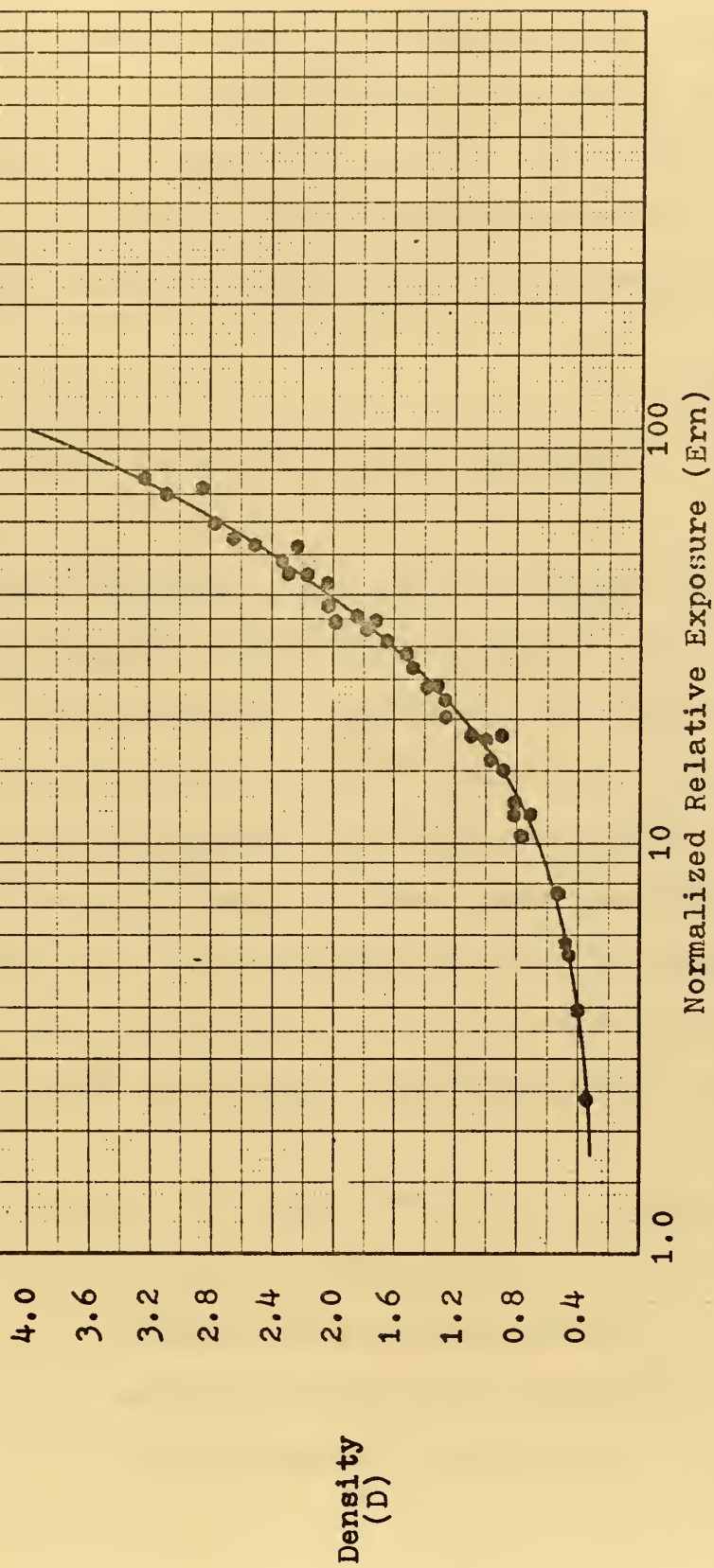


Figure 5-3. Normalized Characteristic Curve

It was also possible from the radiographs to obtain experimental values of the attenuation coefficient (μ_b) and compare it against the theoretical value. The coefficient was determined by measuring the attenuated density (D') and the unattenuated density (D) and using the following equation.

$$D'/D = e^{-\mu_b t} \quad (5-1)$$

where: t is the plate thickness

The measured values of μ_b are shown in Figure 5-4 where they are plotted against the relative exposure. The calculated value of the attenuation coefficient for Hy-80 using the table in Appendix A is 0.123 cm^{-1} while pure iron is 0.118 cm^{-1} . It should be noted that the calculated value (0.123 cm^{-1}) corresponds well with the lower measured values (0.121 cm^{-1}) and also the attenuation coefficient increases with exposure. This increase of the attenuation coefficient with exposure is due to buildup. The buildup can be expressed as follows:

$$I/I_0 = (1 + B) e^{-\mu t} \quad (5-2) \quad (B-8)$$

where: B is the buildup factor

I/I_0 is the intensity ratio

μ is the attenuation coefficient

t is the material thickness

or more simply:

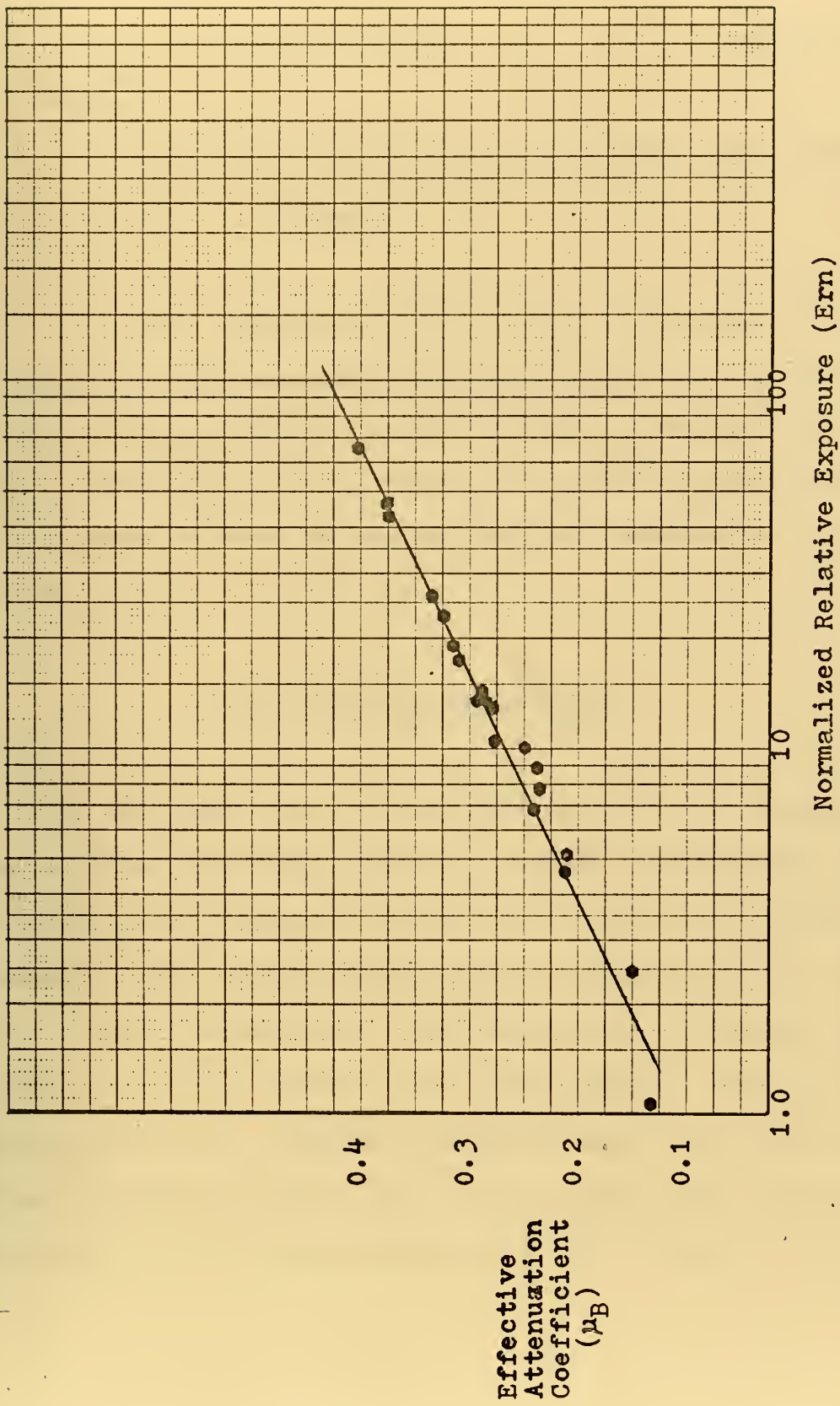


Figure 5-4. Effective Attenuation Coefficient

$$I/I_0 = e^{-\mu_B t} \quad (5-3) \text{ (B-8)}$$

where:

μ_B is the attenuation coefficient with buildup included

It is now possible to use the same procedure outlined in Chapter 3 to determine the irradiation and exposure time (T_{irr} and T_{exp} respectively). But now, a single characteristic curve can be used, Figure 5-3, and μ_B from Figure 5-4, can be used instead of the uncorrected attenuation coefficient.

5.2 NEUTRON RADIOGRAPHS

As was mentioned in the previous section, several radiographs were taken for the purpose of developing the characteristic curves for indium and dysprosium foils. The remaining radiographs taken used the characteristic curves and μ_B curve to determine the feasibility of neutron radiography to detect faults in the weld samples. When radiographing the welds, different incident angles were tried in order to detect cracks, that is the sample was tilted in an attempt to project the widest part of the crack to the film.

In order to try to see the effect of the geometric unsharpness (U_g) and the effect of the ± 1.2 degree deviation from the beam axis by the neutrons, a variation in the collimator to object/film distance was made. The construction of the collimator and its associates shielding permitted only a small variance in elevation of about 5 inches. The data sheets for all the radiographs are in Appendix E. The prints of several radiographs are in the following section where they are compared to other non-destructive tests.

It should be pointed out that the printed radiographs lose some contrast and detail when they are printed due to inefficiencies in the printing process. Another point that should be made is the use of aluminum foil on top of the transfer foil. The purpose of this was to prevent the heavy and rough samples from scratching the transfer foils. This works very well, especially since the thin aluminum is essentially transparent to neutrons. However, in placing the heavy samples on top of the foils, the aluminum tends to wrinkle and if the wrinkles aren't removed the radiographs appear slightly fogged, a minor but very annoying problem which will be pointed out in the radiographs in the following section.

5.3 COMPARISON WITH OTHER NONDESTRUCTIVE TESTS

The other tests performed on the four samples consisted of ultrasonic tests, magnetic particle tests, eddy current tests and convention radiographic examination. The tests provided an interesting basis for comparison with the neutron radiographs and with each other, as seen in the following sections. It should be pointed out that neutron radiography can only best be compared to conventional radiography since the procedures and principles are basic to both. A detailed description of each test and its relative advantages and disadvantages is given in Appendix D.

5.31 MAGNETIC PARTICLE TESTS

One of the oldest methods of NDT, magnetic particle testing, is still used very widely. When it was used to examine the four test samples, it indicated several surface cracks in the heat affected zone (HAZ) around the weld. The magnetic particle test showed the surface cracks between the weld beads in samples F-1 and F-2 extremely well. However, the cracks were sufficiently small and shallow enough that when the weld was dressed (ground to specification) the cracks would be removed. If the cracks remained, the weld would have to be excavated and repaired.

As can be seen in Figures 5-11 and 5-12, radiographs of F-1 and F-2, these cracks didn't show. These cracks didn't show in X-rays of the samples either. This is of no surprise due to the smallness of the cracks, and the fact that they were located within undercuts between weld beads.

5.3.2 EDDY CURRENT EXAMINATION

Eddy current examination is an up and coming method of NDT. It is not presently at PNSY however, they are testing and evaluating several units as a replacement for magnetic particle inspection. The advantages of eddy current testing over magnetic particle inspection is its extreme portability, it produces both an audible and visual output, and it does not require an absolutely clean surface as does magnetic particle or ultrasonic tests.

When the samples were tested with one of the eddy current devices presently being examined it showed the same surface cracks as did the magnetic particle examination. It didn't however pick up any additional cracks in either sample F-1 or F-2, but it did pick up a small crack on "X" side of B-2 which magnetic particle inspection and neither radiographic techniques was able to do.

5.3.3. ULTRASONIC INSPECTION

Ultrasonic testing or "UT" works very similar to sonar i.e. sound is reflected off surfaces and any discontinuity disrupts the beam and appears on a screen. When the samples were tested ultrasonically, the results proved to be very interesting. UT picked up several surface cracks in samples B-1 and B-2, and it also picked up several deep cracks in these two samples as well, (the test report for the "UT" is shown in Appendix E). The test also picked up a small void or inclusion in the B-1 sample, and the latter proved to be the only failure that both radiographic techniques and "UT" detected. It should be pointed out, that there were sufficient number of faults found during the ultrasonic inspection to fail both samples B-1 and B-2 according to standard Mil. Specs.

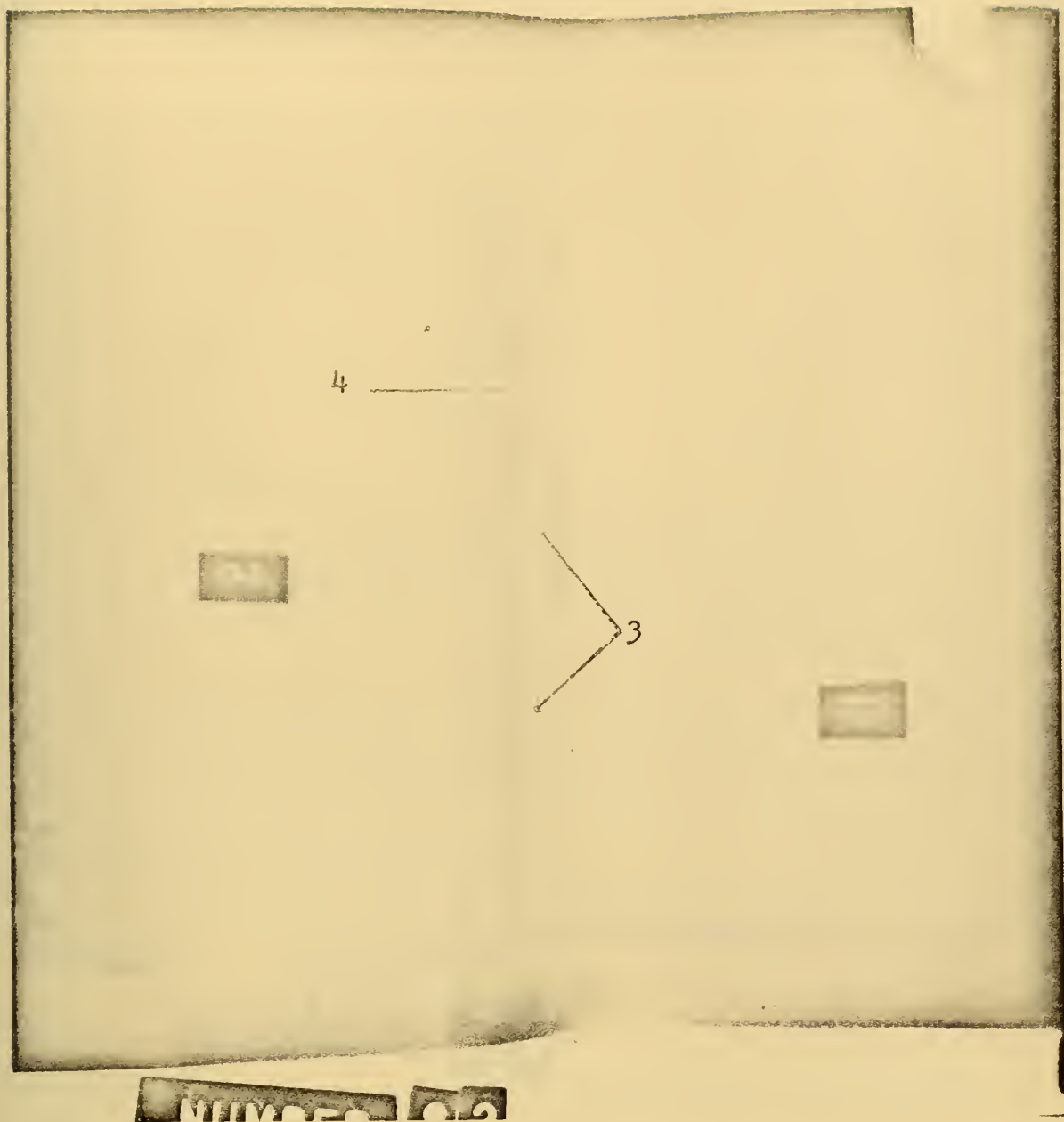
The two fillet samples F-1 and F-2 were impossible to test due to the other than optimum configurations. More precisely, the samples were too small for the "UT" probe to be positioned to get a good reflection from the weld.

5.3.4. RADIOGRAPHIC TESTS

The most popular NDT method in use today, is the in-

dustrial radiography. The procedure, limitations, and capability of this method is discussed in detail in Chapters 2 and 3, and in Appendix D. For the purpose of these experiments, an iridium 192 source with a strength of 65 curies was used. (The details of the tests are given in Appendix E). By using gamma radiography instead of X-rays it was felt that the comparison to neutron radiography would have more meaning since the source of radiation and procedures are more closely related.

Figure 5-5 is a neutron radiograph of sample B-1 taken with a dysprosium transfer foil while Figure 5-6 is a neutron radiograph of the same sample but taken with an indium transfer foil. The pertinent data for each radiograph appears on the figure and additional information is found in Appendix E. Similarly, Figure 5-7 is a gamma radiograph of the same sample. In all three radiographs, the 1.0 penetrameter is visible (1) and in the two neutron radiographs, the 2.0 penetrameter is also visible (2). Also visible in all three radiographs is undercutting between weld beads (3) and also some porosity in the weld (4). This defect does not appear clear in the prints and is not nearly as visible in the neutron radiographs as in the gamma radiographs. Not shown in the print, but which did show in the original radiographs is some porosity in the center of weld-



Ern = 22.9

Dysprosium Foil

S = 4-2T

Figure 5-5 Neutron Radiograph of Sample B-1

95.

4

5

3

NUMBER

80

Ern = 15.6

Indium Foil

S = 1-4T

Figure 5-6 Neutron Radiograph of Sample B-1

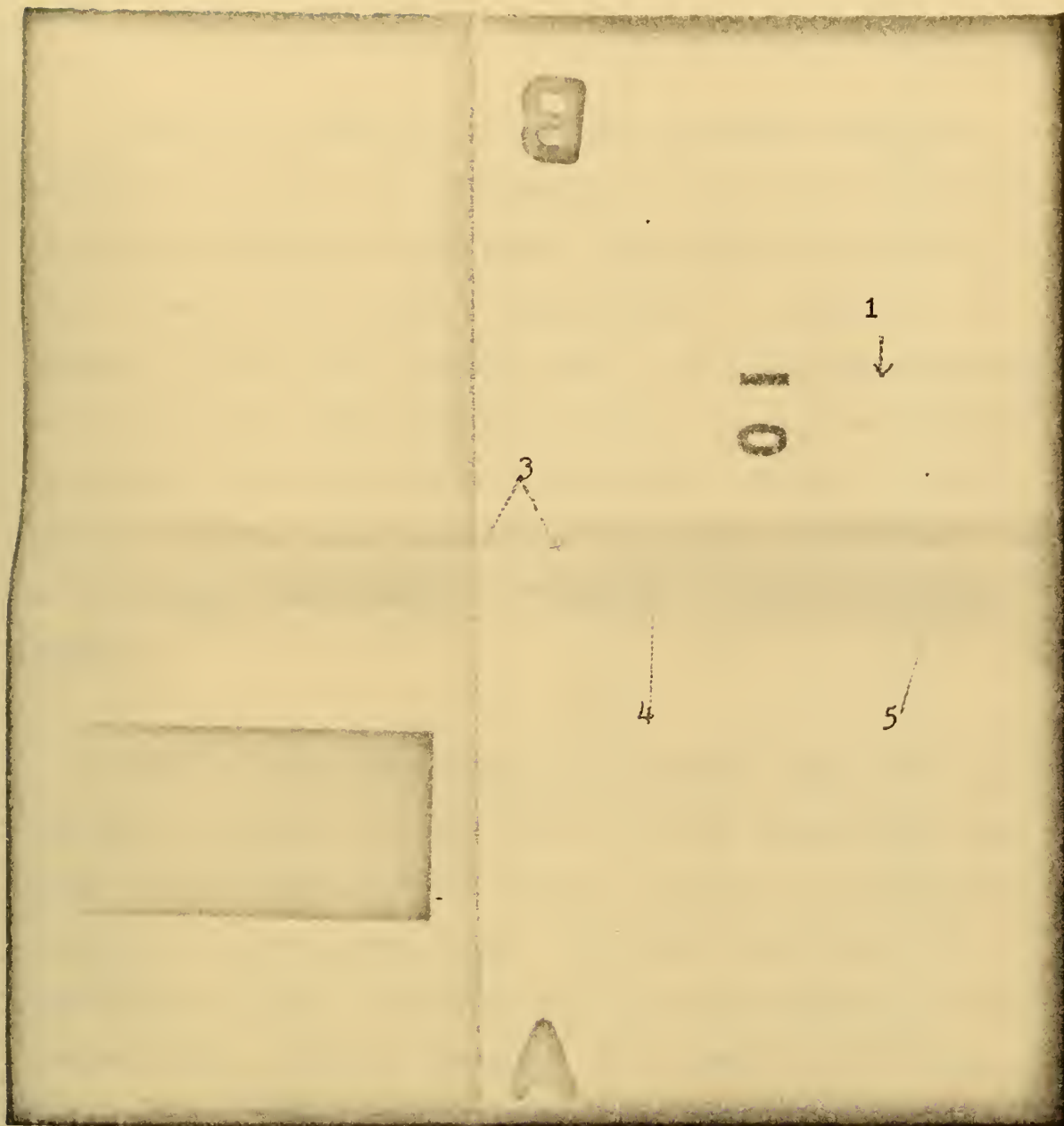
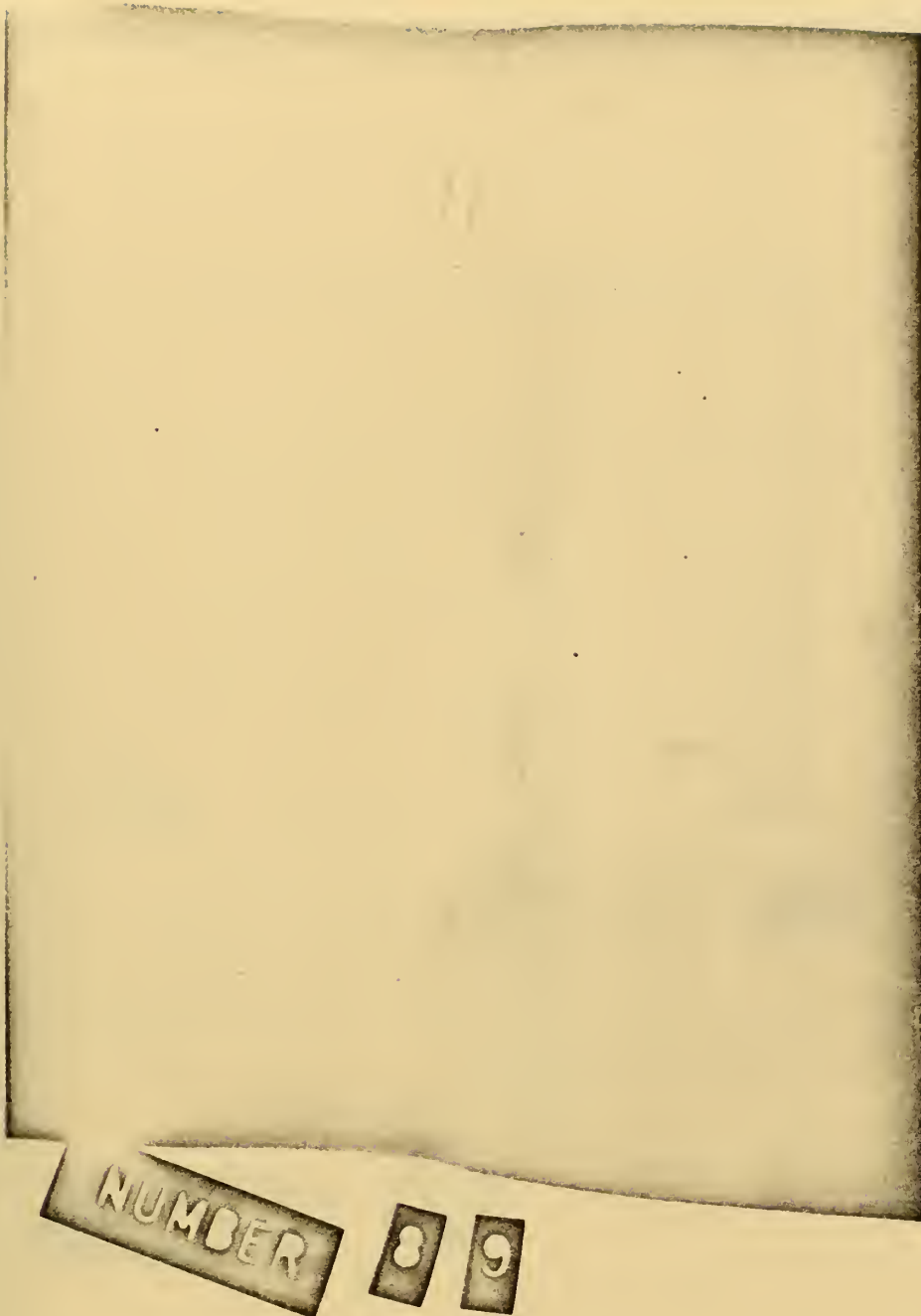


Figure 5-7. Gamma Radiograph of Sample B-1

ment at about point (5).

Also it is possible to see the increased darkness of Figure 5-5 over the radiograph in Figure 5-6 and of the increased darkness of the gamma radiograph of Figure 5-7 over either of the neutron radiographs. It should be pointed out that what appears dark in the radiograph appears as light in the print and vice versa. It is also possible to compare the variation in sensitivity between the radiographs with the gamma radiograph being more sensitive. None of the cracks detected by "UT" appear in any of the radiographs.

Like the three preceeding radiographs Figure 5-8 and 5-9 are of sample B-1, and like the other radiographs they show the penetrameters and faults (1,2,3,4,5). The interesting fact about them is the that they were taken with a collimator to film length (L) of 23 inches and 25.5 inches respectively. This is compared to a normal L of 28 inches. This variation in L resulted in a corresponding variation in geometric unsharpness (U_g) and in widening of the beam ($L \tan 1.2$). This variation is shown in Figure 5-10.



Ern = 22.6

Indium Foil

s = 1-4T

Figure 5-8. Neutron Radiograph of Sample B-1

NUMBER

91

Ern =90.3

Dysprosium Foil

S = 1-4T

Figure 5-9. Neutron Radiograph of Sample B-1

L	28	25.5	23
Ug	.207	.226	.2495
L tan 1.2^0	.587	.532	.482

Figure 5-10 EFFECT OF ELEVATION VARIANCE

As can be seen there is some point where Ug will equal $L \tan 1.2^0$ where the effect of both will be minimized. For a one inch thick sample (t-1) this occurs at L equal to about 16.5 inches. However, due to the collimator construction it was impossible to reduce L to below 23 inches.

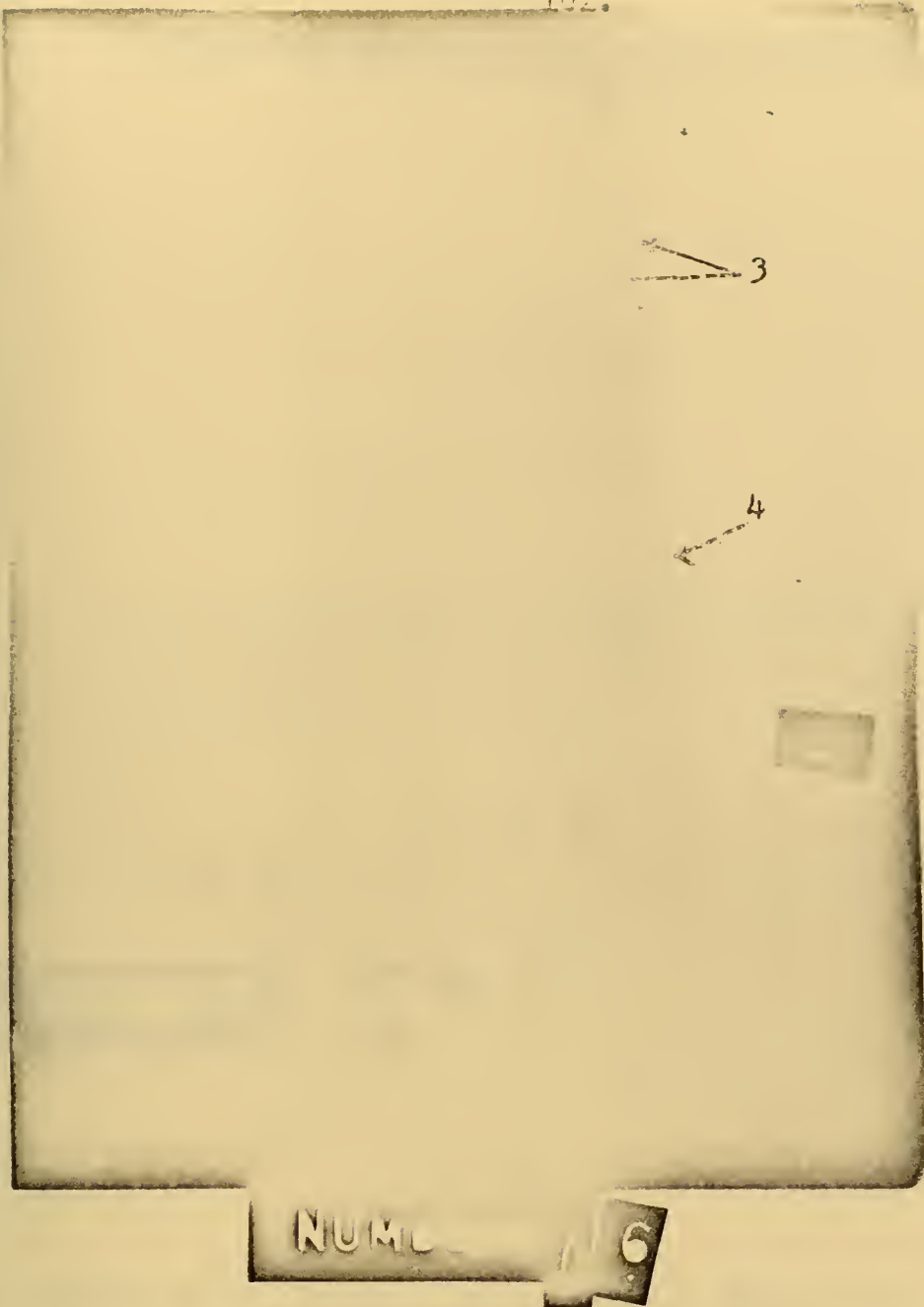
It would be interesting to do this because there is detectable improvement in contrast and sensitivity as L is decreased. This is evident even in the prints by comparing Figures 5-5 and 5-6 to 5-8 and 5-9.

The radiographs shown in Figures 5-11 and 5-12 are of sample F-1 and as before the two penetrameters are shown (1) and (2). Figure 5-11 is a radiograph taken perpendicular to the sample as can be seen by the dark line through the print which is the Tee. The thickness at this point is about seven inches. Radiographs were taken at various angles to the plate. Figure 5-12 is one taken at 45^0 . In this figure the various weld beads can be seen much more clearly than in

Figure 5-11. Similar to Figure 5-13 is a gamma radiograph of the sample also taken at about 45° , and again the various weld beads are visible.

Upon examination of the radiographs, there appears to be some undercutting between a couple of beads (3). It is later evident in Figures 5-12 and 5-13 where the radiographs were taken at an angle. However, in the radiographs taken perpendicular to the sample these don't show up so well. This undercutting probably would be removed when the weld was dressed and would not necessarily require repair. Visible in all the radiographs is weld splatter (4) caused by molten weld metal striking the relatively cold plate.

Figure 5-12 also shows the effect of overlapping transfer foil (5) that is the foil was in two pieces and overlapped. This has the effect of darkening the radiographs. It must also be noted that this radiograph is somewhat foggy compared to the other radiographs, as were all the radiographs taken at the various angles. The only explanation for this is that the inclination of the samples resulted in increased neutron scattering resulting in a fogging effect.



Ern = 81.5

Dysprosium Foil

S = 2-2T

Figure-5-11--Neutron Radiograph of Sample F-1



1

5

2

NUMBER

CF

Ern = 21.9

Indium Foil

s = 4-2T

Figure 5-12. Neutron Radiograph of Sample F-1



Figure 5-13 Gamma Radiograph of Sample F-1

The two inch thick samples B-2 and F-2 proved to be very difficult to radiograph. This was due primarily to the increased irradiation time required to get an adequate radiograph. Figures 5-14 shows a neutron radiograph of sample B-2. This radiograph does not show the weld beads nearly as well as the gamma radiographs of Figures 5-15 and 5-16. However, it does not show an inclusion in the base metal (3) that the gamma radiographs do not show. The gamma radiograph of Figures 5-16 was taken with the sample inclined at about 45° . This radiograph shows some porosity (4) which the other radiographs do not show.

It was mentioned in the previous section that aluminum foil was used to protect the transfer foil from scratches. Figure 5-14 shows scratches in the foil (5).

Figures 5-17 and 5-18 are a gamma radiograph and neutron radiograph of sample F-1 respectively. Both radiographs show the effect of thick sections, particularly Figure 5-17 in which the radiograph was taken with the sample inclined at about 45° with respect to the source. In this radiograph the Tee allowed almost no radiation to pass through to the film, and appears black on the print. Similarly almost the entire neutron beam was attenuated by the sample, resulting in the radiograph shown in Figure 5-18.



NUMBER

6 9

Ern = 9.14

Indium Foil

S = 2-2T

Figure 5-14 Neutron Radiograph of Sample B-2

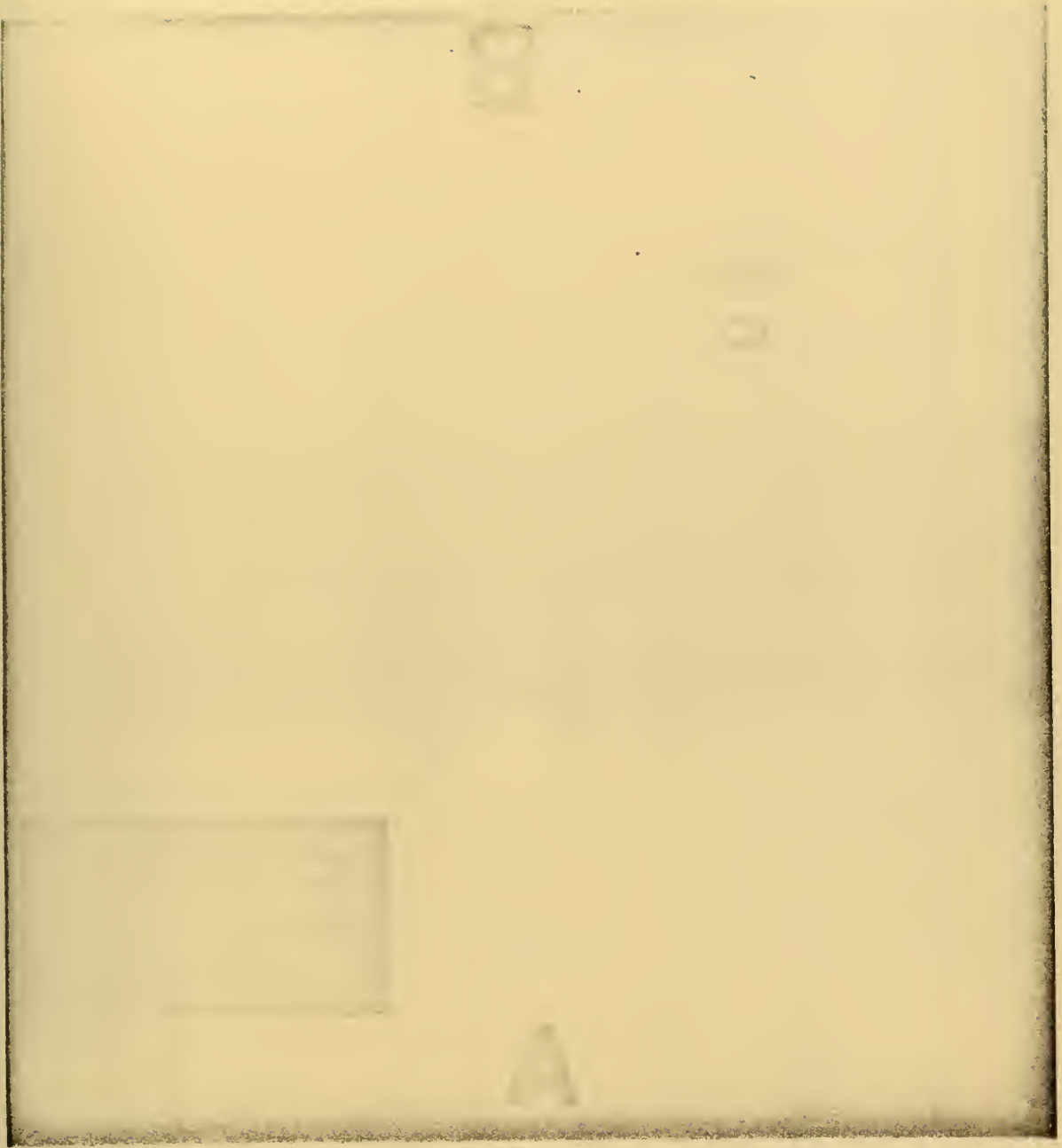


Figure 5-15 Gamma Radiograph of Sample B-2

4

Figure 5-16 Gamma Radiograph of Sample B-2

Figure 5-17 Gamma Radiograph of Sample F-2

Ern = 90.3

Dysprosium Foil

Figure 5-18. Neutron Radiograph of Sample F-2

111.

Neither radiograph showed anything other than the attenuation by thick sections. This is due primarily to the afore accredited thickness, and to the difficulty to radiograph Tee sections.

Finally, an attempt to enhance the surface cracks so that they would show on a radiograph was made. The first method tried was to soak sample B-1 in tap water for several hours. The sample was then patted dry to remove surface water and radiographed. The radiograph when developed proved to be very foggy showing no surface cracks and faults that had previously shown up in other radiographs were not visible due to the fogyness of the radiograph. This extreme fogyness was due to the scattering of neutrons by the water retained by the rough sample surface.

The sample was soaked again, but this time forced air was used to dry the sample before it was radiographed. The radiograph this time was also a failure, it wasn't foggy, but it didn't show any surface cracks either. Either the drying process had removed the water from the cracks as well as the surface, or the water had never entered the cracks.

Sample B-1 was then baked at about 300°F for about three hours to ensure any residual water that might be in sample was removed. The sample was then treated with a

a modified dye penetrant test. That is, it was cleaned with solvent, and then treated with the dye penetrant, however the developer wasn't applied to the sample since it leaves a chlorinated hydrocarbon film which would scatter neutrons and fog the radiograph.

The sample was then radiographed using the previously developed procedures. The resultant radiograph was somewhat fogged and some of the deep defects were not visible, but several surface cracks (1) are visible as are seen in Figure 5-19.

113.



NUMBER 97



Ern = 10.4

Indium Foil

Figure 5-19. Neutron Radiograph of Sample B-]
Enhanced

CHAPTER 6

RECOMMENDATIONS AND CONCLUSIONS

From the work done and observations and examinations made, it is possible to make recommendations in three principle areas. The first two areas concern the radiographic facility and the technique being used. The recommendations deal primarily with safety and limitations of the facility and technique and also the impact on the third area of recommendation ie. the future of neutron radiography in NDT. Similarly the conclusion discusses the work accomplished in this thesis and its potential value.

6.1 RECOMMENDATIONS

The transfer technique is the least expensive of all the radiographic methods available for neutron radiography but it has two big draw backs. The first and undoubtedly the most important is that the transfer method requires more safety precautions.

Requiring more safety precautions, referring to the fact that the activated foil has to be handled when it's removed from the neutron radiographic facility and again when the film is placed on top of it. This latter evolution is perhaps the worst case in that it has to be done in the dark to avoid accidental exposure of the film. Additionally the transfer foil which attains several curies of activity when irradiated still retains sufficient activity after the transfer to give an unsuspecting individual a sizable dose if the proper precautions aren't taken.

The other reason for the transfer technique being a poorer method is that it takes a larger amount of time to produce a radiograph. This increase in time makes it more costly and also makes getting a radiograph requiring a large exposure very difficult. In other words, foil activity is lost while the medical room decays and before the film is transferred to the foil. Depending on the time the foil was irradiated and the degree of background radiation build up in the medical room this can amount to almost 50% of the foil activity. As a result, the irradiation time has to be increased to account for this. Also a large amount of time is taken up while the foil transfers to the film. This time varies from half an hour to 16 to 18 hours depending on the foil.

For the above reasons it is recommended that a direct method be developed for use with the neutron radiographic facility. This would require the use of other foils or scintillation screens to minimize the background gamma. However it would be much safer and reduce the time to produce a radiograph and also reduce the danger involved while handling the foils.

As was mentioned in the previous chapter there is no way to vary the film to collimator length (L) other than shimming up the sample. And this too is limited to a range of about five inches due to the configuration of the shielding surrounding the collimator and camera.

It is recommended that the neutron camera be modified so that L can be varied and also so that there is access for large objects or even so sections of large objects can be radiographed. This would have to be done of course so that the safety and flexibility of the systems is maintained.

It is also recommended that work with neutron radiography at MITR continue, not just with weld examination, but the development of new uses and improving on the old methods and uses. Certainly the development of enhancement methods

would certainly be of considerable importance. Similarly testing and evaluating improvements to the facility and technique would also be invaluable.

6.2 CONCLUSIONS

This thesis did not show that it is possible using neutron radiography and existing facility and test methods to find discontinuities in steel weldments on an equal basis with gamma radiography.

Though not proven conclusively, the thesis did not show that it is possible to enhance defects not normally detectable with conventional radiographic procedures and detect these defects using neutron radiography. The experiments conducted in this area were somewhat crude and used solutions that did not take full advantage of the cross-section difference between steel and a good neutron absorber. However, the thesis left open the door for further experimentation and development in this area.

The thesis also demonstrated the failings of the transfer method. Though it has its place in neutron radiography the transfer method at MITR should be augmented by a direct method similar to those presently being used at other neutron

radiographic facilities.

Though it has been shown to be technically feasible, there appears to be little probability for neutron radiography to become competitive in this area in the very near future due primarily to its lack of development, prohibitive cost and the large amount of time required to make a neutron radiography. However, this is not to say that neutron radiography will not come into its own, after all conventional radiography has been developing and being used for almost a century now. It is not an unrealistic prediction that neutron radiography will soon be a tool of NDT the way X-radiography and ultrasonic testing are today.

APPENDIX AMASS ABSORPTION COEFFICIENTS FOR THE ELEMENTS

The material presented in this table is a summation of attenuation data for thermal neutrons and 120 Kev X-rays for most elements. The information contained can be used with the radiation attenuation equation given in Chapter 2.

$$I/I_0 = \text{Exp} \left(\frac{-\mu x \rho}{\rho} \right) \quad (2.3)$$

ρ

where:

I/I_0 is the ratio of transmitted to
incident intensity

x is the material thickness

μ is the linear attenuation coefficient

ρ is the material density

μ/ρ is the mass absorption coefficient

Thermal Neutrons120 Kev X-rays

Element	Atomic No,	μ/p true	μ/p total	μ/p
H	1	0.11	48.5	0.280
Li	3	3.5	3.7	0.125
Be	4	0.003	0.50	0.131
B	5	24	24	0.138
C	6	0.00015	0.26	0.142
N	7	0.048	0.48	0.143
O	8	0.00002	0.15	0.144
F	9	0.0003	0.11	0.146
Ne	10	0.006	0.006	0.148
Na	11	0.007	0.099	0.150
Mg	12	0.001	0.093	0.152
Al	13	0.003	0.036	0.156
Si	14	0.001	0.044	0.159
P	15	0.002	0.062	0.162
S	16	0.0055	0.029	0.166
Cl	17	0.33	0.59	0.176
A	18	0.0060	0.006	0.184
K	19	0.018	0.049	0.191
Ca	20	0.0037	0.057	0.200
Sc	21	0.09	0.27	0.208
Ti	22	0.044	0.119	0.217
V	23	0.033	0.093	0.227
Cr	24	0.021	0.065	0.238
Mn	25	0.083	0.107	0.250
Fe	26	0.015	0.141	0.265
Co	27	0.21	0.26	0.287
Ni	28	0.028	0.213	0.310
Cu	29	0.021	0.095	0.325

121.

Zn	30	0.0055	0.045	0.350
Ga	31	0.015	0.015	0.380
Ge	32	0.011	0.082	0.41
As	33	0.020	0.076	0.44
Se	34	0.056	0.132	0.48
Br	35	0.029	0.074	0.52
Kr	36	0.0002	0.0002	0.56
Rb	37	0.0029	0.042	0.59
Sr	38	0.0048	0.070	0.61
Y	39	0.0056	0.0056	0.66
Zr	40	0.0006	0.047	0.71
Nb	41	0.0041	0.044	0.75
Mo	42	0.009	0.055	0.79
Ru	44	0.009	0.009	0.90
Rh	45	0.53	0.53	0.95
Pd	46	0.023	0.050	0.99
Ag	47	0.20	0.24	1.05
Cd	48	11.2	11.2	1.09
In	49	0.60	0.60	1.13
Sn	50	0.002	0.027	1.17
Sb	51	0.016	0.037	1.21
Te	52	0.013	0.031	1.25
I	53	0.018	0.036	1.33
Xe	54	0.083	0.083	1.40
Cs	55	0.077	0.109	1.46
Ba	56	0.0027	0.018	1.52
La	57	0.023	0.063	1.60
Ce	58	0.0021	0.014	1.68
Pr	59	0.029	0.046	1.75
Nd	60	0.11	0.21	1.81
Sm	62	25	25	1.95
Eu	63	10	10	2.92
Gd	64	84	84	2.08

Tb	65	0.09	0.09	2.13
Dy	66	2.0	2.0	2.23
Ho	67	0.015	0.015	2.33
Er	68	0.36	0.41	2.40
Tm	69	0.25	0.25	2.48
Yb	70	0.076	0.076	2.55
Lu	71	0.22	0.22	2.63
Hf	72	0.20	0.20	2.72
Ta	73	0.044	0.067	2.80
W	74	0.036	0.058	2.88
Re	75	0.16	0.16	2.95
Os	76	0.028	0.028	3.02
Ir	77	0.80	0.80	3.09
Pt	78	0.015	0.050	3.15
Au	79	0.17	0.20	3.21
Hg	80	0.63	0.71	3.31
Tl	81	0.006	0.027	3.41
Pb	82	0.0003	0.034	3.50
Bi	83	0.00003	0.029	3.57
Th	90		0.033	3.80
U	92	0.005	0.028	3.90

APPENDIX BWELD DEFECTS

The information contained in this appendix is a summation of given in Prof. K. Masubuchi's 13.39 class notes, and chapter 6 of Welding Handbook (M-5, W-5). The purpose is primarily to give a description of and to explain the nature of the common defects found in welded structures for background information. This presentation is by no means all inclusive.

Weld defects can be classified into three general catagories:

1. dimensional discrepancies
2. structural discontinuities
3. detective properties

A satisfactory weld depends on the maintenance of specified properties of the weld or finished structure. Any one or combination of the general defect catagories listed above may result in the weld being unsatisfactory and requiring repair or complete rework. A description of the defects that fall into three general catagories is listed below:

B.1 DIMENSIONAL DISCREPANCIES

a. Warpage or Distortion - warpage or distortion is exactly what the words imply, the structure being welded bends or warps. This type can be controlled by using suitable jigs and the proper welding sequence.

b. Incorrect Joint Penetration - established welding practices require proper joint dimensions for each type of joint consistent with the thickness of the material being welded. Guidance for joint penetration is usually given in the design specifications. Failure to comply with the specification can result in structural discontinuities.

c. Mismatch - This term is sometimes used to denote the amount of offset, usually measured from the centerline (ϕ) of two members in butt welds. Not only does this result in surface discontinuity, but it can also result in the formation of a stress riser. The design specifications usually give the limits on mismatches.

d. Weld size and weld profile - Both weld size and profile are important, they have considerable effect on performance of the weld, and they structurally effect the final product. The reasons are mainly due to strength, stress riser, and improper welding techniques. Again,

the allowable limits for weld profile and size are found in the specifications.

B.2 STRUCTURAL DISCONTINUITIES

Structural discontinuities are cracks, slag, inclusions and other faults that are not metallurgical structural damage but interruptions or discontinuities in the soundness of the weld.

A. Slag Inclusions - The term slag is used to describe the non-metallic solids that are entrapped in the weld metal or between the weld metal and base metal. The slag generally comes from the electrode covering materials or fluxes employed in the arc welding process. Most of the slag inclusions may be prevented by proper preparation of the groove before each bead is deposited, elimination of poor welding conditions, and the use of proper welding techniques.

B. Tungsten Inclusions - The occasional touching of the electrode to the work or to the molten weld metal in the gas tungsten-arc welding process, particularly the manual process, may result in the transfer of tungsten into the weld deposit. These tungsten inclusions generally are undesirable and a limit on the size and number of these

inclusions is usually specified.

C. Inadequate Joint Penetration - Penetration is a term that describes how far the weld extends into a joint, it is relatively limited in application to fillet welds, being used only to describe the depth that the weld fuses or penetrated into the base metal root. Inadequate joint penetration is then used to describe the condition where the joint penetration is less than specified.

D. Incomplete Fusion - Incomplete fusion or lack of fusion is used to describe the failure of adjacent layers of weld metal or adjacent weld metal and base metal to fuse together. Incomplete fusion may be caused by either failure to raise the temperature of the base metal or previously deposited weld metal to the melting point, or failure to remove slag; mill scale, oxides or other foreign material from the surface to which the deposited metal must fuse.

E. Porosity - Porosity is the gas pockets or voids free of any solid material frequently found in welds. Porosity comes from gas released by the cooling weld metals because of reduced solubility as the temperature drops, and from gases formed by chemical reactions in the weld. Porosity may be caused by excessive welding heats or incorrect manipulation.

F. ARC Strikes - Arc strikes represent an unintention-

al melting or heating outside the intended weld deposit area. They are usually caused by the welding arc and result in a small melted area which can produce undercut, hardening, or localized cracking depending on the base metal.

G. Undercut - Undercut is a term used to describe a groove or hollow melted into the base metal adjacent to the toe of the weld which is subsequently left unfilled by the weld metal. Undercut can also describe the melting away of a layer of the sidewall of a welding groove at the edge of a layer of bead, thus forming a sharp recess in the sidewall which the next layer or bead must fuse. The danger of an undercut is it may materially reduce the strength of the joint, particularly with regard to fatigue stresses.

H. Cracks - Cracks result from ruptures of metals under stress and are one of the most harmful of welding defects and are prohibited by most welding specifications. There are numerous types of cracks with just as many causes, some occur in the weld and others occur in the base metal. But no matter what type of crack is found, it more than likely could have been prevented if proper welding techniques were used. A detailed description of each crack type is given in the Welding Handbook (W-5).

As was mentioned before, cracks are extremely harmful. For this reason specifications are reluctant to specify an allowable maximum crack size. Instead they usually specify that only cracks too small to be resolved by inspection procedures will be permitted.

B.3 DEFECTIVE PROPERTIES

Defective properties can occur in both the weld and the base metal. They are usually found by specific destructive tests that are performed on test samples. The properties that the metal must exhibit are generally mechanical and chemical properties set by codes and specifications. Mechanical properties include; tensile strength, yield strength, ductility, hardness, and others. Similarly, the chemical properties usually include correct weld metal composition, base metal composition, and corrosion properties.

It should be pointed out, that not all defects are due to improper welding or welding conditions but are often due to the base metal properties and defects that come through in the base metal. Again, material and product specifications and good quality control must be observed for a satisfactory product. The following Figures

129.

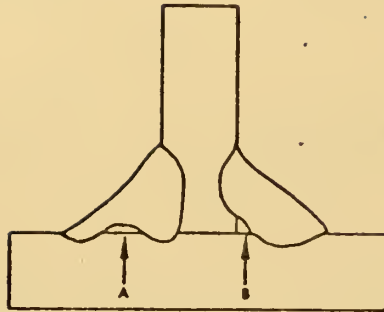
show many of the previously mentioned defects (M-5, W-5).



Figure B-1 Porosity



Figure B-2 Slag Inclusion, Between Passes (A)
Undercut (B)



a. Incomplete Fusion in Fillet Welds.
B is often termed "bridging."



b. Incomplete Fusion in a Groove Weld.

Figure B-3 Incomplete Fusion

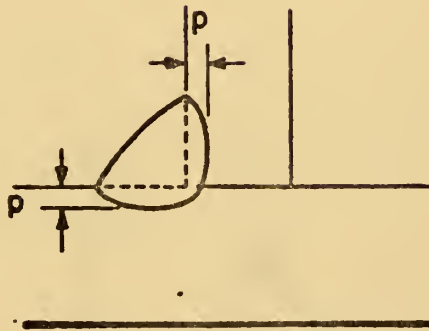
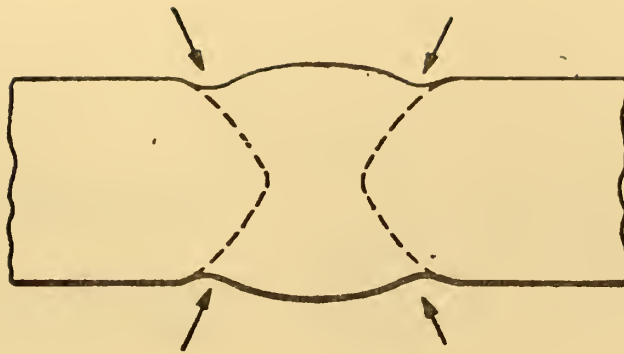
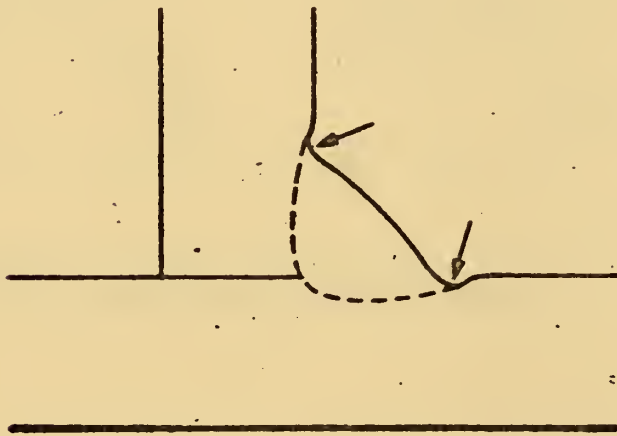


Figure B-4 Penetration (P)



a. UNDERCUTTING IN A BUTT WELD



b. UNDERCUTTING IN A FILLET WELD

Figure B-5 Undercutting

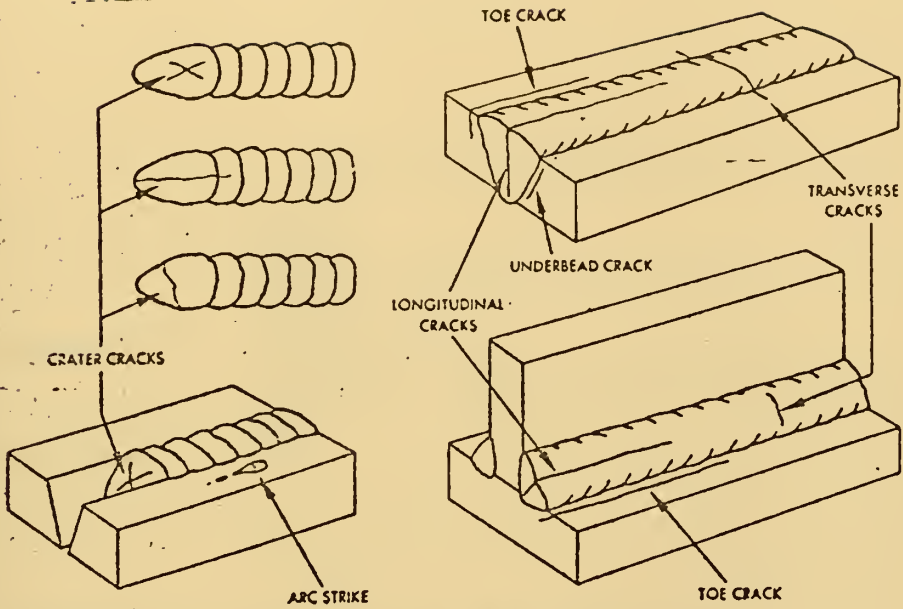


Figure B-6 Cracks in Welded Joints

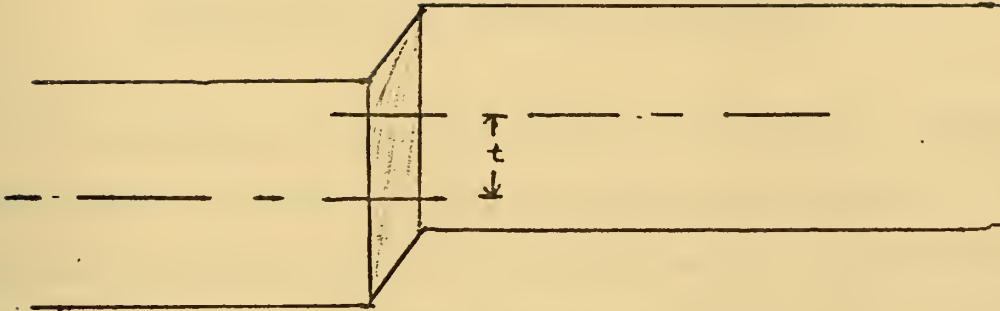


Figure B-7 Mismatch of Butt Weld (t)

APPENDIX CAPPLICATIONS OF NEUTRON RADIOGRAPHY

In addition to the inspection of weldments, neutron radiography can also be used in other areas as well. One of the most promising areas of use for neutron radiography is in the inspection of heavy metals such as lead, bismuth, or uranium. The advantages of neutron radiography over other radiographic techniques in inspecting these metals lies in the fact that neutrons are attenuated less and scatter less than other forms of radiation, resulting in radiographs with very large contrasts (S-2).

Neutron radiography has also proven itself extremely useful in the area of reactor technology where it is used to inspect control rods for content and continuity, inspect shielding materials for defects, locate organic residues from organic coolant, and locate hydrides or boron in fuel cladding, and lastly to inspect fuel elements. This last application, inspection of fuel elements is extremely adaptable to neutron radiography not only due to the fact that the fuel behaves as a heavy metal, but also the fuel tends

to emit radiation itself. This latter problem clouds the radiograph when conventional methods are used. However, it is eliminated when neutron radiography and the transfer technique are used (B-1).

Neutron radiography is also used in the inspection of multi-element components containing fiberglass or similar materials. Materials such as this can often present problems for X-ray inspection because the cross-hatched pattern of the fiberglass strands on the radiograph tends to obscure other detail. On a neutron radiograph, however, the low attenuation of the oxygen and silicon in the fiberglass all but eliminates this background pattern and makes the radiograph easier to view (Y-1). Extensive work with neutron radiography and fiberglass laminates has been done at the Naval Ordinance Research Laboratory (NORL).

Other work done at NORL by the Navy and similar work done by the Army at Watertown Arsenal was the feasibility of using neutron radiography for quality assurance inspection of various explosives and explosive devices. The results obtained were extremely favorable, the contrast between components was exceedingly good and radiographs used to determine explosive mixture continuity were satisfactory (Y-1). The only mark on an otherwise outstanding study

was the almost prohibitive cost of a suitable neutron source. However, since this study the availability of neutron sources has increased and the cost has dropped considerably.

Aerojet General has developed a unique use for neutron radiography. They use it to insure the cooling channels in gas turbine blades they manufacture are clear. They found that X-rays were unable to insure the quality needed, so they tried neutron radiography. It was better, but using an enhancing fluid like cadmium nitrate they were able to image all the channels and also detect cracks or flaws in the blades as well (A-4).

There are numerous other uses for neutron radiography. Some of these include: examination of large-thick sections of cast solid fuel for rockets and missiles, inspection of rubber, plastic or metal gaskets for correct position and seating, inspection of metal plate for homogeneity and continuity, and the inspection of insulation for flaws and defects. Neutron radiography has also shown its value in the field of research in such areas as: diffusion of materials, the study of thin biological specimens, the observation of hydride precipitation in single crystal zirconium and the detection of variations in magnetic properties (B-1).

It should be pointed out that neutron radiography can be an extremely useful method for nondestructive testing, both as a complementary technique to gamma or X-radiography and in a number of specialized areas in which the attenuation differences between X-ray and neutrons are not of primary importance. Although it is unlikely that neutron inspection will ever achieve the wide spread use made of X-ray techniques, continued improvements in detection methods and neutron sources; particularly the latter as applied to other than reactor sources, will undoubtedly stimulate further application of neutron radiography. This addition of neutron techniques to radiographic inspection adds one more useful variable which will contribute to the increasing usefulness of radiography as an inspection method in the industrial and scientific fields.

APPENDIX DNON-DESTRUCTIVE TESTING METHODS

Several methods have been developed to examine welds for defects, some of the more common methods are described herein. The information contained, is sufficient for a basic understanding of how these various NDT methods work and their primary limitations, however more specific information is available. Of particular value are:

Non-Destructive Testing Handbook Vols. 31 and 32 (A-3)

and

Welding Handbook (W-5)

The two above mentioned publications along with Prof. K. Masubuchi's 13.30 class notes (M-5) are the primary sources for this appendix.

D.1 MAGNETIC PARTICLE INSPECTION

Magnetic particle or "Magniflux" inspection is a non-destructive method of detecting the presence of seams, cracks, porosity, inclusions and similar discontinuities in magnetic materials, but is not applicable to nonmagnetic

materials. This method can detect surface discontinuities that are not visible with the naked eye, and those that lie slightly below the material surface. It is also possible with special equipment to test for deeper faults, however with other test methods available, this is not always economical.

The basic principle involved in "Magniflux" inspection is to establish a magnetic field in the test object so that if there is a fault, a small magnetic pole is established. The poles then have a somewhat stronger attraction for magnetic particles than does the remaining test object. As a result, the magnetic particles form a pattern on the surface which is an indication of the approximate shape of the discontinuity.

Direct current, alternating current, and reactivated current can all be used to magnetize the object to be tested. Usually, low voltage high amperage current is used to perform the tests. If alternating current is used, only the surface of the test object is magnetized. It is effective for locating discontinuities extending to the surface, such as service of fatigue cracks, and is usually used to inspect welds where subsurface evaluation is not required.

Direct current testing on the other hand, is more sensitive than alternating current for the detection of subsurface faults because it produces a field which penetrates through out the object. Thee phase rectified current produces results essentially comparable to direct current obtained thru a battery. However, half wave rectified single phase current provides maximum sensitivity. The pulsating field increases the particle mobility and enables the magnetic particles to line up more readily in weak leakage fields.

D.2 ULTRASONIC INSPECTION

Ultrasonic inspection or "UT" depends on the use of high frequency sound waves to detect, locate, and measure discontinuities in an object. Of all the test methods, "UT" requires the greatest degree of skill to get accurate results, and also to interrupt them.

The ultrasonic testing of welds depends on the use of a refined sonar^hlike technique. An electrical pulse is produced by the instrument, and a suitable transducer converts the electrical signal to mechanical vibrations, or sound. The sound waves used in weld inspection are usually in the frequency range between 1 mHz and 5 mHz. The sound beam

generated by the transducer is introduced into the part being tested through a liquid couplement. This thin film of liquid excludes air and permits the passage of the sound, the liquid most commonly used is glycerin. The discontinuities reflect part of the wave and this is picked up and appears as a pip (vertical indication) in the line on the screen of a cathode-ray tube. This is the principle of the ultrasonic reflectoscope. The instrument is designed to register the time required to reflect a wave from a discontinuity, the length of time is then proportional to the distance travelled. Interruption of the sound wave is seen on the screen in the form of a horizontal displacement of the indication. This indication may be photographed if a permanent record is desired. Other special purpose ultrasonic devices have built in recorders, such as tube testers, these units give a permanent record printout of the test and also the location from a zeroing point (usually the tube mouth).

The sound beam interrogates only a small portion of the entire volume of the weld at a given instant. In order to check the entire volume of the weld the transducer must be moved in some adequate scan pattern. It is usually oscillated so that, the sound beam scans the weld in various directions.

D.3 PENETRANT INSPECTION

Penetrant inspection is a sensitive, nondestructive method of detecting and locating minute discontinuities that are open to the surface, such as cracks, pores and leaks. It employs a penetrating liquid which is applied over the surface and enters the discontinuity. Subsequently, after the excess of penetrant has been cleaned from the surface, the penetrant which exudes or is drawn out of the crack is observed, indicating the presence and location of the discontinuity. It is particularly useful on nonmagnetic materials, where magnetic particle inspection cannot be used. In the welding field, it is used extensively for exposing surface defects in aluminum, magnesium and austenitic steel weldments, and for locating leaks in all types of welds.

Penetrant inspection is relatively inexpensive and reasonably rapid. The process is essentially simple and operators find no difficulty in learning to apply it properly. There are a few if any false or non-relevant indications so interpretation is somewhat easier than with magnetic particle inspection. The success of penetrant inspection, like most other inspection methods, depends upon the eye of the inspector and his ability and willingness to do a conscientious job.

Penetrant inspection is the most sensitive method for locating fine, short and shallow cracks in non-magnetic materials. The magnetic particle method is its equal in this respect on magnetic materials and is more reliable on cracks which may be filled with foreign material.

Dye penetrant inspection has several advantages. These include:

1. Dye penetrant equipment is inexpensive.
2. Equipment is portable and suitable for field inspection parts can be inspected in position.
3. The dye indications of a defect often are left on the part to show the location to the grinder and welder.
4. The indications are easily photographed.

D.4 EDDY CURRENT TESTING

An eddy-current testing system consists of a source of alternating electrical current of known frequency applied to a test coil assembly, and an electronic detecting system to sense and indicate variations in the output of the coil assembly resulting from changes in the electromagnetic field of the coil assembly caused by discontinuities in material passing in proximity to the coil assembly. The detecting

system may include an adjustable phase selective system as well as a filter circuit for the purpose of enhancing the response to specific kinds of variations present in the output of the test coil assembly and reducing the effects of unimportant variations. When such selective methods are present, means must be provided to ensure that their correct adjustment may be prescribed or verified. This may be accomplished either by the use of calibrated controls or the incorporation of an indicator to monitor the electrical signals. The stability of the eddy-current testing system shall be such that repeatable results are obtained when a calibration standard is passed through, the equipment at various times.

A suitable means is often utilized to ensure that the portion of the object under inspection and in the vicinity of the test coil assembly is rendered substantially non-magnetic. This means may consist of a suitably cooled coil energized by direct current and the material under inspection. A magnetic circuit energized by direct current or permanent magnets may be utilized where they produce the degree of magnetic saturation required.

D.5 RADIOGRAPHIC INSPECTION

Radiographic inspection involves the use of radiation from specially constructed industrial X-ray machines, or the use of gamma rays from a radioactive source. Short wave length radiations, such as X-rays or gamma rays, penetrate objects opaque to ordinary light. In general, the shorter the wave length, the greater the penetrating power. Should there be a cavity, such as a blowhole, in the weld interior, the beam of radiation will have less metal to pass through than in a sound metal. Consequently, there will be a variation in the absorption of the rays by the weld in the defective region, which variation, if measured or recorded on a film sensitive to the radiation, produces an image that will indicate the presence of the defect. The image is an X-ray shadow of the interior defect. Such a shadow picture is called a radiograph.

A common source of radiation for radiographic inspection is an X-ray tube. X-ray machine up to 2 million volts are available. Table D-1 shows typical industrial radiation sources and their applications. Generally, the higher the voltage, the shorter the wave length and thus greater the penetrating power. Approximate practical thickness limits for steel also are listed in the table.

Gamma rays produced by the atomic disintegration of radium or of several radioisotopes also are used for radiographic examination of welds. Common sources of radiation used in gamm-ray radiography include radium, cobalt 60, iridium, 192, and cesium 137. The radioactive sources are usually sealed in a capsule to provide a means of handling them without harm to the radiographer.

It is not easy to compare the merits of X-rays and gamma rays as a source of radiation for radiography. Each has a definite application in its own field with one hardly a substitute for the other. Because of the lower absorption coefficient of gamma rays as compared to the longer wave lengths of X-rays, the general rule is that lower-contrast radiographs will result. The lower intensity of this radiation as compared to that obtained with X-ray equipment makes necessary the use of long exposure times, which are not always practical or economical. Gamma rays, like high voltage X-rays, are found to be extremely valuable in radiographing materials having high subject contrast. The principal advantage of this source of radiation is that it is extremely portable.

It is generally assumed that radiographic methods will produce films having a sensitivity of 2 percent. When

sensitivity is spoken of, it is considered to mean the least percent of weld thickness difference when can be detected visually on a radiograph.

Cracks in welds produce film images of a line darker than the film background. Because they extend primarily in one plane, some of them require the best techniques to produce a satisfactory image on the film. This is particularly true when the plane in which they lie is not parallel to the radiation beam, as, for example, a crack following the dendritic structure of some welds.

Other defects include inadequate joint penetration, undercut, surface defects and incomplete fusion. The ability to recognize these according to type is largely a matter of experience and acquaintance with standards. The limits of acceptability are defined in applicable codes and specifications.

D.6 COMPARISON OF TESTS

The following tables compares radiographic, ultrasonic, and dye penetrant tests methods. The table indicates when, where, why to use a test methods and limitations of these test methods (M-5).

TABLE D-1

TYPICAL INDUSTRIAL RADIATION SOURCES
AND THEIR APPLICATIONS

<u>Teak Kilovoltage (Kvp), Max.</u>	<u>Screens</u>	<u>Approximate Pract- ical Thickness Limits</u>
	<u>X-rays</u>	
50	None	Microradiography, woods, plastics
100	None	2 in. Al 3 in. Mg
150	None or lead foil	4½ in. Al., 1 in. steel or equivalent
	Fluorescent	1½ in. steel or equivalent
250	Lead foil	2 in. steel or equivalent
400	Lead foil	3 in. steel or equivalent
	Fluorescent	4 in. steel or equivalent
1000	Lead foil	5 in. steel or equivalent
	Fluorescent	7 in. steel or equivalent
2000	Lead foil	9 in. steel or equivalent

Radioactive Material

Radium	Lead foil	8 in. steel or equivalent
Cobalt 60	Lead foil	1 to 6 in. steel or equivalent
Iridium 192	Lead foil	$\frac{1}{2}$ to 2 in. steel or equivalent
Desium 137	Lead foil	1 to $2\frac{1}{2}$ in. steel or equivalent

LIMITATIONS OF NDT METHODS

Category	Radiographic	Magnetic Particle	Ultrasonic (pulse-echo method)	Liquid Penetrant
When to Use	Detection of internal flaws and defects, weld flaw detection, cracks seams, porosity, holes, and inclusions, checking assemblies, and determining thickness variations.	Suitable for the detection of either or sub-surface flaws, cracks, porosity, nonmetallic inclusions and weld defects.	Used to find internal defects, cracks, lack of bond, laminations, inclusions, porosity, Resonance Method used primarily for thickness gaging and laminar flaws.	Used to locate open-to-the surface porosity, laps, cold shuts, lack of weld bond, fatigue and grinding cracks.
Where to Use	Forgings, castings, tubing formed metal parts, welded vessels, field testing of welds, corrosion surveys and assemblies.	Used on all types of ferromagnetic materials, tubing, piping of any size, shape, composition, or state of heat treatment. In-service testing for fatigue cracks.	Used on all metals and hard non-metallic materials, sheet, tube, rod, forgings, castings field and production testing, welds, silver-brazed pipe joints.	Used on all metals, glass, ceramics, castings, forgings, machine parts, cutting tools and field inspection.

Why
Use
It

Detects variety of flaws provides a permanent film record. Gamma sources very portable X-ray machines operable at various energy levels for different materials and thicknesses.

Simple in principle, easy to perform, portable for field testing, fast for production testing. Method is positive and cost is economical.

Fast and dependable easy to operate, lends itself to automation results of test immediately known, relatively portable, highly accurate and high sensitivity.

Simple to apply, Accurate, fast, low initial cost, and per test cost, easy to interpret results no elaborate setup required.

153.

Limita-
tions
of
Test

Power source required for X-ray Both produce radiation hazard. Well trained technician needed to make, interpret radio-graphs.

Test parts must be magnetic. Requires demagnetizing after test. Power source is required and parts must be clean before testing.

Requires contract with part to be tested. Interpretation of defects requires considerable training No permanent record reproduction of test results (without automatic recording devices).

COMPARISON OF NONDESTRUCTIVE TESTING METHODS

	Radio- graphic	Magnaflux	Ultrasonic	Liquid Penetrant

Thick- ness	KVP has to be increased as T in- creases	No effect	Easier for heavy plate	No effect
Mater- ial	Any material	Ferro- magnetic	Any material	Any material
Loca- tion of detect- able de- fects	Any where	Surface and near surface	Anywhere	Surface
Hairline crack	Diffi- cult	Easy	Easy	Easy
Butt weld	Yes	Yes	Yes	Yes
Filet weld	Diffi- cult	Yes	Diffi- cult	Yes
Cost (low ¹) (high ⁴)	4	2	3	1
Permanent record (yes ¹) (diffi- cult ⁴)	1	3	4	1
Skill involved (easy ¹) (diff- cult ⁴)	3	3	4	1

APPENDIX E
DATA SHEETS

Enclosed in this appendix is the data taken from MITR files used to get the first inium characteristic curve (Figure 3-6). This data appears in Figure E-1. The data in Figure E-2 is the data collected while taking radiographs at MITR for this thesis. Figure E-3 is the ultrasonic inspection data sheet and Figure E-4 thru E-7 are the radiographic record sheets for the four test samples.

Ref No.	T _{irr}	$1-e^{-kT_{irr}}$	T _{trans}	$e^{-kT_{trans}}$	T _{exp}	$1-e^{-kT_{exp}}$	Er	Ern	D
11	120	.785	10	.879	120	.785	542.0	24.39	2.4
12	240	.954	10	.879	340	.954	831.0	37.4	2.2
13	30	.319	10	.879	30	.319	89.0	4.0	.8
24	8	.120	10	.879	960	1.0	1.5.0	4.73	1.0
9	60	.536	10	.879	60	.536	252.0	11.3	1.18
10	120	.785	10	.879	120	.785	542.0	24.4	2.2
59	20	.226	10	.879	40	.401	79.7	3.6	.65
58	20	.226	10	.879	30	.319	63.4	2.85	.6
62	30	.319	10	.879	20	.226	63.4	2.85	.8

Figure E-1 Initial Characteristic Curve Data (Indium Foil)

Ref No.	Sample No.	T _{irr}	1-e ^{-λ_{Tirr}}	T _{trans}	e ^{-λ_{Ttrans}}	T _{exp}	1-e ^{-λ_{Texp}}	Er	Ern	D
68	F-1	60	.536	10	.879	30	.319	150.3	6.76	.773
69	B-2	90	.684	16	.825	35	.361	203.7	9.14	1.23
70	F-1	15	.072	15	.928	960	.99	66.1	66.1	5.85
71	F-1	40	.401	15	.825	60	.536	177.3	7.97	.884
72	B-1	90	.684	16	.825	40	.401	226.3	10.1	1.23
73	B-2	25	.117	10	.951	960	.99	115.8	115.8	OS
74	F-1	90	.684	15	.825	60	.536	302.5	302.5	1.74
75	B-1	25	.117	15	.928	960	.99	107.5	107.5	OS
76	F-1	18	.086	10	.951	960	.99	81.5	81.5	OS
77	B-1	20	.221	10	.879	25	.274	54.4	2.45	.405
78	B-1	35	.361	15	.825	40	.401	119.4	5.37	.767
79	B-1	160	.536	15	.825	60	.536	237.0	1.67	1.36
80	B-1	120	.785	25	.726	75	.61	347.6	15.6	1.97
81	F-1	10	.121	10	.819	20	.226	20	1.08	.284
82	B-1	5	.025	15	.928	960	.99	22.9	22.9	2.19
83	B-1	120	.785	20	.774	60	.536	326	14.8	1.79
84	F-1	120	.785	30	.681	120	.785	420	18.9	2.32
85	B-1	150	.853	30	.681	960	.99	581.0	26.1	2.80
86	B-2	15	.072	15	.928	960	.99	66.8	66.8	2.50
88	F-1	120	.785	25	.726	150	.853	486	21.9	2.56
87	F-2	20	.095	10	.951	960	.99	90.3	90.3	OS
89	B-1	120	.785	35	.639	060	.99	22.6	22.6	2.6

157.

Figure E-2 DATA SHEET FOR NEUTRON RADIOGRAPHS

Ref No.	Foil	Position	D'	S	D'/D	t	u
68	In	B/UR	.445		.576	2.54	.217
69	In	X/A	.626	2-2T	.509	5.08	.203
70	Dy	B/UR	2.65	1-2T		2.54	
71	In	B/UR	.528	2-2T	.597	2.54	.203
72	In	Y/A	.64	2-2T	.520	2.54	.257
73	Dy	X/A	2.12			5.08	
74	In	A/UR	.88	4-1T	.313	2.54	.268
75	Dy	X/A				2.54	
76	Dy	A/UR		2-2T		2.54	
77	In	Y/A	.298	2-2T	.735	2.54	.121
78	In	Y/A	.482	2-2T	.633	2.54	.180
79	In	Y/A	.79	1-4T	.581	2.54	.214
80	In	Y/A	.89	1-4T	.452	2.54	.313
81	In	A/UR	.218	1-4T	.768	2.54	.104
82	Dy	Y/A	1.03	4-2T	.470	2.54	.298
83	In	Y/A	.928	2-2T	.511	2.54	.259
84	In	A/UR	1.08	2-2T	.466	2.54	.296
85	In	Y/A	1.26	4-2T	.450	2.54	.314
86	Dy	A/Y	1.16		.144	5.08	.381
88	In	45°	1.19		.464	2.54	.302
87	Dy	A/UR		4-2T		5.08	
89	In	+5	1.83	1-4T	.466	2.54	.301

Figure E-2. (cont)

Ref No.	Sample No.	T _{irr}	1-e ^{-λ_{Tier}}	T _{trans}	e ^{-λ_{Ttrans}}	T _{exp}	1-e ^{-λ_{Texp}}	Er	Ern	D
90	B-2	20	.095	10	.951	960	.99	90.3	90.3	OS
91	B-1	10	.049	10	.951	960	.99	46.6	46.6	4.45
92	B-1	35	.365	10	.879	30	.319	102	4.62	.64
93	B-1	90	.684	15	.825	60	.536	303	13.6	1.64
94	B-2	10	.049	30	.861	960	.99	41.7	41.7	4.3
95	F-1	10	.049	20	.905	960	.99	44.3	44.3	4.68
98	F-1	90	.684	15	.825	90	.684	386	17.4	2.1
96	B-1	15	.072	10	.951	960	.99	67.8	67.8	5.6
97	B-1	90	.684	20	.774	45	.438	232	10.4	1.35

Figure E-2. (cont.)

Ref No.	Foil	Position	D'	S	D'/D	t	u
90	Dy	A/Y		2-2T		5.08	
91	Dy	+2.5	1.83	1-4T	.411	2.54	.35
92	In	Y/A	.399	2-4T	.623	2.54	.186
93	In	Y/A	.856	2-2T	.522	2.54	.256
94	Dy	Y/A	.727	2-2T	.169	5.08	.35
95	Dy	30°	1.97	2-4T	.412	2.54	.349
98	In	60°	1.02	2-4T	.486	2.54	.285
96	Dy	H ₂ O				2.54	
97	In	Dye				2.54	

Figure E-2. (cont.)

PIPE & HULL RADIOGRAPHIC RECORD SHEET
IND-PHS-4730/135 (1679) (REV 10-69)

Non-Destructive Test Branch (Code 133.1)

TECHNICAL DATA NO.	PROCESS INSTRUCTION FOLLOWED	DATE	SHIP
	0152-926-065	3/13/73	BLDG 184
			JOINT IDENT OR ITEM NO.
			1356 B1
			PLAN NO.
			M.I.T. PROJECT

Ref: PHSY Process Instruction 0552-926-199 -0152-926-065

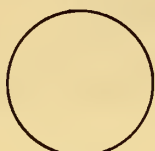
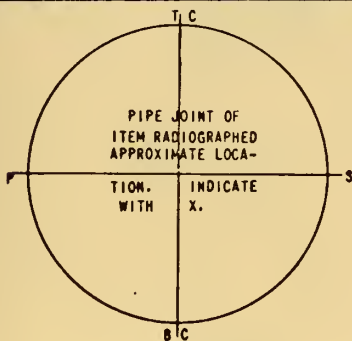
MATERIAL		SHIM OR BLOCK		PENETRATOR(S)	
TYPE	THICKNESS	THICKNESS	<input checked="" type="checkbox"/> SS <input type="checkbox"/> FS	SIZE, (S)	
HY-80	1"	1/4		1.0	
PIPE SIZE		PIPE JOINT TYPE		WELD SURFACE CONDITION	
DIAMETER	WALL THICKNESS	<input type="checkbox"/> BACKING <input type="checkbox"/> INSERT <input type="checkbox"/> OTHER	<input checked="" type="checkbox"/> ACCEPTABLE <input type="checkbox"/> NDT ACCEPTABLE	<input checked="" type="checkbox"/> ETCHED <input type="checkbox"/> NOT ETCHED	
TECHNIQUE		FILM		SCREENS	
<input checked="" type="checkbox"/> A <input type="checkbox"/> B <input type="checkbox"/> C <input type="checkbox"/> D	TYPE	SIZE	<input type="checkbox"/> SINGLE <input checked="" type="checkbox"/> DOUBLE <input type="checkbox"/> SPECIAL	FRONT	BACK
	AA	8X10		10	10
X-RAY			EXPOSURE DATA		
MACHINE	KV	MA	FOCAL SPOT SIZE	EXPOSURE TIME	QUALITY LEVEL
				MIN SEC	
ISOTOPE			EXPOSURE TIME		
<input checked="" type="checkbox"/> IRI92 <input type="checkbox"/> CO60	SHOP NO.	CURIES	SOURCE DIMENSIONS	3 MIN 2415S	24"
	21	65	.100 X .100 IN.		2-2T
WORK SITE			EXCEPTIONS		
BUILDING NO.	BOAT COMPARTMENT	FRAME	FILM LOCATION		
176		<input type="checkbox"/> P <input type="checkbox"/> S <input type="checkbox"/> UL <input type="checkbox"/> LL	A 3 MIN		
RADIOGRAPHER			B " "		
SIGNATURE			AB 2M15S		
33-12145					
WORK STATUS					
<input checked="" type="checkbox"/> COMPLETE <input type="checkbox"/> NDT COMPLETE	NUMBER OF EXPOSURES				
	3				

REMARKS

SOURCE OFFSET 7" LOCS. A & B

SOURCE CENTERED LOC. AB

SIDE X IS SOURCE SIDE



INDICATE STATION LOCATIONS

SKETCH

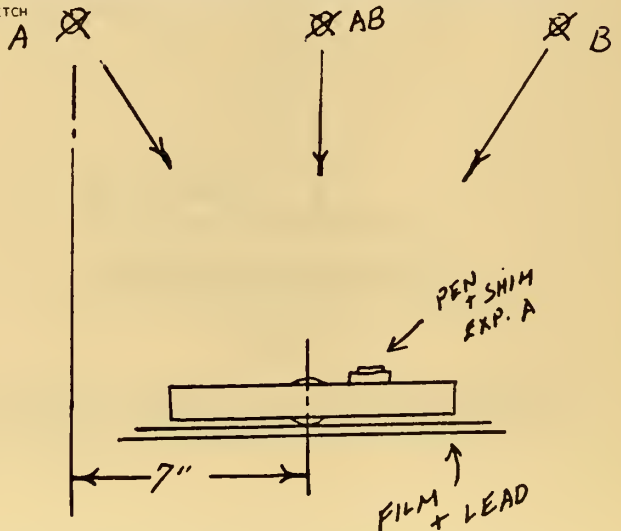


Figure E-4 Radiographic Inspection Sheet for Sample B-1

Non-Destructive Test Branch (Code 133.1)

163.
3/13/73

SHIP *BLDG 184*

JOINT IDENT OR ITEM NO.
1356 T1

PLAN NO.
M.I.T. PROJECT

TECHNICAL DATA NO.

PROCESS INSTRUCTION FOLLOW-UP

0152-926-065

Ref: PHSY Process Instruction 0552-926-199 -0152-926-065

MATERIAL		SHIM OR BLOCK		PENETRATOR(S)	
TYPE HY-80	THICKNESS 1"	THICKNESS 1/8 1/2	<input checked="" type="checkbox"/> SS <input type="checkbox"/> FS	SIZE (S) 1.0	
PIPE SIZE		PIPE JOINT TYPE		WELD SURFACE CONDITION	STATION LOCATIONS
DIAMETER	WALL THICKNESS	<input type="checkbox"/> BACKING RING	<input type="checkbox"/> INSERT <input type="checkbox"/> OTHER	<input checked="" type="checkbox"/> ACCEPTABLE <input type="checkbox"/> NOT ACCEPTABLE	<input checked="" type="checkbox"/> ETCHED <input type="checkbox"/> NOT ETCHED
TECHNIQUE		FILM		SCREENS	
<input checked="" type="checkbox"/> A <input type="checkbox"/> B <input type="checkbox"/> C <input type="checkbox"/> D	TYPE AA	SIZE 8X10	<input type="checkbox"/> SINGLE <input checked="" type="checkbox"/> DOUBLE <input type="checkbox"/> SPECIAL	FRONT 10	BACK 10
X-RAY				EXPOSURE DATA	
MACHINE	KV	MA	FOCAL SPOT SIZE	EXPOSURE TIME MIN SEC	F F O QUALITY LEVEL
ISOTOPE				EXPOSURE TIME MIN SEC	F F O QUALITY LEVEL
<input checked="" type="checkbox"/> IR192 <input type="checkbox"/> CO60	SHOP NO. 21	CRIES 65	SOURCE DIMENSIONS .100 X 100 N.	3 M	24 " 2-RT
WORK SITE				EXCEPTIONS	FILM LOCATION
BUILDING NO. 176	BOAT COMPARTMENT	FRAME			A
RADIOGRAPHER					B
SIGNATURE H. Goulet - PRUNIER		CHECK NO. 33-12145			
WORK STATUS					
<input checked="" type="checkbox"/> COMPLETE <input type="checkbox"/> NOT COMPLETE		NUMBER OF EXPOSURES 2			

SOURCE OFFSET 7"

SIDE X IS A SIDE - B IS ON SIDE Y

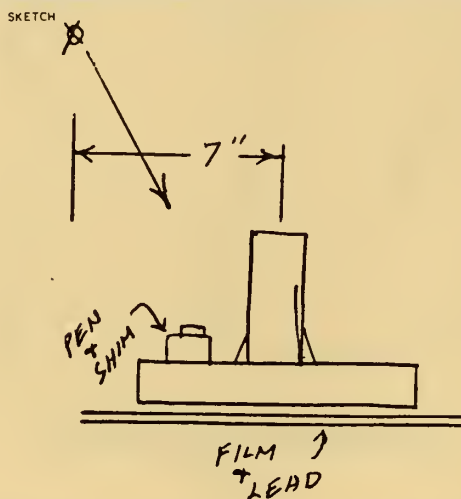
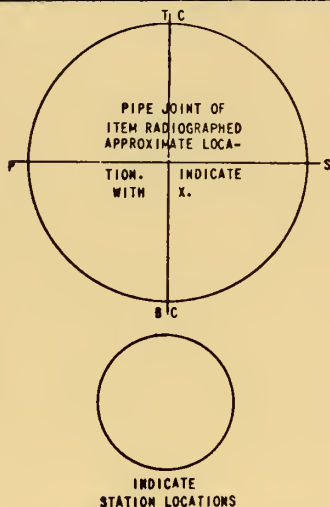


Figure E-5 Radiographic Inspection Sheet for Sample F-1

164.

PIPE & HULL RADIOGRAPHIC RECORD SHEET
IND-PNS-473D/135 (1679) (REV 10-69)

Non-Destructive Test Branch (Code 133.1)

DATE 3/13/73		SHIP BLDG 184	
JOINT IDENT OR ITEM NO. 1356 B 2		PLAN NO. M.I.T. PROJECT	
TECHNICAL DATA NO.		PROCESS INSTRUCTION FOLLOWED OIS2-926-065	
Ref: PNSY Process Instruction 0552-926-199 -0152-926-065			
MATERIAL TYPE HY-80 THICKNESS 2"		SHIM OR BLOCK THICKNESS 1/4	
PENETRATOR(S) SIZE (S) 2.0		PIPE JOINT TYPE <input checked="" type="checkbox"/> SS <input type="checkbox"/> FS	
PIPE SIZE DIAMETER WALL THICKNESS		WELD SURFACE CONDITION <input checked="" type="checkbox"/> ACCEPTABLE <input type="checkbox"/> NOT ACCEPTABLE	
PIPE JOINT TYPE <input type="checkbox"/> BACKING <input type="checkbox"/> RING <input type="checkbox"/> INSERT <input type="checkbox"/> OTHER		STATION LOCATIONS <input checked="" type="checkbox"/> ETCHED <input type="checkbox"/> NOT ETCHED	
TECHNIQUE <input checked="" type="checkbox"/> A <input type="checkbox"/> B <input type="checkbox"/> C <input type="checkbox"/> O		FILM TYPE AA SIZE 8x10 <input type="checkbox"/> SINGLE <input checked="" type="checkbox"/> DOUBLE <input type="checkbox"/> SPECIAL	
SCREENS FRONT 10 CENTER - BACK 10			
X-RAY MACHINE KV MA FOCAL SPOT SIZE		EXPOSURE DATA EXPOSURE TIME F F D QUALITY LEVEL	
ISOTOPE <input checked="" type="checkbox"/> IRI92 <input type="checkbox"/> CO60 SNOP NO. 21 CURIES 65 SOURCE DIMENSIONS 100x100 IN.		EXPOSURE TIME 6 1/2 MIN 10 MIN F F D 24 QUALITY LEVEL 2-2T	
WORK SITE BUILDING NO. 176 BOAT COMPARTMENT FRAME <input type="checkbox"/> P <input type="checkbox"/> S <input type="checkbox"/> UL <input type="checkbox"/> LL		EXCEPTIONS	
RADIOGRAPHER SIGNATURE J. Coull - LIBERTY CHECK NO. 33-12145		FILM LOCATION A 10 MIN B " " A B 6 1/2 MIN	
WORK STATUS <input checked="" type="checkbox"/> COMPLETE <input type="checkbox"/> NOT COMPLETE NUMBER OF EXPOSURES 3			
REMARKS A + B EXPS. 7" OFF CENTER A B EXPS ON CENTER SIDE Y IS AT TOP - SOURCE SIDE			

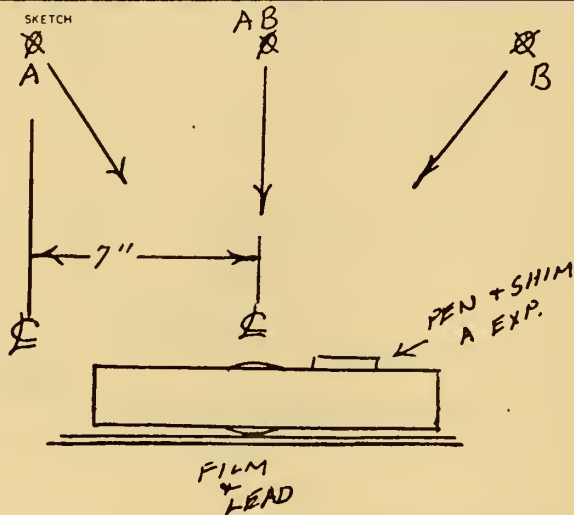
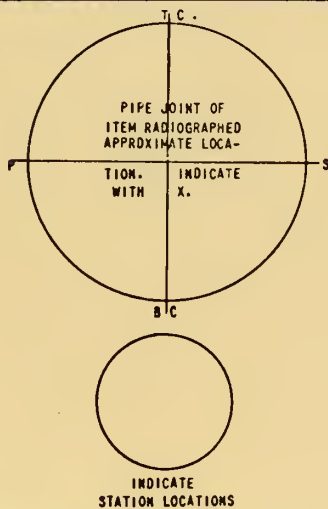


Figure E-6 Radiographic Inspection Sheet for Sample B-2

165.

PIPE & HULL RADIOGRAPHIC RECORD SHEET
IND-PMS-4730/135 (1679) (REV 10-69)

Non-Destructive Test Branch (Code 133.1)

TECHNICAL DATA NO.		PROCESS INSTRUCTION FOLLOWED		DATE 3/13/73	SHIP BLDG 184
Ref: PMSY Process Instruction 0552-926-199 -0152-926-065		0152-926-065		JOINT IDENT OR ITEM NO. 1356-T2	PLAN NO. M.I.T. PROJ.
MATERIAL		SHIM OR BLOCK		PENETRATOR(S)	
TYPE HY-80	THICKNESS 2"	THICKNESS 1/4 3/4	<input checked="" type="checkbox"/> SS <input type="checkbox"/> FS	SIZE (S) 2.0	
PIPE SIZE		PIPE JOINT TYPE		WELD SURFACE CONDITION	
DIAMETER	WALL THICKNESS	<input type="checkbox"/> BACKING <input type="checkbox"/> INSERT <input type="checkbox"/> OTHER		<input checked="" type="checkbox"/> ACCEPTABLE <input type="checkbox"/> NOT ACCEPTABLE	
		<input type="checkbox"/> RING		<input checked="" type="checkbox"/> ETCHED <input type="checkbox"/> NOT ETCHED	
TECHNIQUE		FILM		SCREENS	
<input checked="" type="checkbox"/> A <input type="checkbox"/> B <input type="checkbox"/> C <input type="checkbox"/> D		TYPE AA SIZE 8X10 <input type="checkbox"/> SINGLE <input checked="" type="checkbox"/> DOUBLE <input type="checkbox"/> SPECIAL		FRONT 10 CENTER - BACK 10	
X-RAY				EXPOSURE DATA	
MACHINE	KV	MA	FOCAL SPOT SIZE	EXPOSURE TIME	QUALITY LEVEL
			MM	MIN SEC	
ISOTOPE				EXPOSURE TIME	
<input checked="" type="checkbox"/> IRI92 <input type="checkbox"/> CO60 SHOP NO. 21 CURIES 65 SOURCE DIMENSIONS 100 X 100 IN.				16 MIN 24" 2-2T	
WORK SITE				EXCEPTIONS	
BUILDING NO. 176	BOAT COMPARTMENT	FRAME		FILM LOCATION	
		<input type="checkbox"/> P <input type="checkbox"/> S <input type="checkbox"/> LL		A	
RADIOGRAPHER				B	
SIGNATURE 26. Bond-LIBERTY		CHECK NO. 33-12145			
WORK STATUS					
<input type="checkbox"/> COMPLETE <input type="checkbox"/> NOT COMPLETE		NUMBER OF EXPOSURES 2			
REMARKS					
EACH EXP. 7" OFF CENTER					
"A" IS ON SIDE "Y"					

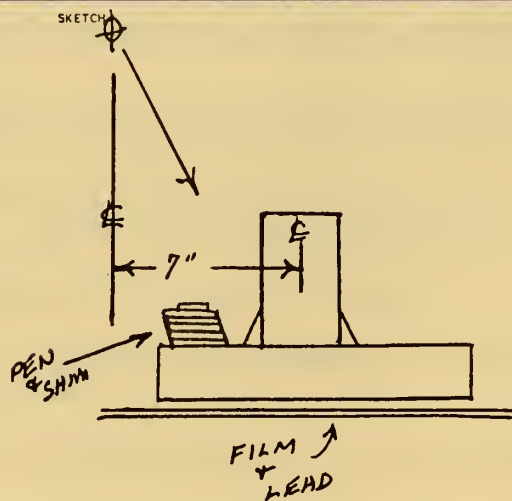
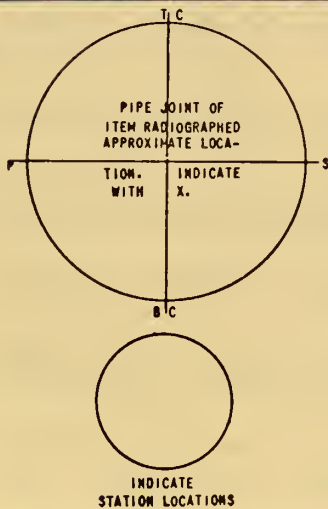


Figure E-7 Radiographic Inspection Sheet for Sample F-2

APPENDIX F

REFERENCES

- A-1. Annual ASTM Standards, NDT, 1972.
- A-2. ANL-4800, Reactor Physics Constants, USAEC, 1963.
- A-3. ASTM, Non Destructive Testing, Section E-142, 1972.
- A-4. Areojet General, Private Communication 1972.
- B-1. BERGER, Harold, Neutron Radiography, New York: Eisenuler Publications Co., 1965.
- B-2. BERGER, Harold, "Neutron Radiography", Annual Review of Nuclear Science, Vol. 21, 1971.
- B-3. BERGER, Harold, "Some Experiments in Fast Neutron Radiography", Materials Evaluation, Dec. 1969.
- B-4. BERGER, Harold, Annual Review of Nuclear Science, 21:337, 1971.
- B-5. BERGER, Harold, Materials Evaluation, 27:245, 1969.
- B-6. BARTON, J. P., "Divergent Beam Collimator for Neutron Radiography", Materials Evaluation, May 1967.
- B-7. BERGER, Harold, Journal of Applied Physics, 34, 1963.
- B-8. BONILLA, Charles F., Nuclear Engineering, McGraw Hill Book Co., New York, 1957.
- E-1. EVANS, Robley D., The Atomic Nucleus, McGraw Hill Co., New York, 1955.
- E-2. EHELICH, M., Health Physics, April, 1960.
- G-1. Gamma Industries, Advertisement, "Portable Neutron Radiography Camera".

- G-2. Gamma Industries, "Industrial Neutron Radiography Device", Advertisement, 1972.
- H-1. HASKINS, J. J., HILL, K. R., and TUNNELL, G. W., Transactions of The American Nuclear Society, Vol. 14, 1971.
- H-2. HAGEMAIER, D. and BASIL, G., Material Evaluation, Vol. 27, 1969.
- H-3. HALMSHAW, R., Physics of Industrial Radiology, American Elsevier Publishing Co., New York, 1966.
- H-4. HUGHES, Donald J., Neutron Cross Sections, Pergamon Press, New York, 1957.
- H-5. HELLER, S.R., FIORITI, Ivo, AND VASTA, John, An Evaluation of HY-80 Steel As A Structural Material For Submarines, Naval Engineers Journal, ASNE, Feb., 1965.
- K-1. KANNO, A., Journal of Non Destructive Inspection, Vol. 14, 1965.
- K-2. KOSANKE, H. D., Transactions of The American Nuclear Society, Vol. 14, 1971.
- K-3. KIEHLE, William D., Factors Affecting Radiographic Sensitivity, Eastman Kodak Co., Rochester, N.Y., 1961.
- L-1. LAMARSH, John R., Introduction to Nuclear Reactor Theory, Addison-Wesley Publishing Co., Reading, 1966.
- L-2. LARSON, E. T., The Meaning of Characteristic Curves, Ansco, Binghamton New York, 1961.
- M-1. M.I.T. Bulletin 72/73, MIT Press, 1972.
- M-2. MITR Neutron Radiography Facility, Reactor Operations Information Publication, 1971.
- M-3. MOMSEN, Bruce, Sensitometric Properties of Neutron Radiography at MIT Research Reactor, 22.39 Project, 1972.
- M-4. MIT Required Procedures for Radiation Protection, MIT Radiation Protection Committee, 1971.
- M-5. MASUBUCHI, K., 13.39 Class Notes, MIT, 1972.

- M-6. MASUBUCHI, K., Materials for Ocean Engineering, MIT Press, Cambridge Mass, 1970.
- P-1. PHILLIPS, Arthur L., Current Welding Processes, American Welding Society, New York, 1968.
- S-1. SUN, K.H., Nucleonics, 14:7, 1960.
- S-2. SCHULTZ, A.W., and LEAVITT, W. Z., 24th National Convention of the Society for N.D.T., Phila., 1964.
- W-1. WILSON, L.E., and SWANSON, G.W., Component Inspection Using Neutron Radiography, High Voltage Engineering Corp., 1971.
- W-2. WESTBERG, Eric L., Neutron Radiography at M.I.T. Research Reactor, Masters Thesis, Cambridge, Mass., 1972.
- W-4. WILSON, Lester E., and SWANSON, G.W., Component Inspection Using Neutron Radiography, High Voltage Engineering Corp., Burlington, Mass., 1971.
- W-3. WHITTEMORE, W.L., Ga-9472, San Diego, 1969.
- W-5. Welding Handbook, American Welding Society, New York, 1968.
- Y-1. YOUSHAU, Robert, U.S. Naval Ordinance Laboratory, Private Communication.



Thesis
E2325 Edgar

145670

Nondestructive test-
ing of high strength
steel welds by neutron
radiography. **DISPLAY**

16 OCT 73

Thesis
E2325 Edgar

145670

Nondestructive test-
ing of high strength
steel welds by neutron
radiography.

thesE2325

Nondestructive testing of high strength



3 2768 001 90320 6

DUDLEY KNOX LIBRARY